

ABSTRACT

Transcriptional Landscape of Human Blood Monocyte and Dendritic Cell Subsets at Steady State and Upon Vaccination

Yuanyuan Wang, Ph.D.

Mentors: A. Karolina Palucka, M.D., Ph.D.
Gerlinde Obermoser, M.D.

Influenza virus remains a major global public health concern that causes annual epidemics and occasional pandemics. The best way to prevent infection is by vaccination. Vaccines work through the generation of protective antibodies against hemagglutinin. Whereas a majority of people respond to vaccination by generating neutralizing antibodies, some vulnerable populations fail to respond including young children, the elderly and immunocompromised people. The reasons for this lack of response to influenza vaccination are under intense study. Ideally, the adaptive immune response to influenza vaccine should include helper $CD4^{+}$ T cells that can help B cells produce antibodies and $CD8^{+}$ T cells that can eliminate infected cells. These responses are elicited and regulated by antigen presenting cells (APCs) such as dendritic cells (DCs). DCs capture antigens and present them to T and B lymphocytes leading to generation of cellular and humoral immunity. This study aims to identify a transcriptional signature of APCs to predict vaccine responsiveness. Using systems biology approaches, we examined transcriptional profiles of APCs, including monocyte

and DC subpopulations, in order to identify signatures in vaccination response. We measured the transcriptional profiles of APCs at steady state, post vaccination, and potential correlation with development of immune response defined by antibody titers. We determined that the early innate immune response to the influenza vaccination peaks at day one after vaccine administration with a prominent type I interferon (IFN) signature contributed by monocytes and CD1c⁺ DCs. We found that monocytes and CD2⁺ pDCs were the main contributors to global transcriptional changes. Finally, we established transcriptional signatures at baseline that correlated with the magnitude of serological response to vaccination. Thus, this dissertation offers a proof-of-concept that transcriptional profiles of APCs at baseline might enable the identification of people who do not respond to influenza vaccination and therefore are at greater risk for infection. Larger studies are needed to confirm these pilot observations; however this work provides a framework for evaluating strategies aimed at the improvement of vaccination outcomes, such as the combination of vaccine with additional adjuvants.

Transcriptional Landscape of Human Blood Monocyte and Dendritic Cell Subsets
at Steady State and Upon Vaccination

by

Yuanyuan Wang, B.S., M.S.

A Dissertation

Approved by the Institute of Biomedical Studies

Robert R. Kane, Ph.D., Director

Submitted to the Graduate Faculty of Baylor
University in Partial Fulfillment of the
Requirements for the Degree
of
Doctor of Philosophy

Approved by the Dissertation Committee

Karolina Palucka, M.D., Ph.D., Chairperson

Gerlinde Obermoser, M.D.

Virginia Pascual, M.D.

Gerard Zurawski, Ph.D.

Robert R. Kane, Ph.D.

Cheolho Sim, Ph.D.

Accepted by the Graduate School
May 2015

J. Larry Lyon, Ph.D., Dean

Copyright © 2015 by Yuanyuan Wang

All rights reserved

TABLE OF CONTENTS

LIST OF FIGURES	v
LIST OF ABBREVIATIONS	ix
ACKNOWLEDGMENTS	xiii
CHAPTER ONE	1
Introduction.....	1
Influenza and Influenza Vaccine	1
Roles of Antigen Presenting Cells in Immunity	3
Transcriptional Programs in DC and Monocyte Subsets	11
CHAPTER TWO	17
Objectives	17
Aim 1: Study Transcriptional Profiles of Whole Blood and Major Cellular Sources at Baseline and in Response to Influenza Vaccination	17
Aim2: Study Transcriptional Response of APC Subsets to Influenza Vaccination	18
Aim 3: Investigate Correlations between Steady State Transcriptional Signatures of APCs and Serological Response to Vaccination	18
CHAPTER THREE	19
Materials and Methods.....	19
Healthy Donors and Samples.....	19
Genome-wide Transcription Analysis	23
Influenza Hemagglutinin Inhibition and Virus Neutralization Assays	26
CHAPTER FOUR.....	28
Results.....	28

Global Responses of Whole Blood and Responses of Major Cellular Components to Influenza Vaccination.....	28
Transcriptional Profiles of Monocytes and Dendritic Cell Subsets in the Steady State and Upon Influenza Vaccination.....	35
Correlations between Baseline Transcriptional Signatures of APCs and Antibody Responses After Influenza Vaccination.....	61
CHAPTER FIVE	72
Discussion.....	72
CHAPTER SIX.....	87
Conclusions.....	87
APPENDIX.....	88
APPENDIX.....	89
List of Current and Future Publications.....	89
BIBLIOGRAPHY	91

LIST OF FIGURES

Figure 1. Dendritic cells (DCs) play an important role in initiating the immune response to vaccination.	5
Figure 2. DC and monocyte subset in the blood.	7
Figure 3. Global changes in blood transcript abundance elicited by influenza and pneumococcal vaccinations.	30
Figure 4. Study design for studying the kinetics of immune responses to influenza vaccination using finger prick sampling during 2009-2010 influenza season.....	31
Figure 5. Profiling the interferon response within the first 48 hr following vaccination.	32
Figure 6. Deconvolution of whole blood signatures elicited by influenza vaccination....	33
Figure 7. The purity gating strategy of purified CD4 ⁺ T cells in 2009 isolated leukocytes study.	33
Figure 8. IFN responses in whole blood and isolated leukocyte populations from healthy donors.	34
Figure 9. Human monocyte and DC subsets in the blood.....	36
Figure 10. Unsupervised clustering analysis of human monocyte and DC subsets at steady state (day 60).....	38
Figure 11. Distances of distinct APCs subsets.....	40
Figure 12. Differentially expressed genes in human monocyte and DC subsets at steady state.	40
Figure 13. mRNA expression of surface markers in monocyte and DC subsets at steady state.	41
Figure 14. CLEC10A expression on DC subsets.....	42
Figure 15. Common and unique gene signatures characterized in monocytes, CD1c ⁺ and CD141 ⁺ DCs.....	43
Figure 16. Common and unique gene signatures characterized in distinct monocyte subsets.	46

Figure 17. Human blood monocyte subsets show differences in transcriptomic signatures at the steady state.	48
Figure 18. Common and unique gene signatures characterized in two cDC subsets.	50
Figure 19. Human blood cDC subsets show different transcriptomic signatures at the steady state.	51
Figure 20. Common and unique gene signatures characterized in two pDC subsets.	52
Figure 21. Human monocyte and DC subpopulations in healthy donors with TIV vaccination.	54
Figure 22. Numbers of interferon-stimulated genes (ISGs) with changes at day 1 and day 3 after influenza vaccination in monocyte and DC subsets.	55
Figure 23. Most transcriptional changes upon vaccination occurred in monocytes and CD2 ⁺ pDCs.	55
Figure 24. Genes with changes in each monocyte subsets after influenza vaccination.	56
Figure 25. Genes with changes in each monocyte subsets after influenza vaccination.	57
Figure 26. Genes with changes in each cDC subset after flu vaccination from 2010 cohort.	58
Figure 27. Genes with changes in each cDC subset after flu vaccination from 2010 cohort.	59
Figure 28. Genes with changes in each pDC subset after flu vaccination from 2010 cohort.	60
Figure 29. Genes with changes in each pDC subset after flu vaccination from 2010 cohort.	60
Figure 30. Study design of small blood draw study during 2012 flu season.	62
Figure 31. Gating strategy for monocyte and DC cell populations.	62
Figure 32. Commonly expressed genes of CD14 ⁺ monocytes sorted from 2010 apheresis and 2012 small blood draws. Line graphs showed genes present in CD14 ⁺ monocytes for each year of study. Common genes are at the intersection venn diagram.	64
Figure 33. Numbers of transcripts correlating with each serology parameter.	66
Figure 34. IPA network analysis of transcripts correlated with “Fold_B_VN” in BDCA2 ⁺ pDCs.	69

Figure 35. GSEA of transcripts correlated with Fold_B_VN using blood module gene sets..... 71

LIST OF TABLES

Table 1. Advantages of RNA-Seq compared with microarray.	12
Table 2. Overview of studies.	19
Table 3. Compositions of trivalent inactivated seasonal influenza vaccines.	20
Table 4. The purity of isolated leukocytes was assessed by flow cytometry.	33
Table 5. Demographic information of six healthy volunteers in 2010 apheresis study...	36
Table 6. Purity of sorted myeloid cell populations.	37
Table 7. The study design and the classification of serological responder in 2012 small blood draw study.	63
Table 8. Top genes ranked by correlation (R) with antibody response in CD14 ⁺ monocytes.	66
Table 9. Top genes ranked by correlation (R) with antibody response in CD1c ⁺ cDCs. .	67
Table 10. Top genes ranked by correlation (R) with antibody response in CD141 ⁺ cDCs.	67
Table 11. Top genes ranked by correlation (R) with antibody response in BDCA2 ⁺ pDCs.	68

LIST OF ABBREVIATIONS

Ag	antigen
AIF1	allograft inflammatory factor 1
APCs	antigen presenting cells
CCL	chemokine (C-C motif) ligand
CD	classification determinant
CDC	centers for disease control and prevention
cDCs	classical dendritic cells
CLEC	C-type lectin domain
CLR	C-type lectin receptors
CMP	common myeloid progenitor
CpG-ODN	CpG oligodeoxynucleotides
CXCL	chemokine (C-X-C motif) ligand
DCIR	Dendritic Cell Immunoreceptor
DCs	dendritic cells
DC-SIGN	Dendritic Cell-Specific ICAM-3-Grabbing Non-Integrin 2
DEGs	differentially expressed genes
EHR	extremely high responder
ELR	extremely low responder
FACS	fluorescence-activated cell sorting
FcγR	Fc gamma receptor
FDA	food and drug administration

FDR	false discovery rate
GMP	granulocyte/macrophage progenitor
GO	gene ontology
HA	haemagglutinin
HI	hemagglutination inhibition
HSC	hematopoietic stem cell
IFNs	interferons
IL-1B	interleukin-1 beta
IPA	ingenuity pathway analysis
IP-10	interferon-inducible cytokine IP-10
ISGs	interferon-stimulated genes
LCs	Langerhans cells
LINC RNA	long non-coding RNA
LogCPM	log ₂ transformed counts per million
LPS	lipopolysaccharide
M	matrix protein
MDP	macrophage/DC progenitor
MEK	mitogen-activated protein kinase kinase
MHC	major histocompatibility complex
MNCs	mononuclear cells
MoDCs	monocyte-derived DCs
MRC1	mannose receptor, C type 1
MRC2	mannose receptor, C type 2

MyD88	myeloid differentiation primary response 88
NA	neuraminidase
NK cells	natural killer cells
NLR	NOD-like receptor
NP	nucleoprotein
NS1	nonstructural protein
PA	polymerase acidic protein
PAMPs	pathogen associated molecular patterns
PB	polymerase basic
PBMC	peripheral blood mononuclear cell
PCA	principal component analysis
pDCs	plasmacytoid dendritic cells
PRR	pathogen recognition receptor
PTPN6	Protein Tyrosine Phosphatase, Non-Receptor Type 6
RLRs	RIG-I-like receptors
RNA-Seq	RNA sequencing
RNP	ribonucleoprotein
SA	sialic acid
TAP	transporter associated with antigen processing
TF	transcription factor
TGFB1	transforming growth factor, beta 1
Th	T helper
TIE2	TEK tyrosine kinase, endothelial

TIV	trivalent inactivated influenza vaccine
TLRs	toll-like receptors
TNF	tumor necrosis factor
TNFSF	tumor necrosis factor super family
Tregs	regulatory T cells
TSLP	thymic stromal lymphopoietin
VNA	virus neutralization assay
YF-17D	yellow fever 17D vaccine

ACKNOWLEDGMENTS

First and foremost I want to thank my mentor Prof. A. Karolina Palucka. It has been an honor to be her student. I appreciate all her contributions of time, ideas, and efforts to make my Ph.D. experience productive and stimulating. I am very thankful to my co-mentor Dr. Gerlinde Obermoser for her encouragement, instructions, time and efforts on my dissertation and many experimental supports. The enthusiasm they have for their research was motivational for me during the entire time of my studies.

I would also like to thank my committee members, Prof. Virginia Pascual, Prof. Gerard Zurawski, Prof. Robert R. Kane and Prof. Cheolho Sim, for their encouragement, insightful comments and suggestions.

My sincere thanks also goes to Dr. Jacques Banchereau and Dr. Damien Chaussabel for encouraging me to start my Ph.D. study and their contributions in initiating my project. I would also like to thank Dr. Hideki Ueno for offering me the summer rotation opportunities in his group and leading me working on diverse exciting projects.

I want to thank all present and past members of the Palucka lab. Thanks to Drs. Chun I Yu, LuAnn T. Snipes and Jason Skinner for reviewing and giving comments on my dissertation. Thanks to Dr. Chun I Yu, Florentina Marches, Kristina Goller and Patrick Metang for helping me on experiments and collecting samples. Also thanks to Dr. Te Chia Wu, Cheng Han Chung, Dr. Kangling Xu, Dr. Qiumei Du, Stephane Pourpe, Jan Martinek and Pierre Authie for their support and discussion.

My sincere thanks also goes to Esperanza Anguiano from Genomics Core at BIIR for her continuous supports and efforts on multiple RNA-Seq experiments, data analysis and discussion. I would also like to thank other members in the Genomics Core: Benjamin Lemoine, Rahul Maurya, Abhilasha Cheruku, Indira Munagala, Durgha Nattamai, Lindsey Gibbons and Phuong Nguyen for their help on RNA-Seq experiments and other support.

My special thanks also goes to Dr. LuAnn T. Snipes for teaching me cell culture techniques and her great help on collecting samples and summarizing clinical information for this project. I am also thankful to Dr. Carson Harrod, Lynnette Walters and Jean-Phillip Blanck for their help on clinical information collection and sample preparation. I also want to especially thank our healthy volunteers, the apheresis core, the flow core and Dr. Randy Albrecht at Mount Sinai medical school for serology assays. I would like to acknowledge Dr. Brandi Cantarel, Dr. Nicole Baldwin, Dr. Romain Banchereau, Dr. Aaron Chang and Dr. Guorong Xu for their help on RNA-Seq analysis and bioinformatics support. I am also grateful to Cindy Samuelsen, Cheryl Gibson, Angela Plata, Annie Mathew, Darlene Pleiner and Bonnie Walters from Baylor Research Institute and Rhoda Bellert from Baylor University for their administrative supports. Support for this project was made through the U19AI089987-01 grant from National Institutes of Health.

Lastly, I would like to thank my family for all their love and encouragements. I would like to thank my parents who faithfully support and encourage me during all stages of this Ph.D.

CHAPTER ONE

Introduction

Influenza and Influenza Vaccine

Influenza remains a global health threat due to its pandemic potential.

Vaccination is the most effective method to prevent diseases and severe outcomes caused by influenza infection (Fiore et al., 2009).

Influenza Remains a Clinical Threat

Influenza is a viral infection that causes acute respiratory diseases (World Health Organization, 2014). In the United States, seasonal influenza epidemics account for >200,000 hospitalizations and about 36,000 deaths annually (Thompson et al., 2009; Thompson et al., 2004). Globally, it is still a major public challenge causing about 3 to 5 million cases of severe illness and about 250,000 to 500,000 deaths yearly (World Health Organization, 2014). 1918 influenza pandemic virus caused severe pneumonia and resulted in >500,000 deaths in the United States and over 50 million deaths on a global scale (Taubenberger and Morens, 2008). The 2009 influenza H1N1 pandemic virus was more pathogenic compared with seasonal influenza viruses and it accounted for about 22 million cases of infection, about 98,000 H1N1-related hospitalizations, and 10,000 2009 H1N1-related deaths in the United States (CDC, 2010).

Current Influenza Vaccines

Vaccination is an important strategy to prevent influenza epidemics and pandemics (Fiore et al., 2009). In the United States, three types of influenza vaccines are

commercially available: the most widely used unadjuvanted injectable trivalent inactivated influenza vaccines (TIV) for eligible individuals aged ≥ 6 month, an intranasal live attenuated influenza vaccine (LAIV) for eligible individuals aged 2-49 years (Ambrose et al., 2011), and a recently approved recombinant HA protein subunits adult vaccine (Treanor et al., 2011). The seasonal flu vaccines are constituted with the two influenza A strains (H3N2 and H1N1) and one B virus strain. For 2014-15, U.S.-licensed influenza vaccines are quadrivalent containing two viral strains of influenza A and B, respectively (Grohskopf et al., 2014). Currently licensed vaccines are updated for each new influenza season to counter the threat of the antigenic drift in HA. The World Health Organization (WHO) predicts the virus strains that will circulate in the new coming season and this provides the instruction for vaccine production every year (Schotsaert and Garcia-Sastre, 2014).

Challenges of Vaccination Against Influenza

Successful vaccination against influenza results in generating neutralizing antibody targeting HA that is the main surface antigen of influenza virus (Clements et al., 1986). One of the challenges in the current vaccination is that different populations have variable efficacy (Wong and Webby, 2013). The majority of healthy children and adults generate robust antibody responses after influenza vaccination (La Montagne et al., 1983; Neuzil et al., 2001). However, the most vulnerable segment of the population, such as young children, the elderly and immunocompromised individuals, generally benefits less from active immunization (Thompson et al., 2004). In 2008, seasonal influenza viruses were responsible for 90 million new infections globally in children younger than 5 years of age (Nair et al., 2011). In the elderly, influenza caused increased morbidity and

mortality because that an aging immune system reduces their ability to control infections (Reber et al., 2012). In young healthy adults, there is still a proportion of individuals that respond poorly to influenza vaccination with very low levels of antibody titers (Nakaya et al., 2011). The immunological mechanisms that underlie the different outcomes of vaccination still need to be identified.

Roles of Antigen Presenting Cells in Immunity

The mammalian immune system comprises two important aspects: innate and adaptive immunity. The innate immune system consists of cells and proteins that are present and ready to mobilize and fight microbes at the site of infection. On the other hand, the adaptive immune system takes action against pathogens that are able to evade or overcome innate immune defenses by generating a diverse repertoire of pathogen-specific antigen receptors on T and B lymphocytes to neutralize or eliminate pathogens (Schenten and Medzhitov, 2011). A key player involved in the initiation of effective immune responses after vaccination are antigen presenting cells (APCs) (Palucka et al., 2010). Dendritic cells are professional APCs crucial for linking innate and adaptive immune responses (Banchereau and Steinman, 1998). Their precursors, monocytes, are also professional APCs that express proinflammatory cytokine proteins, MHC class II and costimulatory molecules upon activation (Iwasaki and Akashi, 2007; Lauvau et al., 2014; Manz et al., 2001; Traver et al., 2000).

Biology Functions of Dendritic Cells

Pathogen recognition. Dendritic cells can recognize diverse microbes or vaccine antigens and initiate innate immune response to set the stage for an effective adaptive

immune response (Palucka et al., 2007; Palucka et al., 2010). At steady-state, DCs are immature and unable to stimulate T cells but are well equipped to capture and process antigens (Banchereau and Steinman, 1998). They play a major role in tolerance by circulating through tissues and capturing self-antigens and innocuous environmental proteins (Steinman et al., 2003). During inflammation and infection, immature DCs are triggered by pathogen-derived activation signals to migrate to the draining lymph node, where they become mature and highly efficient at presenting antigens and stimulating T cells (Palucka et al., 2010; Real et al., 2004). DCs detect a limited set of conserved molecular patterns that are associated with microbes, called pathogen-associated molecular patterns (PAMPs). PAMPs are recognized through pattern recognition receptors (PRRs) which include toll-like receptors (TLRs), C-type lectin receptors (CLRs) and nucleotide oligomerization domain-like receptors (NLRs) (Akira and Takeda, 2004; Geijtenbeek and Gringhuis, 2009; Krishnaswamy et al., 2013).

Presenting antigen. There are two classical antigen presentation pathways: major histocompatibility complex (MHC) class I and class II presentation. MHC class I molecules present peptides primarily derived from endogenous proteins in the cytosol. These proteins are degraded into peptides by the proteasome and then transported through the transporters of antigen-processing (TAP) molecules into the endoplasmic reticulum for loading on MHC class I molecules (Joffre et al., 2012). MHC class II molecules present proteins through an endocytic route. Their peptide cargo is loaded in endosomal compartments via proteolytic degradation. These peptides are derived from both exogenous material that is from the extracellular environment, and endogenous components (Villadangos and Schnorrer, 2007). DCs have both functional MHC class I

and MHC class II presentation pathways. They can also process exogenous antigens into the MHC class I pathway. This ability, known as cross-presentation, is essential for the initiation of CD8⁺ T cell responses (Heath and Carbone., 2001; Joffre et al., 2012).

Initiating adaptive immunity. DCs are efficient stimulators of T and B lymphocytes. After exposure to pathogens, tissue-resident DCs capture the antigens and become activated. Activated DCs migrate to secondary lymphoid organs via chemokine receptors (e.g., CCR7) where they interact with T cells to initiate the selection and expansion of antigen-specific T cells and simultaneously they become terminally mature

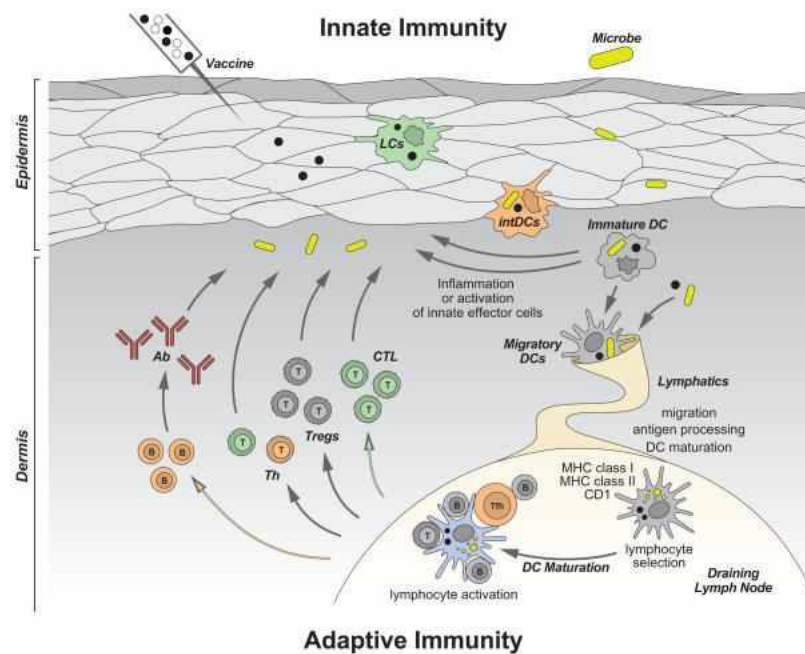


Figure 1. Dendritic cells (DCs) play an important role in initiating the immune response to vaccination. DCs can recognize and capture foreign antigens (vaccines) in the tissue. Activated DCs migrate toward secondary lymphoid organs and present antigens to T lymphocytes via classical MHC class I and class II or non-classical CD1 molecules, which results in the selection and expansion of antigen-specific T cells. Activated T cells migrate to the infection sites and eliminate pathogens or infected cells. DCs and T cells activate B cells that further differentiate into plasma cells which secrete antibodies against the pathogen. Antigens can also drain into the adjacent lymph node and be captured by lymph node-resident DCs directly.

(Palucka et al., 2010). Mature DCs can induce different CD4⁺ T helper cell subsets: T_H1, T_H2, T_H17 or regulatory T cells (Tregs). Additionally, activated DCs can induce naïve CD4⁺ T cells to become IL-21-producing follicular helper T (T_{fh})-like cells through IL-12 (Schmitt et al., 2009). Furthermore, DCs and T cells drive B cells to differentiate into plasma cells secreting antibodies against the pathogen (Palucka et al., 2007; Palucka et al., 2010) (Figure 1).

Human Dendritic Cell Subsets

DC subsets. Dendritic cells (DCs) comprise heterogeneous populations of rare leukocytes found in all tissues. Different DC subsets are equipped with distinct receptors for antigen uptake and signaling, and undergo different pathways of antigen processing and presentation (Steinman, 2007). Human blood-circulating DCs can be divided into two major subsets: plasmacytoid DCs (pDCs) and classical DCs (cDCs). cDCs can be further divided into CD1c⁺ (BDCA1⁺) and CD141⁺ (BDCA3⁺) cDCs. CD2 can be used to distinguish pDCs into CD2⁺ and CD2⁻ subsets (Andrzej Dzionek, 2000; Boltjes and van Wijk, 2014; Matsui et al., 2009) (Figure 2). In the blood at the steady state, DCs constitute 0.25-0.84% of peripheral blood leukocytes and 0.6-1.69% of mononuclear cells (MNCs) in healthy adults (Haller Hasskamp et al., 2005). The total blood DCs are comprised of 5-10% CD141⁺ cDCs and equal parts of CD1c⁺ cDCs and pDCs (MacDonald et al., 2002). The skin contains a much higher frequency of CD1c⁺ cDCs, which constitute about 12%-28% of CD45⁺ MNCs. The frequencies of CD141⁺ cDCs (~0.2-0.5% of MNCs) are both higher in liver and lung compared to frequencies observed in the blood (Haniffa et al., 2012). Skin tissues contain the highest percentage (~0.8-1.8% of MNCs) of CD141⁺ cDCs (Haniffa et al., 2012).







Dendritic cells		
	cDC1	CD1c+ CD11c+++ 45-50%
	cDC2	CD141+ CD11c++ CLEC9A+ XCR1+ 5-10%
	pDC	CD11c+ CD123+ BDCA-2+ BDCA-4+ 45-50%
Monocytes		
		Surface markers Distribution
	"classical"	CD14++ CD16- ~85%
	"intermediate"	CD14++ CD16+ ~5%
	"non-classical"	CD14+ CD16++ ~10%

Figure 2. DC and monocyte subset in the blood. Monocyte and dendritic cell populations in human peripheral blood in steady-state conditions. The expression of markers commonly used to identify and discern these populations are indicated. The frequencies of monocyte and DC subsets are specified (Boltjes and van Wijk, 2014).

Different patterns in antigen recognition and presentation. DCs are efficient in recognizing distinct pathogens and induce distinct innate responses to trigger the immune system. Many of the markers used to divide DCs into distinct subsets are receptors involved in pathogen recognition and antigen presentation, those important in initiating immune responses (Steinman, 2008) suggesting a division of labors between various DC

subsets. pDCs express and secrete large amounts of type I interferons in response to viral or self-nucleic acids through TLR7- and/or TLR9-dependent pathways (Barrat et al., 2005; Boonstra et al., 2002; Boule et al., 2004; Christensen et al., 2006; Kadowaki et al., 2000; Lande et al., 2007). The two cDC subsets are different in TLR expression pattern and responsiveness. CD141⁺ cDCs are characterized by high expression of TLR3 and TLR10 and low expression of other TLRs, but lack the expression of TLR4, 5, 7 and 9. In contrast, CD1c⁺ cDCs express TLR4, 5 and 7 (Hemont et al., 2013; Jongbloed et al., 2010). Stimulation of two cDC subsets with TLR3 agonist (poly I:C) showed that CD141⁺ cDCs have a more restricted response by secreting CXCL-10 (IP-10), CCL5, IFN- β and IFN- λ , a type III IFN with anti-viral properties compared to CD1c⁺ cDCs (Hemont et al., 2013; Jongbloed et al., 2010; Lauterbach et al., 2010). The expression of CLRs also varied in distinct cDC subsets. CLEC9A was shown to be restricted to CD141⁺ cDCs (Jongbloed et al., 2010) CD1c⁺ cDCs showed higher frequency for CD206/MRC1, DCIR and CD301/CLECSF14, whereas CD141⁺ cDCs had a higher surface expression of Dectin-1, Dectin-2, CD209/DC-SIGN, CD207/Langerin and CD280/MRC2 (Lundberg et al., 2014).

DC subsets initiate different adaptive immune responses. Previous studies have shown that distinct cDC subsets can induce T cell polarization via different mechanisms (Hemont et al., 2013). These differences may be caused by differential TLR and cytokine/chemokine expression profiles. CD141⁺ cDCs were found to be more efficient to promote T_H1 response upon poly I:C activation and induce the highest percentage of IFN- γ -producing T cells (Hemont et al., 2013). Blood DCs are not able to induce efficient T_H2 polarization (Segura et al., 2012); however, they can drive a strong T_H2

response under the influence of TSLP (Ito et al., 2005). Whereas blood/lung CD1c⁺ cDCs are more efficient in inducing IL-17 production by autologous CD4⁺ T cells comparing with CD141⁺ cDCs or CD14⁺ DCs/monocytes (Kelly et al., 2014), CD141⁺ cDCs are more efficient in inducing IL-4/IL-13 producing T_H2 cells in response to live-attenuated influenza virus (Yu et al., 2014). Human CD141⁺ DCs, comparable to their counterpart of mouse CD8α⁺ DCs, can produce IL-12 and cross-present antigens to CD8⁺ T effector cells when activated by poly I:C (Bachem et al., 2010; Haniffa et al., 2012; Jongbloed et al., 2010). However, a recent study compared the capacities of CD1c⁺, CD141⁺ cDCs and pDCs in priming cytotoxic T cells. CD1c⁺ cDCs were surprisingly the only human DC that secreted high amounts of IL-12p70 with a combination of TLR (LPS+R484) stimulation (Nizzoli et al., 2013). Function studies on pDC subsets showed that both subsets express IFN-α, granzyme B and trail but CD2⁺ pDCs uniquely expressed IL12p40 and CD80 under the activation. Therefore, CD2⁺ pDCs have more potential in initiating T cell immune responses (Matsui et al., 2009). Formal studies indicated that DC subsets use different machineries in antigen presentation responding to different TLR stimulations, which leads to initiating different adaptive immune responses.

Human Monocyte Subsets

Monocyte subsets. Human monocytes can be divided into three different subsets based on the expression of CD14 and CD16 (FcγRIII): classical CD14⁺CD16⁻, intermediate CD14⁺CD16⁺ and non-classical CD14^{dim}CD16⁺ monocytes (Figure 2; modified from (Boltjes and van Wijk, 2014). Monocytes constitute about 20-40% of blood peripheral MNCs (de Almeida et al., 2000). Eighty-five percent of total circulating

monocytes are classical monocytes with 5% intermediate and 10% non-classical monocytes (Boltjes and van Wijk, 2014; Passlick et al., 1989; Zawada et al., 2011; Ziegler-Heitbrock, 2007) (Figure 2).

Different functions of monocyte subsets. Monocytes are derived from progenitors in the bone marrow and migrate to peripheral tissues via the bloodstream (Shi and Pamer, 2011). They are equipped with a wide array of scavenger and pattern recognition receptors which enable them effectively to control and clear viral, bacterial, fungal and protozoal infections (Boltjes and van Wijk, 2014). The stimulation of TLR receptors in monocyte subsets showed that all TLR agonists trigger a rapid expansion of blood monocytes whereas only R-848 (TLR7/8-L) and CPG-ODN (TLR9-L) can induce a rapid and transient increase in CD16⁺ (intermediate and non-classical) monocytes (Kwissa et al., 2012). Initially, monocytes were thought to circulate in the blood for a few days before entering tissues where they differentiated into macrophages and DCs, however they were also found to play critical roles in pathogen defense and driving inflammatory diseases (Boltjes and van Wijk, 2014).

Like DCs, distinct monocyte subsets exhibit different functional characteristics. Classical CD14⁺CD16⁻ monocytes can be rapidly recruited to tissues in response to inflammation. CD16-positive (CD14⁺CD16⁺ and CD14^{dim}CD16⁺) monocytes are likely to carry effector functions related to antigen processing and presentation with DC and macrophage-like characteristics. Gene ontology (GO) analysis indicates that intermediate CD14⁺CD16⁺ monocytes have diverse immunological functions related to inflammation and monocyte activation (e.g., TGFB1, AIF1, PTPN6), and angiogenesis (e.g., TIE2, CD105) (Zawada et al., 2011). In contrast, non-classical CD14^{dim}CD16⁺ monocytes can

produce TNF α , IL-1 β and CCL3 in response to viruses and immune complexes containing nucleic acids following the TRL7-TLR8-MyD88-MEK pathway (Cros et al., 2010).

Transcriptional Programs in DC and Monocyte Subsets

With recent advances in technology and methodology, it is now possible to study the human immune system on a systems level. Technologies such as genome-wide expression analysis enable the simultaneous assessment of thousands of genes in heterogeneous tissue or in an isolated cell population (Chaussabel et al., 2010).

Approaches to Study Transcriptomes

Understanding the transcriptome is essential for studying the molecular constituents of cells and tissues and interpreting the functional elements of the genome. Various technologies, including real-time PCR, Nanostring, hybridization and sequence-based approaches, have been developed to analyze the transcriptome (Chaussabel et al., 2010; Wang et al., 2009). Real-time PCR is used as a gold standard for measuring gene expression but it is limited by the numbers of genes that can be simultaneously tested (Chaussabel et al., 2010). Nanostring can detect the abundance of up to 500 transcripts with high sensitivity (Geiss et al., 2008). On the other hand, microarray and RNA-Seq both can measure the abundance of transcripts on a genome wide scale. Microarray, a typical hybridization-based approach, is high throughput and relatively inexpensive. However, it relies on existing knowledge about genome sequence and also suffers from high background levels by cross-hybridization (Okoniewski and Miller, 2006; Royce et al., 2007). In contrast to microarray, RNA-Seq has several advantages including the ability to detect (a) novel transcripts, (b) low abundant transcripts, (c) non-coding and

small RNAs, (d) alternatively spliced isoforms (Table 1) (Wang et al., 2009). In addition, RNA-Seq has relatively low noise compared to microarray, has a high levels of accuracy for quantifying expression levels and is highly reproducible for both biological and technical replicates (Nagalakshmi et al., 2008).

Table 1. Advantages of RNA-Seq compared with microarray (Wang et al., 2009).

Technology	Tiling microarray	RNA-Seq
Technology specifications		
Principle	Hybridization	High-throughput sequencing
Resolution	From several to 100 bp	Single base
Throughput	High	High
Reliance on genomic sequence	Yes	In some cases
Background noise	High	Low
Application		
Simultaneously map transcribed regions and gene expression	Yes	Yes
Dynamic range to quantify gene expression level	Up to a few-hundredfold	>8,000-fold
Ability to distinguish different isoforms	Limited	Yes
Ability to distinguish allelic expression	Limited	Yes
Practical issues		
Required amount of RNA	High	Low
Cost for mapping transcriptomes of large genomes	High	Relatively low

Transcriptional Profiling of DC Subsets

Miller and colleagues have identified cell type specific transcriptional programs by analyzing DC subsets, macrophage DC precursors and common DC precursors in vivo across the entire murine immune system (Miller et al., 2012). Distinct DC populations were isolated from lymphoid tissues, secondary lymphoid tissues and nonlymphoid tissues. This study identified both known and unknown potential regulators that control DC lineages in vivo. They also predicted the regulators that maintained DC functional

diversity in tissues. Core gene sets were identified to compose cDC and pDC signatures. Several transcription factors have been identified to control DC development. For instance, zinc-finger protein Ikaros 25 was identified to be responsible for the differentiation of pDCs and cDCs. Moreover, transcription factors including E2-2 (encode by Tcf4), Spi-B and IRF8 were identified to control pDC differentiation. Bcl-6 was found to control the development of cDCs but not of pDCs in the spleen. Unique gene signatures were characterized for distinct tissue DC clusters as well (Miller et al., 2012). Our group recently published the data analyzing transcriptional signatures of APC subsets in human. The transcriptional programs of human DC subsets were established by characterizing the responses of human APCs to pathogens, innate receptor ligands and vaccines (Banchereau et al., 2014). A modular framework with 204 transcript clusters was built by stimulating monocyte-derived DCs with different pathogens. The framework was further used to determine the specialization of APC subsets in response to 13 different vaccines. The data showed that different vaccines activated distinct APC subsets. Monocyte-derived DCs, monocytes and CD1c⁺ blood DCs become activated by culturing with Fluzone, Pneumovax and Gardasil, respectively (Banchereau et al., 2014). In addition, transcriptional profiles of CD1c⁺ and CD141⁺ DCs purified from human blood and lungs and from humanized mouse spleens and lungs were also investigated (Yu et al., 2013). CD1c⁺ DCs over-expressed genes involved in TGF- β 1 activation including furin, MMP-9 (matrix metalloproteinase 9), CD36 and PLAUR. This observation, based on transcriptional profiling, led to investigation on their biological functions. We demonstrated that lung-tissue-resident CD1c⁺ DCs, but not CD141⁺ DCs, were able to drive CD103 expression on CD8⁺ T cells via TGF- β 1 and promoted CD8⁺ T cell accumulation in lung epithelia in vitro and in vivo (Yu et al., 2013).

Transcriptional Profiling of Monocyte Subsets

Classification of monocyte heterogeneity was based on CD14 and CD16 surface markers (Ziegler-Heitbrock et al., 2010). Transcription profiles of CD16⁺ and CD16⁻ monocytes were analyzed using microarray. CD16⁺ monocytes were found to have a more macrophage (CSF1R/CD115, MafB, CD97, C3aR) and DC (SIGLEC10, CD43, RARA)-like transcription program. CD16⁻ monocytes overexpressed transcripts for myeloid (CD14, MNDA, TREM1, CD1d, C1qR/CD93) and granulocyte markers (FPR1, GCSFR/CD114, S100A8-9/12). These distinct transcriptional programs also suggest that CD16⁺ and CD16⁻ monocyte give rise to functionally distinct DC and macrophage in vivo (Ancuta et al., 2009). In another study, all three human monocyte subsets and mouse blood monocytes Gr1⁺ and Gr1⁻ were analyzed using microarray. Gene expression analysis indicated that CD14⁺CD16⁻ CD14⁺CD16⁺, and CD14^{dim}CD16⁺ subsets segregated in independent clusters. Transcription profiling revealed the similarities between human CD14^{dim}CD16⁺ monocytes and mouse patrolling Gr1^{dim} monocytes. In contrast, both CD14⁺CD16⁻ and CD14⁺CD16⁺ cells are similar to mouse Gr1⁺ inflammatory monocytes (Cros et al., 2010). Zawada and his colleagues used SuperSAGE sequencing to analyze transcriptional profiles of all three human monocyte subsets (Zawada et al., 2011). A specific gene set was identified for each monocyte subset. The differences between CD14⁺CD16⁺ and CD14^{dim}CD16⁺ monocytes were analyzed extensively since no previous studies had focused on this subject. Differentially expressed genes were defined between the two subsets and functional annotations of present genes were analyzed based on GO categorization as well. GO enrichment analysis revealed diverse immunologic functions of CD14⁺CD16⁺ monocytes including antigen processing and presentation (CD74, HLA-DR, IFI30, CTSB), inflammation and

monocyte activation (TGFB1, AIF1 and PTPN6), and angiogenesis (TIE2 and CD105). In contrast, CD14^{dim}CD16⁺ monocytes were more abundant in gene expression related to MHC I-restricted processes (HLA-B, B2M), migration and transendothelial motility (LSP1, LYN, CFL1, MYL6), and cell-cycle progression (CDKN1C, STK10) (Zawada et al., 2011).

Using Systems Biology Approaches to Study Immune Responses to Vaccination

Vaccination not only protects individuals from illnesses caused by pathogens but also provides a good opportunity to study human immune response that leads to protective immunity. Inactivated influenza vaccination offers a model to study immune responses to an inactivated immunogen. Studies with these and other vaccines are beginning to reunite the estranged fields of immunology and vaccinology, yielding unexpected insights about mechanisms of viral immunity (Pulendran et al., 2013).

Blood acts as a pipeline of the immune system since it carries the immune cells flowing throughout the body (Chaussabel et al., 2010). Profiling blood transcript abundance on a systems scale has been successfully implemented to investigate vaccine responses in human. System biology approach has been employed because it gives an unbiased and comprehensive view of the immune system (Nakaya et al., 2011; Obermoser et al., 2013; Querec et al., 2009). Vaccination not only protects individuals from illnesses caused by influenza but also provides excellent strategies for learning human immunity by perturbing the immune system in vivo (Pulendran et al., 2013). Thus this system biology approach has been used to identify global biomarkers to predict adaptive immune responses induced by various vaccines (Li et al., 2014; Nakaya et al., 2011).

Live attenuated yellow fever vaccine (YF-17D) is one of the most successful vaccines ever developed and it has been used to study human innate and adaptive responses. System studies with YF-17D were used to identify early molecular signatures of vaccination that could be explored to predict immunogenicity such as the development of antigen-specific CD8⁺ T cells and neutralizing antibody response (Gaucher et al., 2008; Querec et al., 2009). Nakaya and his colleagues have employed a system biology approach to study healthy donors' immune responses for both TIV and LAIV. The expression of kinase CaMKIV at day 3 postvaccination was discovered to be inversely correlated with later antibody titers from the TIV group (Nakaya et al., 2011). Similar approaches were used by other groups to study immune responses to seasonal influenza, pneumococcal and meningococcal vaccines (Li et al., 2014; Nakaya et al., 2011; Obermoser et al., 2013; Tsang et al., 2014).

Previous studies have focused on global immune responses to vaccination by analyzing transcriptomes of whole blood or peripheral blood mononuclear cell (PBMCs) (Li et al., 2014; Nakaya et al., 2011; Obermoser et al., 2013; Tsang et al., 2014). Roles of APCs in vaccination still need to be further investigated. Due to the rarity of these cells in the circulation and difficulties acquiring human tissue, it presents substantial challenges to the study of monocyte and DC subsets in human. We here employed transcription profiling as a tool to study monocyte and DC subsets in vivo. We used a systems biology approach to investigate circulating monocyte and DC subsets in the steady state and upon influenza vaccination. We further identified their transcriptional signatures at baseline that correlate with serologic response after vaccination.

CHAPTER TWO

Objectives

Influenza vaccines are designed to initiate protective immunity by generating neutralizing antibody against viral HA. However, vaccination outcome varies among individuals. APCs are critical in eliciting this adaptive immune response.

Transcriptional profiling of whole blood allows us to identify the status of the immune system (Chaussabel et al., 2010). However, transcriptional profiling of the vaccine response in whole blood or PBMC cannot easily provide insight into the changes in individual cell populations, in particular when the populations are rare. As important initiators of the immune response, the specialization of each APC subset in response to vaccination requires investigation. Here we employed RNA-Seq for genome-wide transcriptional profiling to investigate three subsets of monocytes, CD14⁺CD16⁻, CD14⁺CD16⁺, and CD14^{dim}CD16⁺ monocytes as well as four blood DC subsets, CD1c⁺ DCs and CD141⁺ (BDCA3⁺) cDCs, and CD2⁺ and CD2⁻ pDCs at steady state and their transcriptional changes after TIV vaccination in healthy volunteers.

Aim 1: Study Transcriptional Profiles of Whole Blood and Major Cellular Sources at Baseline and in Response to Influenza Vaccination

a) Study Global Responses to Influenza Vaccination in the Whole Blood

b) Identify Major Cellular Sources of Early Innate Transcriptional Responses

To gain a comprehensive view of the immune system upon vaccination, we first investigated the global responses induced by the vaccination in whole blood. Besides influenza vaccine, we also studied the transcriptional changes elicited by non-live

pneumococcal vaccine (Pneumovax23®) in healthy individuals. Furthermore, we studied the kinetics of the immune response to influenza vaccination by analyzing changes in blood transcript abundance at different days and within hours after the vaccine administration. Moreover, we investigated contributions of major immune cell populations to the global responses elicited by influenza vaccination.

Aim2: Study Transcriptional Response of APC Subsets to Influenza Vaccination

a) Establish Transcriptional Signature of Monocyte and DC Subsets at the Steady State

b) Study Transcriptional Responses of APC Subsets Upon Vaccination

Distinct cell populations may play different roles in response to vaccination. Besides monocyte subsets, we expanded our investigation to blood DC subsets. Because of the rarity of certain APCs in the circulation, the overall contribution to the blood transcriptome is very small. Therefore, we isolated APCs from the blood to study their transcriptional profiles. Before we investigated their responses to the vaccination, we first studied their transcriptional signatures in the steady state.

Aim 3: Investigate Correlations between Steady State Transcriptional Signatures of APCs and Serological Response to Vaccination

There is variability in serological response to seasonal influenza vaccination in healthy adults, with some individuals showing very low antibody response. We hypothesized that the baseline transcriptional signature of APCs contributes to this. We sorted APC subsets at baseline, investigated their transcriptomes using RNA-Seq and applied correlation analysis with serology response to influenza vaccination.

CHAPTER THREE

Materials and Methods

Healthy Donors and Samples

A series of studies with healthy adult volunteers were conducted between 2009 and 2012 to collect whole blood or apheresis samples for the study of transcriptional response to influenza vaccination (Table 2). All protocols were approved by the Institutional Review Board at Baylor Research Institute (Dallas, TX).

Table 2. Overview of studies.

Study Title	Whole blood and isolated leukocytes study 2009	Apheresis study 2010	Small blood draw sorted APCs 2012
IRB #	009-179 & 009-282	010-305	011-221
Subjects	Healthy adults (30)	Healthy adults (6)	Healthy adults (26)
Vaccine	2009/10 TIV	2010/11 TIV	2012/13 TIV
Sample	Whole blood (venous and finger stick) and bead isolated leukocytes	Apheresis sample and FACS isolated myeloid APCs	PBMC FACS isolated APCs
Assay	Microarray	RNA-Seq	RNA-Seq

Whole Blood and Isolated Leukocytes Study 2009

Healthy adults, aged 18 to 64 years, were enrolled to receive a single intramuscular dose of 2009 influenza vaccine (Fluzone®, Sanofi Pasteur, PA; Table 3), 23-valent pneumococcal vaccine (Pneumovax23®) or placebo (saline) (n=6 subjects per group). Exclusion criteria were pregnancy, active allergy symptoms, or vaccinations within the previous 2 months. Blood samples were collected by venipuncture at days 0 (prior to vaccination), 1, 3, 7, 10, 14, 21 and 28 (Figure 3). In an independent cohort, capillary blood samples from 6 donors of each treatment were collected in customized

baby tempus tubes via finger stick at hours 0, 1.5, 3, 6, 9, 12, 15, 24, 36, and 48, for whole-genome transcriptional profiling using microarray (Figure 4).

Table 3. Compositions of trivalent inactivated seasonal influenza vaccines.

2009 Fluzone®	2010 Fluzone®	2012 Fluzone®
A/Brisbane/59/2007 (H1N1)	A/California/07/2009 (H1N1)	A/California/07/2009 (H1N1)
A/Uruguay/716/2007 (H3N2) (an A/Brisbane/10/2007-like)	A/Victoria/210/2009 (an A/Perth/16/2009– like virus) (H3N2)	A/Victoria/361/2011 (H3N2)
B/Brisbane/60/2008	B/Brisbane/60/2008	B/Texas/6/2011 (a B/Wisconsin/1/2010-like virus)

In a third, independent cohort, 6 healthy adults received the influenza vaccine. Whole blood samples were collected in Tempus blood RNA tubes (Life Technologies, Carlsbad, CA) at day 0 prior, days 1 and 28 post vaccination. At day 0 and day 1 after vaccination, freshly ficolled PBMC were used for sequential isolation of white blood cell subsets. Neutrophils were first separated from mononuclear cells by Ficoll gradient centrifugation, followed by hypotonic lysis of red blood cells in KHCO_3 and NH_4Cl and finally purified by negative selection by using the EasySep Human Neutrophil Enrichment Kit (StemCell, Vancouver, Canada); monocytes (CD14^+) and T lymphocytes positive for the CD4 and CD8 antigen were sequentially isolated from PBMC using Dynabeads (Invitrogen, Carlsbad, CA) according to the manufacturer's instructions. Blood and isolated leukocytes samples were prepared for microarray analysis (for study design see Figure 6). The purities of neutrophils, CD4^+ and CD8^+ T cells were analyzed using flow cytometry on an LSR II (BD, San Jose, CA). A cocktail of antibodies have been used to identify possible cellular contaminants: CD15-FITC, CD8-PE, HLA-DR-PerCP-Cy5.5 (BD), CD19-ECD (Beckman Coulter, Pasadena, CA), CD123-PC5, CD56-

PC7 (BD), CD16-APC (Invitrogen), CD3-AF700, CD14-APC-Cy7 (BD), CD4-Pacific Blue and CD45-Pacific Orange (Invitrogen). The gating strategy for purity checking was shown in Figure 7.

Apheresis Study 2010

Six healthy adult volunteers, aged 35 to 61 years, were recruited in the study, following the same exclusion and inclusion criteria as in the 2009 flu season study. At day 0, one dose of 2010 Fluzone® (Table 3) was administered intramuscularly to the volunteers. The six volunteers were randomly and evenly divided into two study groups receiving a single body volume leukapheresis either at day 1 or day 3 as early time points and underwent an additional apheresis at steady state, approximately 60 days later. The collection of apheresis products was set to collect mononuclear cells and sample was separated into two parts for the isolation of blood cDC subsets and monocyte subsets.

DC purification. Leukapheresis samples were collected and enriched for dendritic cells by negative depletion of CD3, CD9, CD14, CD16, CD19, CD34, CD56, CD66b and glycoporphin A using magnetic beads with a Human Pan-DC Pre-Enrichment Kit (StemCell Technologies) for dendritic cells. Enriched DCs were stained with the following antibodies: Lin 1-FITC (CD3, CD8, CD14, CD16, CD19, CD20, CD56 and NKp46), CD11c-Pacific Blue, CD303 (BDCA2) -PE (all from BD), CD1c-PE-Cy7 (BioLegend, San Diego, CA), BDCA-3(CD141)-APC (Miltenyi Biotec, San Diego, CA), HLA-DR-Pacific Orange (Invitrogen), and CD2-ECD (Beckman Coulter, CA). cDCs were sorted using flow cytometry by first gating on singlets for exclusion of doublets and then gating on Lin⁻HLA-DR⁺CD11c⁺ cells and further separated by the differential expression of CD1c and CD141 (Figure 9).

Monocyte purification. Monocytes were enriched by negative selection using magnetic beads (Dynabeads® Pan Mouse IgG, Life technologies) and by adding the antibody cocktail including CD19, CD56 and CD66b mAbs (Beckman Coulter, Brea, CA) and Glycophorin A tetramer (StemCell Technologies) in a customized kit. Enriched monocytes were stained with CD14-PE-Cy7 (BioLegend, San Diego, CA), CD16-PE, HLA-DR-Pacific Blue, CD19-APC, CD20-APC, CD56-APC, CD3-APC, CD8-APC and NKp46-APC (all from BD, San Diego, CA). Monocytes were isolated by gating on dump⁻ (CD3, CD8, CD19, CD20, CD56 and NKp46) HLA-DR⁺CD14⁺ monocytes and separated based on CD16 expression into three subsets: CD14⁺CD16⁻, CD14⁺CD16⁺, and CD14^{dim}CD16⁺ monocytes (Cros et al., 2010) (Figure 9). Cells were sorted on a custom BD Fluorescence-activated cell sorting (FACS) Aria II high speed cell sorter. Purified cells were lysed in QIAzol (Qiagen, Valencia, CA) for RNA sequencing analysis.

Small Blood Draw Sorted Myeloid APCs 2012

26 healthy donors were recruited to receive 2012-2013 seasonal influenza vaccine (Fluzone®). A 60 ml blood draw was collected from each individual at day 0 prior to influenza vaccination. 5 million freshly ficolled PBMCs were stained with the following antibodies: Lin-1-FITC, CD66b-FITC, CD8-FITC, CD11c-V450, CD14-APC-H7 (all from BD), CD41-FITC, NKp46 (R&D systems, Minneapolis, MN), HLA-DR-Pacific Orange (Invitrogen), BDCA-2-APC and BDCA3-PE (Miltenyi Biotec, San Diego, CA) and CD62P-FITC and CD1c-PC7 (BioLegend). Serum of healthy donors was also collected at day 0 prior to influenza vaccination and 28 days later for serology (Figure 30). Four cell populations were sorted from the blood samples at day 0 including CD1c⁺

and CD141⁺ cDCs, CD14⁺ monocytes and BDCA2⁺ pDCs for RNA-Seq analysis (Figure 30; Figure 31).

Genome-wide Transcription Analysis

Microarray Assay

Total RNA was either isolated from whole-blood lysate in Tempus tubes (Ovcharenko et al., 2005) followed by depletion of globin messenger RNA (Whitley et al., 2005) or extracted from isolated leukocytes using Qiagen RNeasy® Micro Kit (Qiagen). All samples passing quality control were then amplified and labeled using the Illumina TotalPrep-96 RNA amplification kit. Amplified RNA was hybridized to Illumina HT-12 V3 beadchips (48,803 probes) and scanned on an Illumina Beadstation 500. Illumina's BeadStudio version 2 software was used to generate signal-intensity values from the scans. After background subtraction, the average normalization recommended by BeadStudio 2.0 software (Illumina, San Diego, CA) was used to rescale the difference in overall intensity to the median average intensity for all samples across multiple arrays and chips. For modular analysis, a set of 260 transcriptional modules was used as a pre-existing framework for the analysis of this data set. The approach used for the construction of such framework was previously described by our group (Chaussabel et al., 2008). A modular framework was constructed based on coordinately expressed gene sets from a data-drive process of recapitulating fluctuation in blood transcript abundance measured across a wide range of diseases (Chaussabel et al., 2008). Following the transformation of gene level data into module level activity scores (calculated by proportion of significant transcripts for each module), both unsupervised and supervised analyses of the complete data set were conducted.

RNA-Seq Sample Preparation and Sequencing

Isolated total RNA was run on a NanoDrop 8000 (Thermo Scientific) and a Bioanalyzer 2100 Nano Chip (Agilent Technologies, Inc.) to check RNA quantity and quality. Sequencing libraries for whole transcriptome analysis were prepared using Illumina® TruSeq™ RNA Sample Preparation V2 kit (Illumina, San Diego, CA). Twelve 6-base index sequences were used to prepare barcoded libraries (twelve barcodes per lane) for multiplexing (RNA Adapter Indexes, Illumina). Libraries were quantified using Qubit™ dsDNA HS Assay Kits (Life technology, Carlsbad, CA). The quality of libraries was checked on a 2100 Bioanalyzer using a DNA-1000 chip (Agilent Technologies, Inc.). TruSeq™ PE Cluster Kits v2 (Illumina Inc.) were used for cluster generation on an Illumina cBOT™ instrument following the manufacturer's protocol. Single indexed libraries were loaded into each lane of flow cells. Sequencing was performed on an Illumina HiSeq®2000 instrument (Illumina) by the manufacturer's protocol. Multiplexed paired-end read runs were carried out with a total of 2x50 cycles per run and 7 cycles for the index sequences.

Bioinformatics and Statistics

Background-subtracted microarray data were obtained from Illumina's GenomeStudio software. Expression values less than 10 were set to 10, log (base 2) transformed, and quantile normalized. Microarray derived variables were analyzed by using linear mixed models (LMMs), which included time as a categorical variable with a first-order autoregressive residual covariance matrix. Specific contrasts were used to test for differences between postvaccination and both prevaccination time points. When applicable, differences between the two prevaccination time points were also tested as a

control. A FDR of 0.10 was used to adjust for multiple testing (Benjamini and Hochberg, 1995). The number and proportion of differentially expressed probes (both up and down-regulated) was determined per module and time point comparison. Modules containing a proportion of probes greater than an FDR of 0.10 were considered active at the specified time point and further investigated. Statistical analyses of microarray data was performed by using SAS software (v9.2), JMP (v8), and JMP/Genomics (v4.0) (each from SAS Institute, NC). Heatmaps were generated using GeneSpring (Agilent Technologies, v12.6).

Besides the application of microarray, we also employed RNA-Seq technology to analyze myeloid cell subsets from the 2010-2011 and 2012-2013 influenza seasons. All primary analysis of RNA-Seq was processed using CASAVA pipeline (Illumina, San Diego, CA., v1.8.2). Sequences were aligned with TopHat2 (Kim et al., 2013), duplicates were removed using Picard (picard.sourceforge.net/) and counts were generated using HTSeq (Anders et al., 2014) using the annotations from Gencode V19 (Harrow et al., 2012). Genes identified as globins, rRNAs, and pseudogenes were removed. The alignment files were converted to BAM format by using SAMtools (Li et al., 2009). Differential expression analysis was performed using edgeR (Robinson et al., 2010) and a p-value cutoff of 0.05 and a fold change cutoff of 5 for comparing monocyte and DC subsets at steady state and cutoff of 1.5 for comparing vaccine responses at early time points with steady state for each APC cell subset. Pre-processed data was further analyzed by using GeneSpring (Agilent Technologies). One-way ANOVA with Benjamini Hochberg multiple testing correction was used for comparison of three or more groups. Statistical comparisons between two groups were approached using paired t-test. Heat maps were generated by using hierarchical

clustering with Pearson distance metric and linkage rule as centroid. Downstream regulatory effects and upstream regulator analysis for each APC cell subset at steady state was performed by using Ingenuity Pathway Analysis (Qiagen, Redwood City, CA). Correlation analysis of gene expression at baseline and serological parameters was accomplished by using JMP/Genomics (v7.0) (SAS Institute, NC). GESA (Broad Institute, MA) was also used to analyze baseline transcriptional signatures for 2012 cohort.

Influenza Hemagglutinin Inhibition and Virus Neutralization Assays

All virus strains corresponding to the influenza virus vaccine compositions for the 2009-10, 2010-2011 and 2012-2013 influenza seasons were propagated in 8 day old specific pathogen-free embryonated hen's eggs (Charles River, North Franklin, Connecticut, USA). Hemagglutinin Inhibition (HI) assays were performed as previously described for the detection of neutralizing antibodies (Wang et al., 2006). Briefly, two-fold serial dilutions of human sera were mixed and preincubated in 96-well V-bottom microtiter plates for 30 min at room temperature with the indicated influenza virus vaccine strain. The HI assays were developed by adding 0.5% suspension of turkey red blood cells (Lampire Biological Laboratories, Pipersville, PA) and incubating the assays until the red blood cells pelleted in control wells containing only saline. Neutralizing antibody titers were determined as the reciprocal value of the highest dilution that displayed no hemagglutinating activity. Virus Neutralization Assays (VNA) were

performed with the same influenza virus vaccine strains. To conduct the assay, two-fold dilutions of the serum were mixed with the influenza vaccine virus strains and incubated for 45 min at 37°C. Madin-Darby canine kidney cells (cell line) were added in the virus-antibody mixtures and incubated for 45 min at 37°C. The neutralization titer is expressed as the reciprocal of the highest dilution at which virus infection is blocked (Steel et al., 2009).

CHAPTER FOUR

Results

We first investigated the early innate immune responses to influenza vaccination in whole blood and four major types of leukocytes. Next, we studied the transcriptional profiles of APC subsets at both steady state and early time points after influenza vaccination. Furthermore, we applied correlation analysis of baseline transcriptional profiles of APC subsets with serologic responses to identify the potential predictive transcripts for later vaccination outcomes.

Global Responses of Whole Blood and Responses of Major Cellular Components to Influenza Vaccination

We wanted to investigate the transcriptional response of APCs to the stimulation in vivo by studying immune responses to influenza vaccination. To this end, we first wanted to gain an overview of transcriptional changes in whole blood following influenza vaccination.

The Global Innate Immune Response Peaks at Day 1

First, we investigated the global immune responses to vaccination from whole blood. Besides influenza vaccine, we also included another widely used vaccine, 23-valent pneumococcal vaccine, to learn if there was a difference of immune responses to two vaccines. Pneumovax23® comprises polysaccharide extracts from the 23 most common disease-causing serotypes of *Pneumococcus pneumonia*. Healthy donors were recruited and randomly assigned to three study groups receiving either 2009-2010

seasonal influenza vaccine (Fluzone®), 23-valent pneumococcal vaccine (Pneumovax23®), or saline injection (n= 6 subjects per group) (Figure 3). Blood samples were collected by venipuncture at days 0, 1, 3, 7, 10, 14, 21 and 28 (see methods section). Vaccine responses were assessed through the analysis of global changes in transcript abundance in whole blood samples. A modular repertoire analysis was conducted. Modules were developed based on co-expressed gene sets associated with a particular cell type, biological pathway, or processed from 239 PBMC patient samples with eight different diseases (Chaussabel et al., 2008)(Chaussabel et al., 2008)(Chaussabel et al., 2008)(Chaussabel et al., 2008)(Chaussabel et al., 2008). A module is considered to be „responsive“ to vaccination when the proportion of significant transcripts is greater than what could be expected by chance (FDR = 0.10). Out of 62 modules, 17 and 14 were responsive at day 1 in the influenza vaccine and pneumococcal vaccine groups, respectively. Subsequently, changes in transcripts abundance were detected for a single module at day 7 and day 21 in the influenza vaccine group, and for 3 modules and 1 module at day 7 and day 10 in the pneumococcal vaccine group (Figure 3A). We further mapped responsive modules on a grid for both vaccine groups at day 1 and day 7. We observed the influenza vaccine produced an IFN-inducible transcriptional signature whereas myeloid- and inflammation-related gene transcripts were enriched in pneumococcal vaccine group at day 1 after vaccination. Thus, we observed that the early innate immune responses peak at day 1 followed by a smaller peak at day 7 caused by the adaptive immune responses in both vaccine groups but with different magnitudes of transcriptional responses.

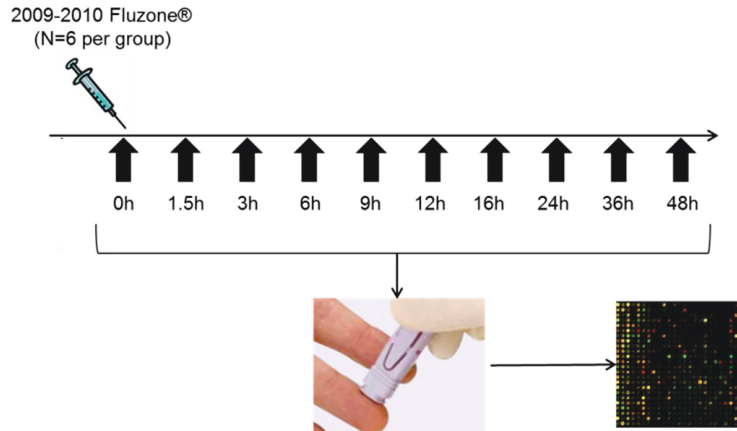


Figure 4. Study design for studying the kinetics of immune responses to influenza vaccination using finger prick sampling during 2009-2010 influenza season.

An Interferon Signature Is Detected at 15 Hours Post-Vaccination in Whole Blood Following Influenza Vaccination

Next, we analyzed finger prick whole blood transcriptome profiles from a second independent cohort using the modular analysis approach to explore the kinetics of early innate responses within hours after vaccination. We collected the capillary blood samples from 6 donors receiving either 2009-2010 seasonal influenza vaccine (Fluzone®) or saline injection prior and after vaccine administration. Finger prick blood samples were collected at hours 0, 1.5, 3, 6, 9, 12, 16, 24, 36, and 48 to study the kinetics of the innate response to vaccination (Figure 4). Collected samples were analyzed for whole genome transcriptional profiling using microarray. For each gene, its expression level was normalized to the baseline values. We calculated the average fold changes of genes within a module. IFN-inducible modules were found to be up-regulated at early time points post administration of influenza vaccine. We discovered significant changes of IFN-inducible modules 1.2, 3.4 and 5.12 as early as 15 hr following influenza vaccine injection and persisting to 48 hr post vaccination (M1.2 and M3.4) (Figure 5).

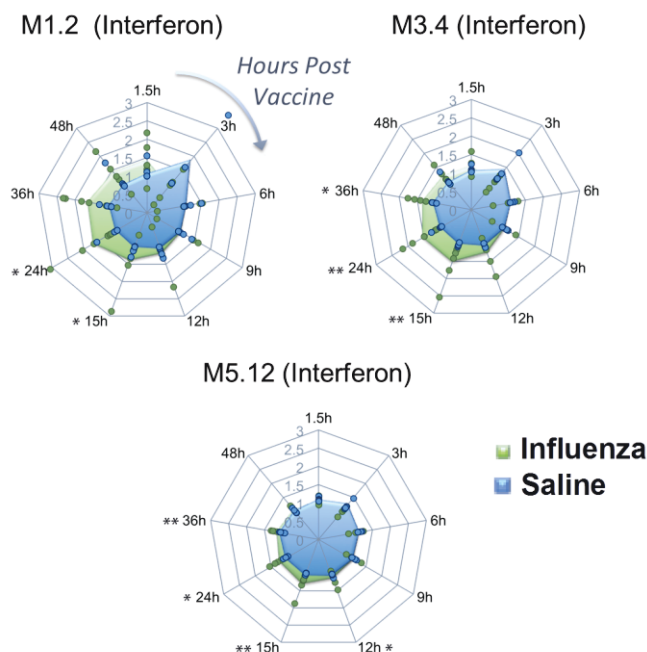


Figure 5. Profiling the interferon response within the first 48 hr following vaccination. Spider plot shows the average fold changes of genes forming module 1.2, 3.4 and 5.12 (IFN-inducible gene modules) at multiple consecutive time points for the influenza vaccine comparing with saline control groups. The dots represented the fold change at different time points post vaccination as compared the baseline from individual donors. The filled regions represented the average fold change within either influenza vaccine or saline group. * $p < 0.05$; ** $p < 0.01$.

Neutrophils and Monocytes Show IFN Signature at Day 1 Post Influenza Vaccination

To validate the observation of IFN signature made from finger prick study, we collected venous blood samples from healthy subjects ($n=6$) at day 0, 1, and 28 in a third, independent cohort. To deconvolve these data and identify the cellular origin of the IFN signature observed in the whole blood of healthy subjects following the administration of vaccines, we purified four populations of leukocytes. We isolated neutrophils, monocytes, and $CD4^+$ and $CD8^+$ T cells from the blood of the same donors before and 24 hr after the administration of the influenza vaccine (48 samples in total) (Figure 6). After removal of enrichment beads, purities of all isolate leukocytes except $CD14^+$ monocytes were checked by flow cytometry. Bead detachment was not possible for the removal of

CD14⁺ enrichment beads (gating strategy shown in Figure 7). The average purities of isolated cell populations were all above 90% (Table 4)

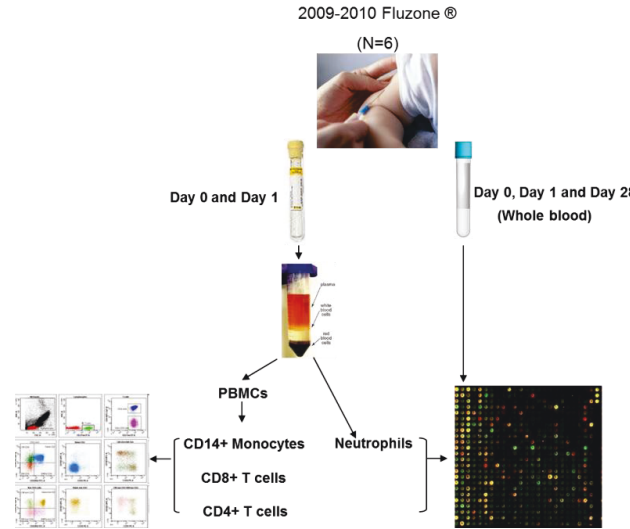


Figure 6. Deconvolution of whole blood signatures elicited by influenza vaccination. Neutrophils, monocytes, CD4⁺ T cells and CD8⁺ cells were isolated 24 hours post influenza vaccinations from healthy donors' venous blood. Whole transcriptome profiling using microarray was performed on isolated cells

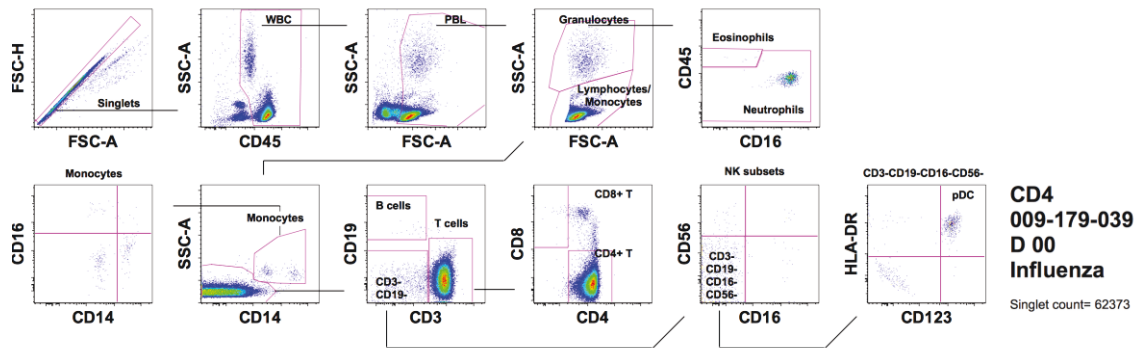


Figure 7. The purity gating strategy of purified CD4⁺ T cells in 2009 isolated leukocytes study. 1 of 12 experiments is shown.

Table 4. The purity of isolated leukocytes assessed by flow cytometry.

Purity	Neutrophils	CD4 ⁺ T cells	CD8 ⁺ T cells
Purity average	99.4	95.6	90.4
Purity min	96.5	92.6	81.9
Purity max	100.0	98.2	96.7

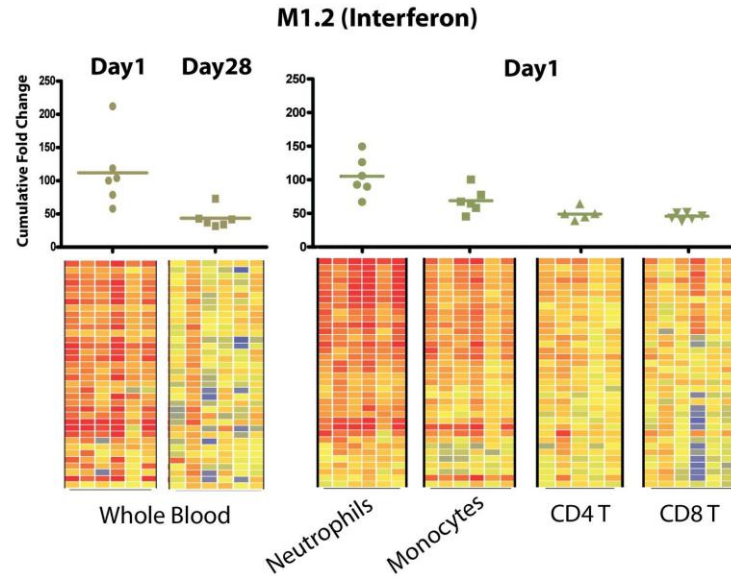


Figure 8. IFN responses in whole blood and isolated leukocyte populations from healthy donors. Cumulative fold changes normalized to baseline day 0 for each gene within module 1.2 were calculated and plotted for each donor from blood and isolated leukocyte samples (upper panel). The up-regulation of genes from module 1.2 was also visualized using heat maps (lower panel).

First, we validated previous observations from finger prick study in venous blood samples. We analyzed expression levels of genes forming interferon annotated module M1.2 from whole blood samples. For each donor, gene expression values at day 1 were normalized to their corresponding baseline value. Cumulative fold changes were calculated for each gene within module 1.2. Our analysis shows that the gene expression level of IFN-inducible genes was elevated on day 1 and diminished by day 28 when compared with baseline day 0 (Figure 8). Next, we analyzed the IFN signature from isolated leukocytes after influenza vaccination. The analysis revealed differences in the expression levels for IFN-inducible transcripts in neutrophils and monocytes following influenza vaccination while CD4⁺ and CD8⁺ cells showed only a mild IFN signature (Figure 8). To summarize, a systems immunology approach was employed to investigate immune responses to influenza and pneumococcal vaccines. These two non-live vaccines

showed different quality of transcriptional responses at early time points after vaccination. The innate response, measured within hours in the peripheral blood, was dominated by an interferon transcriptional signature after influenza vaccination. We discovered this interferon signature in the blood was dominated by gene expression change in by neutrophils and monocytes.

Transcriptional Profiles of Monocytes and Dendritic Cell Subsets in the Steady State and Upon Influenza Vaccination

To understand the contributions of APCs in immune responses to vaccination, we first needed to characterize those cells in the steady state. Both monocytes and DCs comprise heterogeneous populations. We employed RNA-Seq technology and established the transcriptional profiles of distinct subsets of monocytes, cDCs and pDCs at the steady state.

Transcriptional Profiles of Human Monocyte and DC Subsets at Steady State

Seven monocyte and DC subsets from 6 healthy volunteers at the steady state were investigated in the 2010 apheresis study (Table 5). $CD14^+CD16^-$, $CD14^+CD16^+$ and $CD14^{dim}CD16^+$ monocytes; $CD1c^+$ and $CD141^+$ cDCs; and $CD2^+$ and $CD2^-$ pDCs were isolated by FACS (Figure 9). Monocytes were isolated by gating on dump channel⁻ $HLA-DR^+$ population and separated based on CD14 and CD16 expression into three subsets: $CD14^+CD16^-$, $CD14^+CD16^+$, and $CD14^{dim}CD16^+$ monocytes (Figure 9A). A similar approach was taken for sorting DCs. CD11c expression is found on cDCs and monocytes while BDCA2 is exclusively expressed on pDCs. $CD11c^{high}$ cells were gated and further separated into $CD1c^+$ and $CD141^+$ cDC subsets. $BDCA2^{high}$ cells were gated and CD2 was used to further separate pDCs into two subsets (Figure 9B). After the sort,

we reran the FACS for the purified cells to check the purity. The purities of sorted monocyte and DC subpopulations were $\geq 95\%$ (Table 6).

Table 5. Demographic information of six healthy volunteers in 2010 apheresis study.

Donor ID	Age (yr)	Gender	Race	Ethnicity
1005	48	Female	African American	Not Latino
1006	43	Female	Caucasian	Latino
1014	61	Male	Caucasian	Not Latino
1008	48	Female	Caucasian	Not Latino
1009	56	Male	Caucasian	Not Latino
1010	35	Male	Caucasian	Not Latino

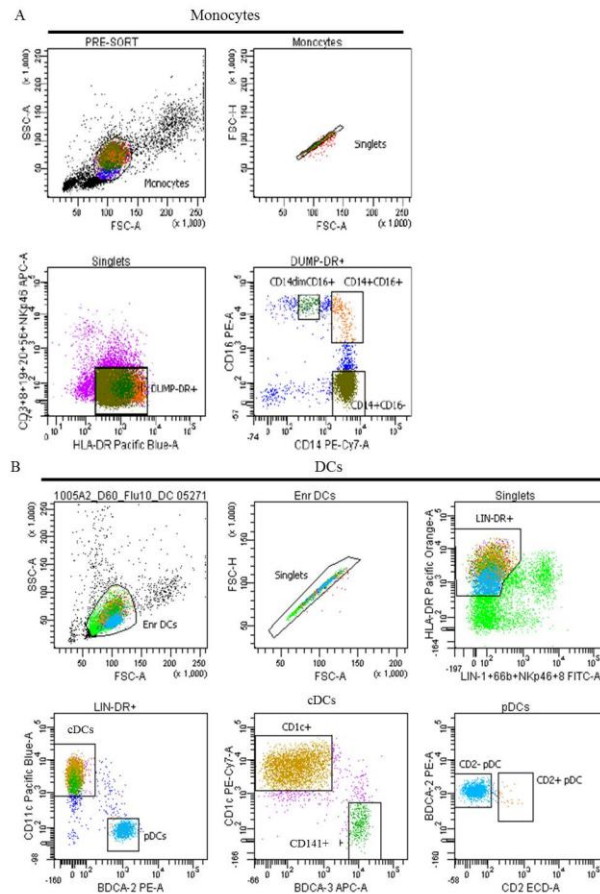


Figure 9. Human monocyte and DC subsets in the blood. Monocytes were isolated by gating on dump⁻ HLA-DR⁺CD14⁺ monocytes and separated based on CD16 expression into three subsets. Enriched human blood DCs were gated on Lin⁻HLA-DR⁺ cells and further separated into cDCs and pDCs by differential expression of CD11c and BDCA2. cDCs were further divided into two subsets using CD11c and CD141. pDCs were further separated into two subsets by differential expression of CD2. 1 representative example of 12 sorting experiments is shown.

Table 6. Purity of sorted myeloid cell populations.

Donors	Cell subsets	Purity (%)		
		Day 1	Day 3	Day 60
1005	CD14 ⁺ CD16 ⁻ monocytes	100		100
	CD14 ⁺ CD16 ⁺ monocytes	99.6		99
	CD14 ^{dim} CD16 ⁺ monocytes	100		99.4
	CD1c ⁺ cDCs	98.7		100
	CD141 ⁺ cDCs	100		100
	CD2 ⁺ pDCs	99.5		99
	CD2 ⁻ pDCs	99		99.7
1006	CD14 ⁺ CD16 ⁻ monocytes	100		99.8
	CD14 ⁺ CD16 ⁺ monocytes	98.8		99.5
	CD14 ^{dim} CD16 ⁺ monocytes	99.8		100
	CD1c ⁺ cDCs	100		100
	CD141 ⁺ cDCs	100		99.7
	CD2 ⁺ pDCs	100		99.7
	CD2 ⁻ pDCs	99.6		100
1014	CD14 ⁺ CD16 ⁻ monocytes	99.6		100
	CD14 ⁺ CD16 ⁺ monocytes	98.3		99.1
	CD14 ^{dim} CD16 ⁺ monocytes	99.8		99.8
	CD1c ⁺ cDCs	100		100
	CD141 ⁺ cDCs	100		100
	CD2 ⁺ pDCs	99.4		100
	CD2 ⁻ pDCs	100		100
1008	CD14 ⁺ CD16 ⁻ monocytes		100	100
	CD14 ⁺ CD16 ⁺ monocytes		99.3	98.6
	CD14 ^{dim} CD16 ⁺ monocytes		99.8	99.2
	CD1c ⁺ cDCs		100	100
	CD141 ⁺ cDCs		99.4	98.4
	CD2 ⁺ pDCs		96.5	99.6
	CD2 ⁻ pDCs		99.6	100
1009	CD14 ⁺ CD16 ⁻ monocytes		99.9	100
	CD14 ⁺ CD16 ⁺ monocytes		100	95.5
	CD14 ^{dim} CD16 ⁺ monocytes		99.6	99.7
	CD1c ⁺ cDCs		100	100
	CD141 ⁺ cDCs		100	99.2
	CD2 ⁺ pDCs		100	98.9
	CD2 ⁻ pDCs		100	100
1010	CD14 ⁺ CD16 ⁻ monocytes		99.9	100
	CD14 ⁺ CD16 ⁺ monocytes		98.8	99.8
	CD14 ^{dim} CD16 ⁺ monocytes		99.3	99.8
	CD1c ⁺ cDCs		99.2	100
	CD141 ⁺ cDCs		100	100
	CD2 ⁺ pDCs		100	99.2
	CD2 ⁻ pDCs		99.8	100

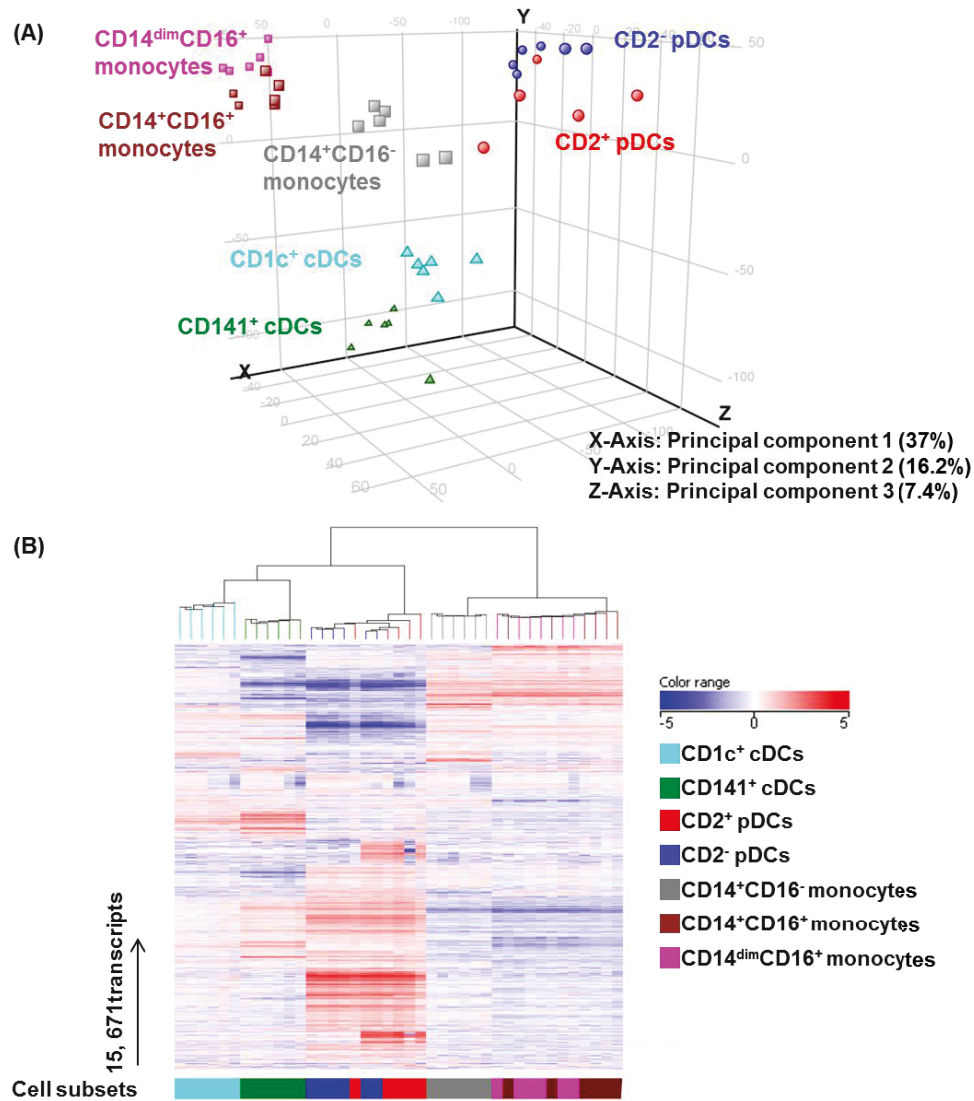


Figure 10. Unsupervised clustering analysis of human monocyte and DC subsets at steady state (day 60). Gene expression profiles of purified blood CD1c⁺ and CD141⁺ cDCs, BDCA2⁺CD2⁺ and BDCA2⁺CD2⁻ pDCs, and blood CD14⁺CD16⁻, CD14⁺CD16⁺ and CD14^{dim}CD16⁺ monocytes from 6 healthy donors at steady state were analyzed by RNA sequencing. (A) Principal component analysis of gene expression by different cell subsets. Principal component 1, 2 and 3 were selected as the axes explaining most of the data variance. (B) Hierarchical clustering of different monocyte and DC subsets. 15,671 highly expressed genes were selected with raw counts greater or equal to 30 in at least one sample.

Total RNA of sorted cells was extracted for RNA-Seq analysis (Figure 10A and B). First, we ran principal component analysis (PCA). PCA is a mathematical algorithm reducing the number of variables while retaining the variability in the data (Ringner,

2008). PCA three-dimensional scatter plot represented the differential gene expression patterns of DC and monocyte subsets. Three axes represented three principal components with a variance of 37%, 16.2% and 7.4%, respectively. In the PCA, CD1c⁺ cDCs, CD141⁺ cDCs and CD14⁺CD16⁻ monocytes clustered independently. CD14⁺CD16⁺ and CD14^{dim}CD16⁺ monocytes were grouped closer to each other compared to other cell subpopulations. CD2⁺ and CD2⁻ pDCs also clustered closer together compared to the other cell subsets (Figure 10A). 15,671 genes with raw counts ≥ 30 in at least one sample were identified as highly expressed genes. Hierarchical clustering unsupervised analysis was performed to analyze the clustering of different monocyte and DC subsets in the steady state using Pearson distance metric and centroid linkage rule. The read counts per million of highly expressed genes were log₂ transformed (LogCPM) and plotted on a heat map. Four blood DC subsets and three monocyte subsets were segregated in independent clusters. Among three monocyte subsets, CD14⁺CD16⁺ and CD14^{dim}CD16⁺ monocytes were closer to each other compared with CD14⁺CD16⁻ monocytes (Figure 10B). cDC and pDC subsets were segregated into two subgroups. Two subsets of cDCs clustered separately while two subsets of pDCs were close to each other (Figure 10B). This finding further confirmed the result from PCA.

In order to have an overview of similarities of all investigated APC subsets, we used a correlation matrix (Pearson correlation) to describe the relationships across all the subsets. Each square represented the correlation between any two APC subsets in the steady state (Figure 11). Correlation analysis led to similar conclusions given by PCA and hierarchical clustering analysis.

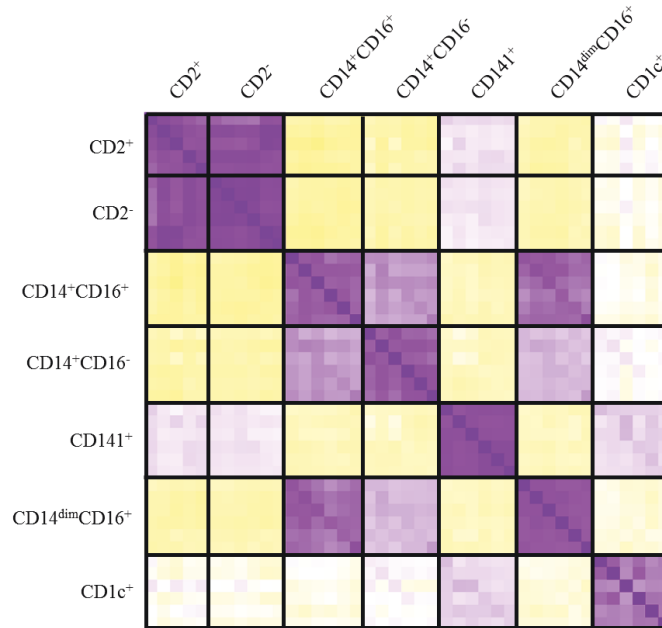


Figure 11. Distances of distinct APCs subsets. Correlation plot displays the correlation coefficient for each pair of samples. Black vertical and horizontal lines delineate myeloid cell subpopulations.

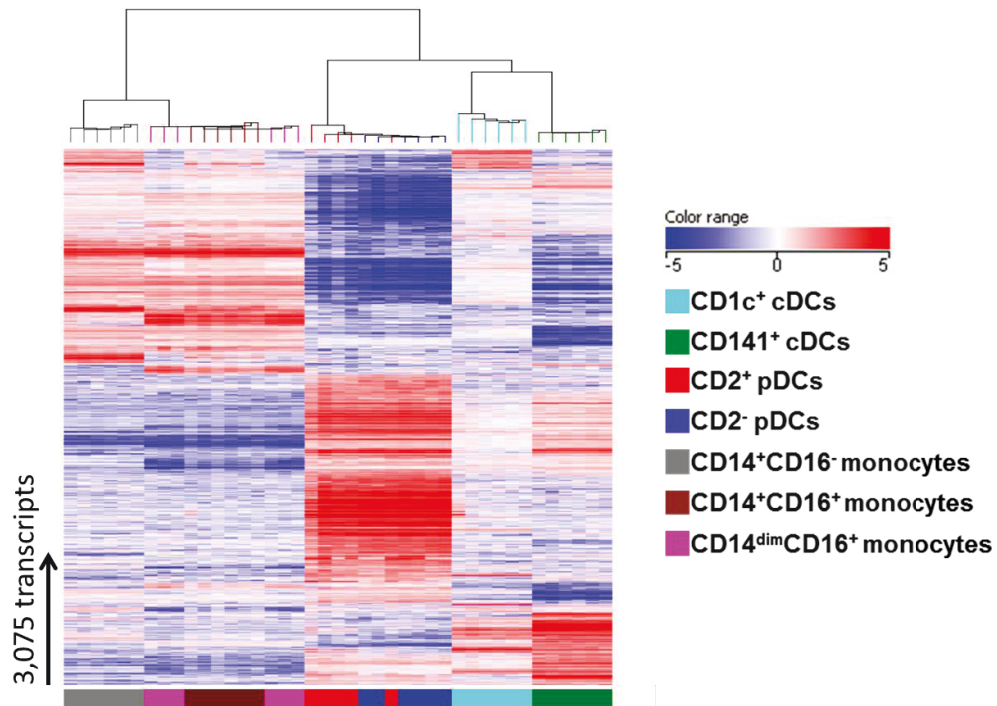


Figure 12. Differentially expressed genes in human monocyte and DC subsets at steady state. Transcripts with significant differential abundance were selected based on ANOVA test with stringent FRD=0.0001 and a 10 fold-change difference.

Next, we investigated the top differentially expressed genes (DEGs) that were most representative for the differences in human APC subsets. 3, 075 transcripts were identified using ANOVA test, which compares three or more groups simultaneously (Figure 12). Among those significant DEGs, we found the surface markers that we used for sorting cells and other known markers specific for monocyte and DC subsets as reported in the literature. All myeloid APC subsets expressed CD11c, but at different expression levels: highest in CD1c⁺ cDCs and CD16⁺ monocytes, followed by

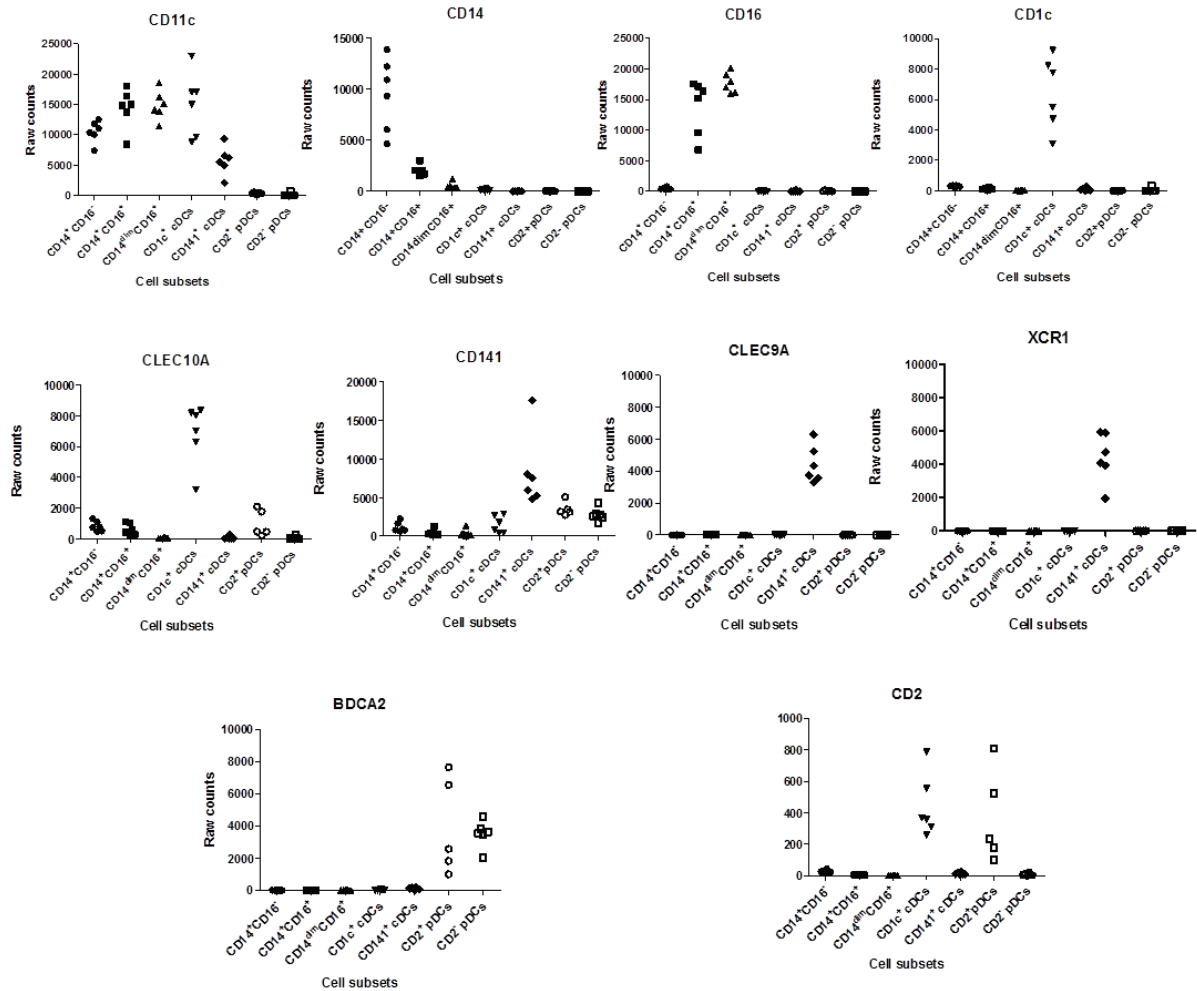


Figure 13. mRNA expression of surface markers in monocyte and DC subsets at steady state. Expression of mRNA encoding CD11c, CD14, CD16, CD1c, CLEC10A (DC-ASGPR), CD141, CLEC9A, XCR1, BDCA2 and CD2.

CD14⁺CD16⁻ monocytes and lowest in CD141⁺ cDCs (Figure 13). CLEC10A (DC-ASGRP) was found to be highly expressed in CD1c⁺ cDC subset and also expressed in monocytes and CD2⁺ pDCs but at a lower level. We further confirmed this observation on the protein level. Only CD1c⁺ cDCs but not CD141⁺ cDCs or pDCs express CLEC10A on the surface (Figure 14). The gene expression levels of CD14, CD16, CD1c, CD141, BDCA2 and CD2 confirmed the identity of sorted cell subsets. Finally, CLEC9A and XCR1 were highly expressed in CD141⁺ cDCs (Figure 13) as reported previously (Haniffa et al., 2012). Together, both unbiased clustering and supervised ANOVA analysis demonstrated the differences in transcriptional profiles of blood APC subsets.

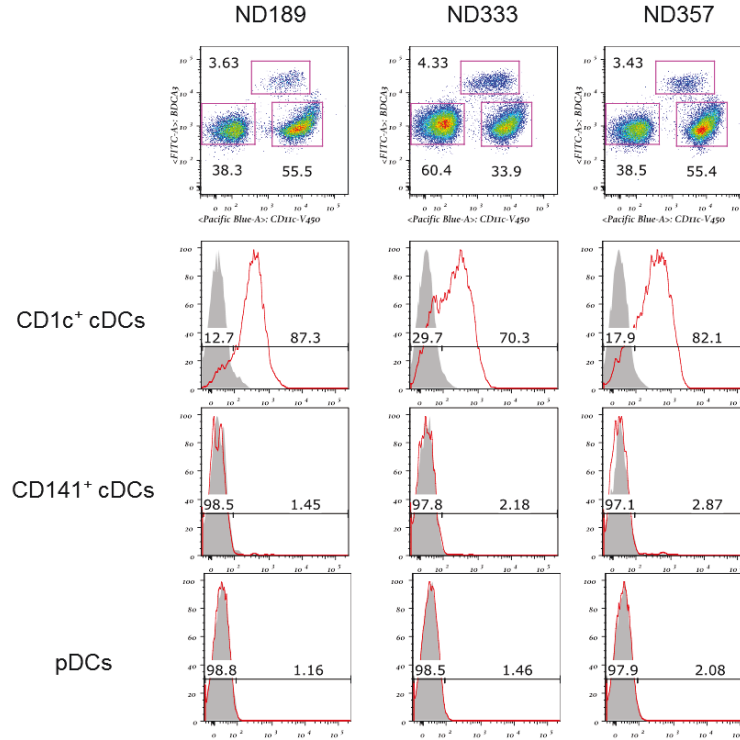


Figure 14. CLEC10A expression on DC subsets. CLEC10A (DC-ASGRP) staining was analyzed in three healthy donors.

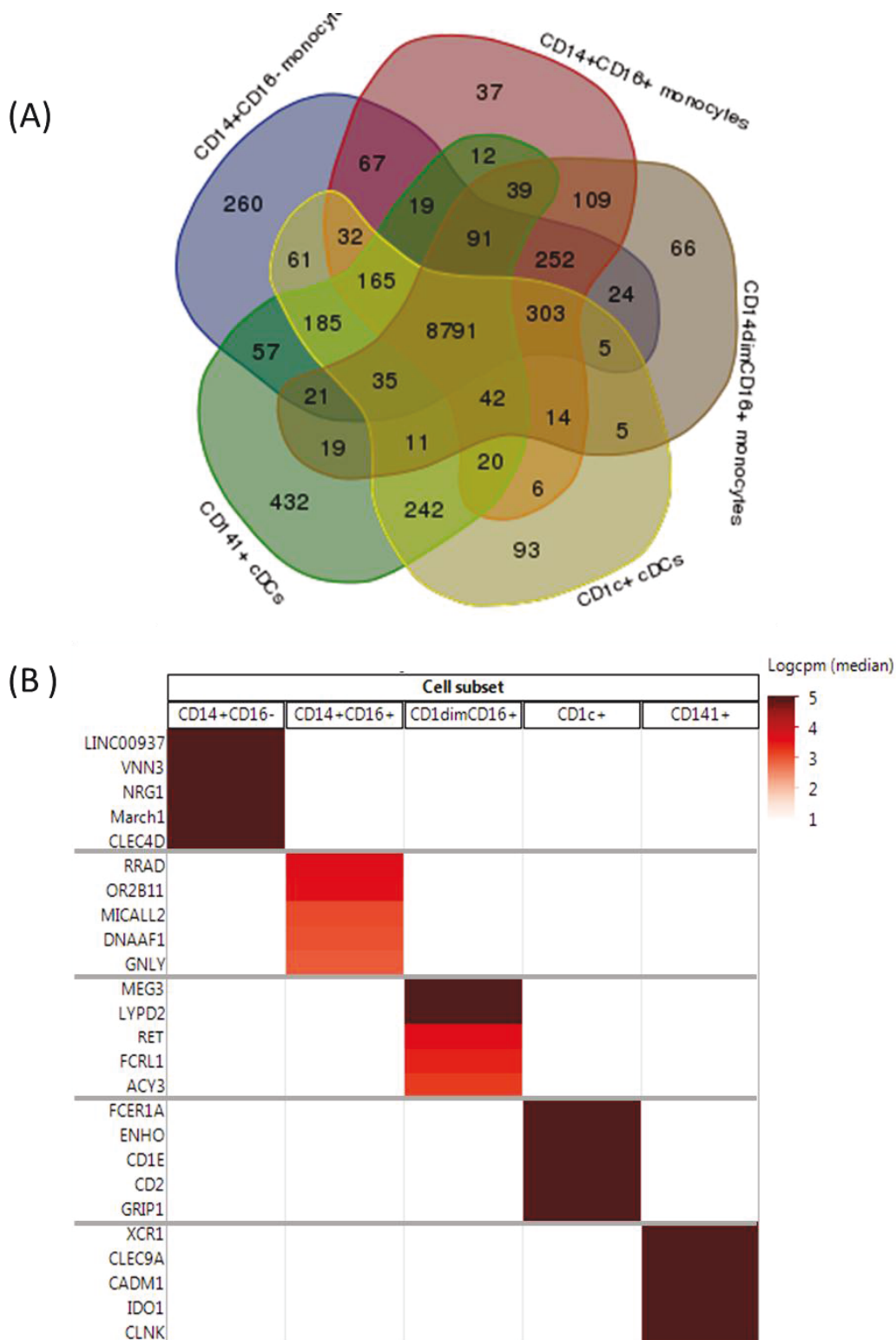


Figure 15. Common and unique gene signatures characterized in monocytes, CD1c+ and CD141+ DCs. (A) Venn diagram shows genes commonly and uniquely expressed by each monocyte and cDC subset. (B) Top expressed unique genes in each APC subset. Top 5 unique transcripts with highest abundance were selected for each cell subpopulation. Raw counts were normalized to \log_2 transformed counts per million (logcpm) and presented into a heatmap.

Common and Unique Transcriptional Signatures in Myeloid APC Subsets

As discussed above, monocytes are the circulating precursors of DCs in vivo (Auffray et al., 2009). To understand their relationships on the molecular level, we first analyzed the transcriptional signature in monocyte, CD1c⁺ and CD141⁺ cDC subsets at the steady state. We identified their common and unique transcripts by overlapping highly expressed genes with raw counts ≥ 30 in at least 80% of donors for each subset using a venn diagram (Figure 15A). 8,791 transcripts were found commonly expressed in all monocyte and cDC subsets which formed the core gene set of myeloid APCs. Subsequently, unique transcripts were identified for each APC subsets: 260 transcripts in CD14⁺CD16⁻ monocytes, 37 transcripts in CD14⁺CD16⁺ monocytes, 66 transcripts in CD14^{dim}CD16⁺ monocytes, 93 transcripts in CD1c⁺ cDCs and 432 transcripts in CD141⁺ cDCs. We further analyzed the top five unique genes with highest expression levels (logcpm) in each cell subset. Significant enrichment of Linc00937 (lincRNA), CLEC4D (C-type lectin), March1 (E3 ubiquitin-protein ligase), VNN3 (amidohydrolase) and NRG1(neuregulin) was found in CD14⁺CD16⁻ monocytes (Figure 16B). We also identified uniquely expressed genes in CD14⁺CD16⁺ monocytes including RRAD (calmodulin binding and GTP binding), OR2B11 (olfactory receptors), MICALL2 (cell adherence; regulates E-cadherin), DNAAF1 (Cilium-specific), and GNLY (granulysin) (Figure 16B). Top unique transcripts in CD14^{dim}CD16⁺ monocytes were identified comprising RET (Receptor Tyrosine Kinase), FCRL1 (Immunoglobulin superfamily), MEG3 (lincRNA), LYPD2 (LY6/PLAUR domain containing 2) and ACY3 (acylase) (Figure 16B). Furthermore, top unique transcripts in CD1c⁺ cDCs including Fc receptor FCER1A, CD1E (antigen presentation; DC maturation), CD2 (LFA-3 receptor), ENHO (glucose homeostasis), and GRIP1 (Glutamate Receptor-Interacting) (Figure 16B). Finally,

we analyzed the top unique transcripts in CD141⁺ cDCs. Besides previously identified markers XCR1 and CLEC9A (Bachem et al., 2010; Haniffa et al., 2012), we also found CADM1 (cell adhesion molecule), IDO1 (indoleamine 2, 3-dioxygenase 1) and CLNK (immunoreceptor signaling) to be significantly enriched (Figure 16B).

Common and Unique Transcriptional Signatures in Monocyte Subsets

Next, we wanted to focus on the transcriptional programs in monocyte subsets. We first identified the common and unique transcripts for all the monocyte subsets in the steady state by overlapping highly expressed genes (same definition as above) for each subset using a venn diagram (Figure 16A). 9,437 transcripts constitute the core gene set of monocytes which were abundant in all three subsets. In addition, 563 transcripts were identified as unique genes in CD14⁺CD16⁻ monocytes identified as unique genes for CD14⁺CD16⁺ and CD14^{dim}CD16⁺ monocytes, respectively (Figure 16A). In order to capture the most representative features in each monocyte subset, we identified top 10 unique transcripts with highest abundance (logcpm) for each subset (Figure 16B). Beside previously identified unique markers in myeloid APCs, CD14⁺CD16⁻ monocytes also uniquely expressed high levels of CCR2 (chemokine receptor), ADAM19 (disintegrin and metalloprotease-family; DC maturation marker), CES1(carboxylesterase), ALOX5AP (Lipoxygenases activating protein), and STEAP4 (TNF α –induced protein) (Figure 16B). We also identified additional uniquely expressed genes in CD14⁺CD16⁺ monocytes mainly including LYPD3 (LY6/PLAUR domain containing 3), GFRA2 (Neurturin Receptor Alpha), and ADRA2B (Adrenergic Receptor) (Figure 16B). Finally, additional top unique transcripts in CD14^{dim}CD16⁺ monocytes comprised RP11-1008C21.1 (lincRNA) and other function genes of unknown function (Figure 16B).

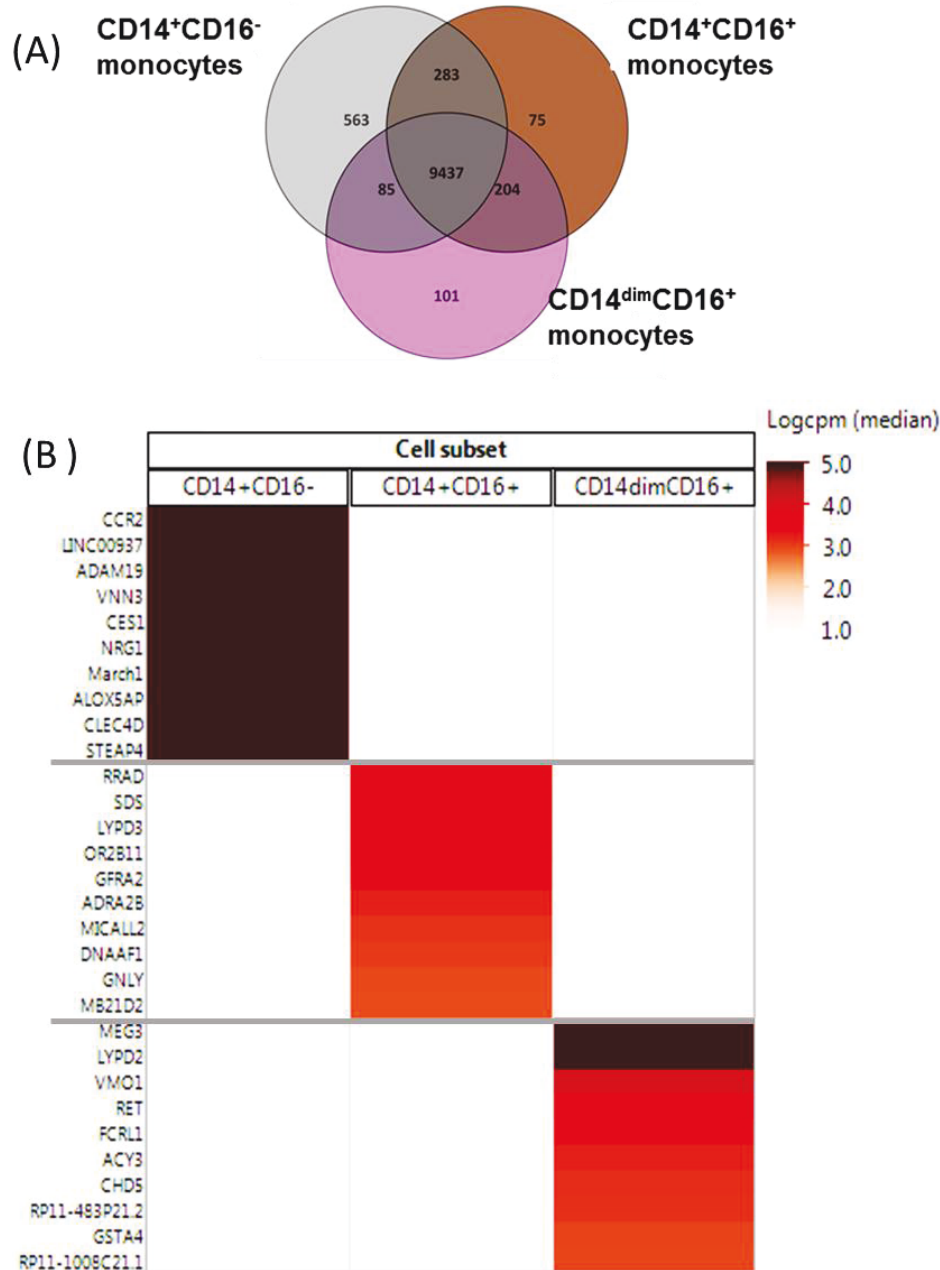


Figure 16. Common and unique gene signatures characterized in distinct monocyte subsets. A) Venn diagram shows genes commonly and uniquely expressed by each monocyte subset. (B) Top expressed unique genes in each monocyte subset. Top 10 unique transcripts with highest abundance were selected for each monocyte subsets. Raw counts were normalized to log₂ transformed counts per million (logcpm) and presented into a heatmap.

To gain insights on monocyte subset gene regulation, we also analyzed the expression of known transcription factors (TFs) (Vaquerizas et al., 2009). We further

explored different family molecules using GO by which is widely recognized as the premier tool for the functional annotation of molecular aspects of cellular systems (Lovering et al., 2008). We focused on the major biological roles of APCs and analyzed the gene expression of pathogen recognition receptors (PRRs) (GO: 0002221), Ag processing and presentation (GO: 0019882), inflammasomes (GO: 0044546, GO: 0072557, GO:0072558, GO:0072559, GO:0097169, GO:1900225, GO:1900226 and GO:1900227) and chemotaxis (GO:0006935) in three monocyte subsets. An ANOVA test (FDR=0.05) with Benjamini Hochberg multiple testing correction and a fold change $\geq 5x$ was applied to the selected family molecules. Among the transcription factors, RNASE2, ID1 and CD36 were over-expressed in CD14⁺CD16⁻ monocytes. BATF3 and E2F1 were over-expressed in CD14^{dim}CD16⁺ monocytes. CD14⁺CD16⁻ monocytes showed upregulation of genes including CD1 family molecules, CD36 and FCGR1A involved in antigen processing and presentation while there were very few such transcripts overexpressed in intermediate and non-classical monocytes. Among the pathogen recognition receptors, CD14⁺CD16⁻ monocytes were found to over-express CD14, CD36, ITGAM (CD11B), and SCARB1 while DUSP4 and IRAK2 were found to be over abundant in CD14⁺CD16⁺ monocytes. CD14⁺CD16⁻ monocytes and CD14^{dim}CD16⁺ monocytes have comparable numbers of over-expressed chemotaxis genes (Figure 17). The expression of inflammasome genes was found to be similar in three monocyte subsets (data not shown).

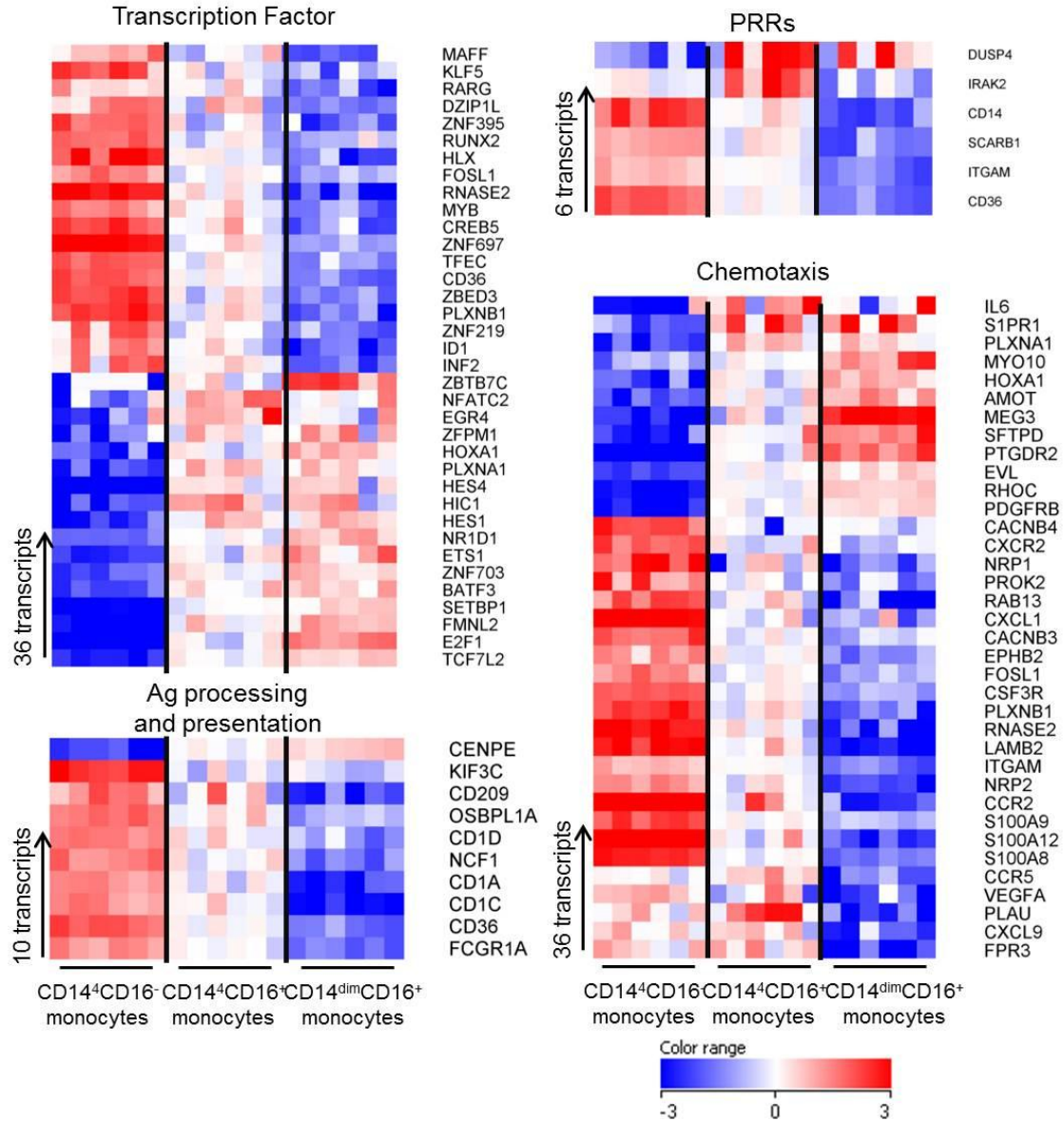


Figure 17. Human blood monocyte subsets show differences in transcriptomic signatures at the steady state. Heat maps representing relative gene expression of transcriptional factors, antigen processing and presentation, pathogen recognition receptors (PRRs), and chemotaxis. Paired t-test (FDR=0.05) with Benjamini Hochberg multiple testing correction plus a 5-fold change. Each gene expression was normalized to the median of all samples from monocytes.

Common and Unique Transcriptional Signatures in DC Subsets

The similar analysis approach to that employed above was also used to study DC subsets in the steady state. We investigated their transcriptional features by comparing two cDC subsets and two pDC subsets, respectively.

Two subsets of cDCs. We first identified common and unique genes expressed by each cDC subset. The core gene set of cDCs comprised 9,491 transcripts (Figure 18A). 519 and 690 genes were identified as uniquely expressed genes for CD1c⁺ and CD141⁺ cDCs, respectively (Figure 18A). Abundant unique genes in CD1c⁺ cDCs included FCER1A and FCGR2C of Fc receptors, CLEC10A, CD1D (antigen-presenting glycoprotein), transcriptional factor ZEB2, SIRPA (ligand of CD47), CD163 (macrophage-associated antigen), and CD300E (surface protein on myeloid cells). Subsequently, we determined top unique transcripts significantly enriched in CD141⁺ cDCs including previously introduced XCR1 and CLEC9A, CADM1 (cell adhesion molecule), IDO1 (indoleamine 2, 3-dioxygenase 1), TACSTD2 (an EpCAM-like molecule) and DBN1 (drebrin) (Figure 18B). Furthermore, we addressed the extent of differential gene expression between cDC subsets and pDC subsets pre-selected family molecules. We first analyzed the expression of transcription factors (TFs) in two cDC subsets. IRF4, PRDM1 and RNASE2 were highly expressed in CD1c⁺ cDCs while IRF8 and BATF3 were found to be over abundant in CD141⁺ cDCs (Figure 19). CD1c⁺ cDCs were found to over-express genes related to pathogen recognition except RAB33A and MHC class II molecule, HLA-DOB, which were more abundant in CD141⁺ cDCs. As for inflammasome related molecules, AIM2 was over-expressed in CD141⁺ cDCs while CAPS1 and 5 were highly expressed in CD1c⁺ cDCs. Finally, significant enrichment for genes related to chemotaxis was found in CD1c⁺ cDCs (Figure 19).

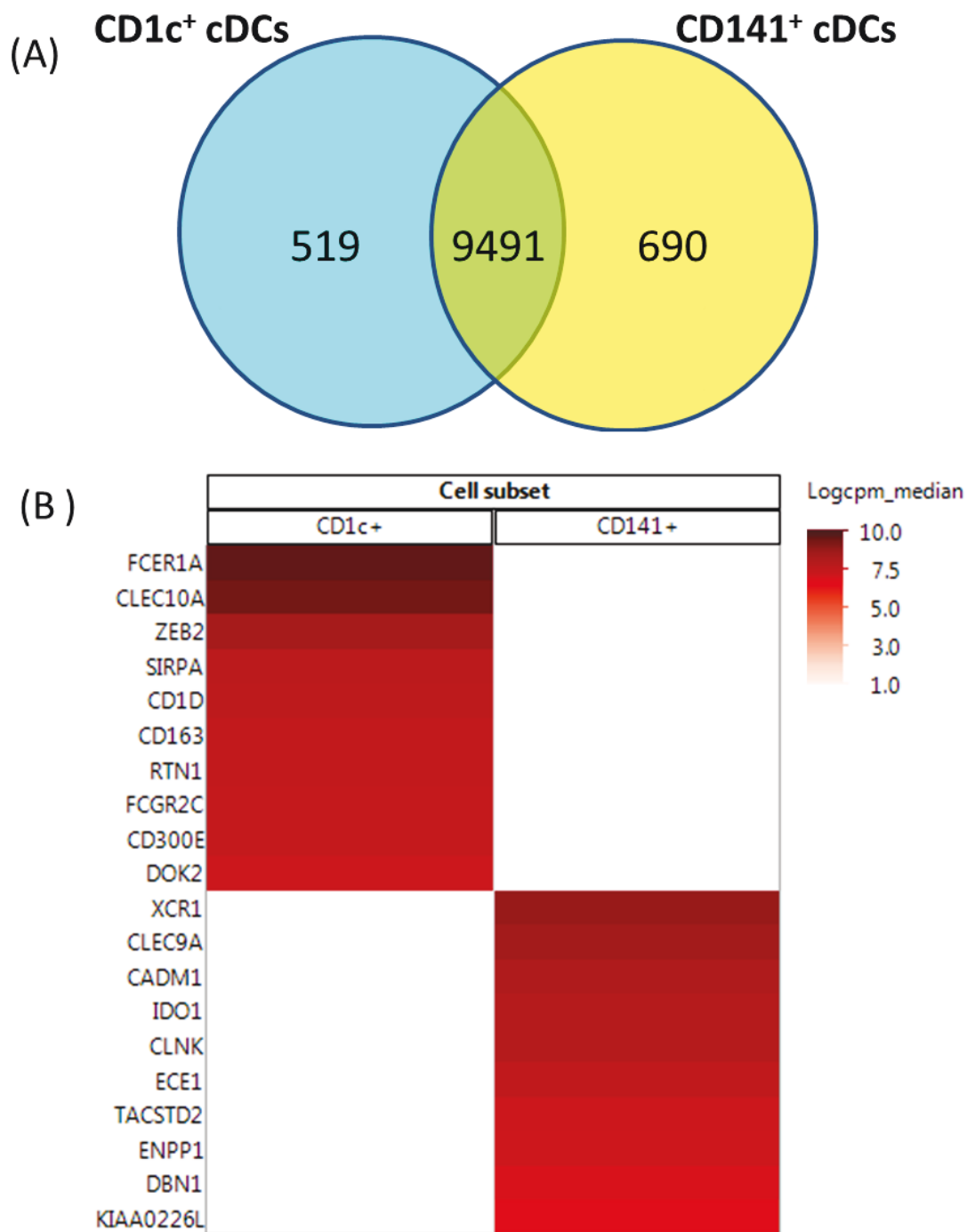


Figure 18. Common and unique gene signatures characterized in two cDC subsets. A) Venn diagram shows genes commonly and uniquely expressed by each cDC subset. (B) Top expressed unique genes with highest abundance in each cDC subset. Top 10 unique transcripts were selected based on expression levels. Raw counts were normalized to log₂ transformed counts per million (logcpm) and presented into a heatmap.

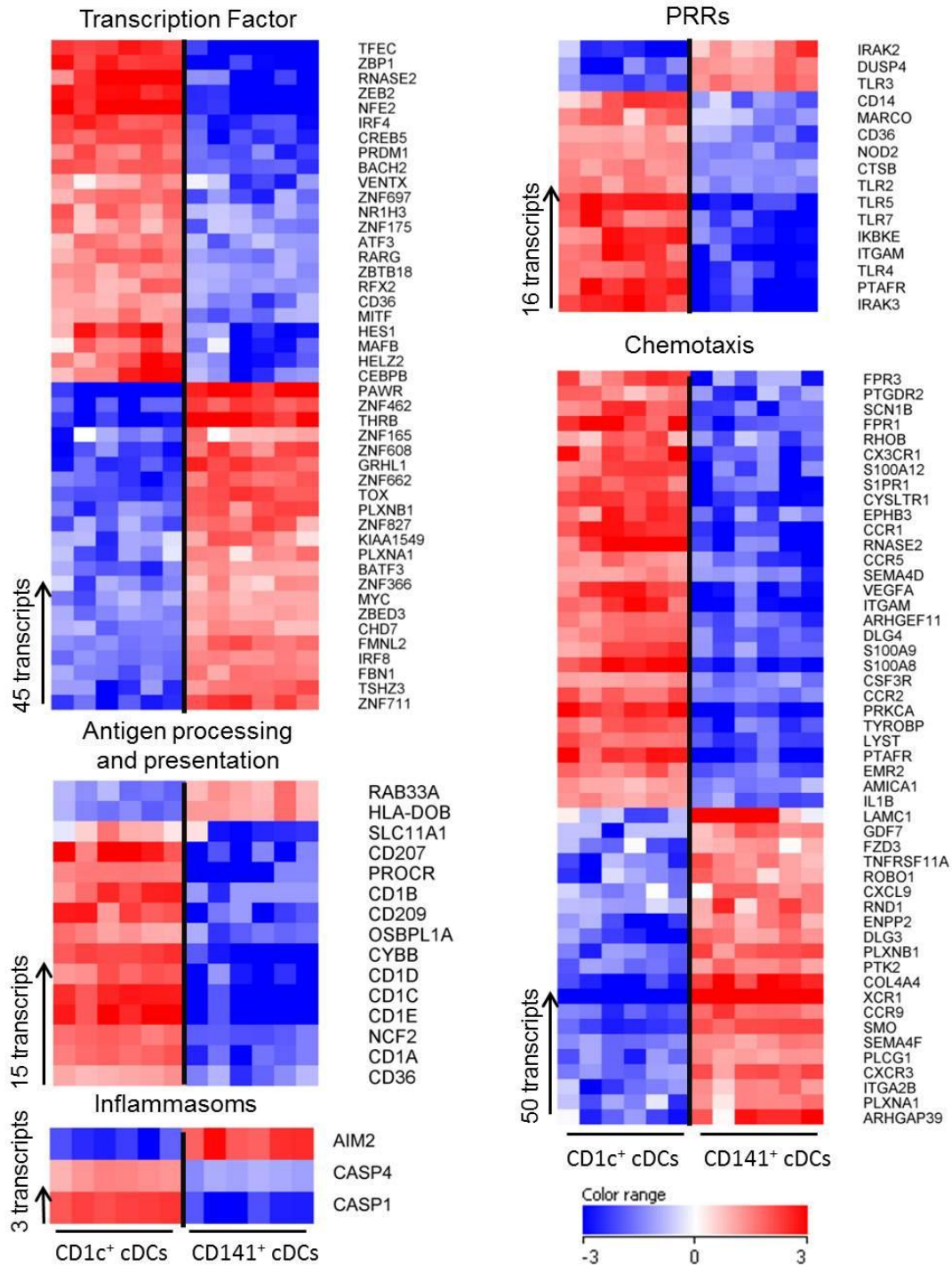


Figure 19. Human blood cDC subsets show different transcriptomic signatures at the steady state. Heat maps representing relative gene expression of transcriptional factors, antigen processing and presentation, pathogen recognition receptors (PRRs), inflammasomes and chemotaxis. Paired t-test (FDR=0.05) with Benjamini Hochberg multiple testing correction plus a 5-fold change. Each gene expression was normalized to the median of all samples from cDCs.

Two subsets of pDC. Finally, we compared transcriptional profiles of two pDC subsets. We first determined commonly and uniquely expressed genes for each pDC subsets (Figure 20A). 10,229 transcripts were identified as core genes of pDC subsets. 219 and 597 transcripts were selected as unique genes for CD2⁺ and CD2⁻ pDCs, respectively.

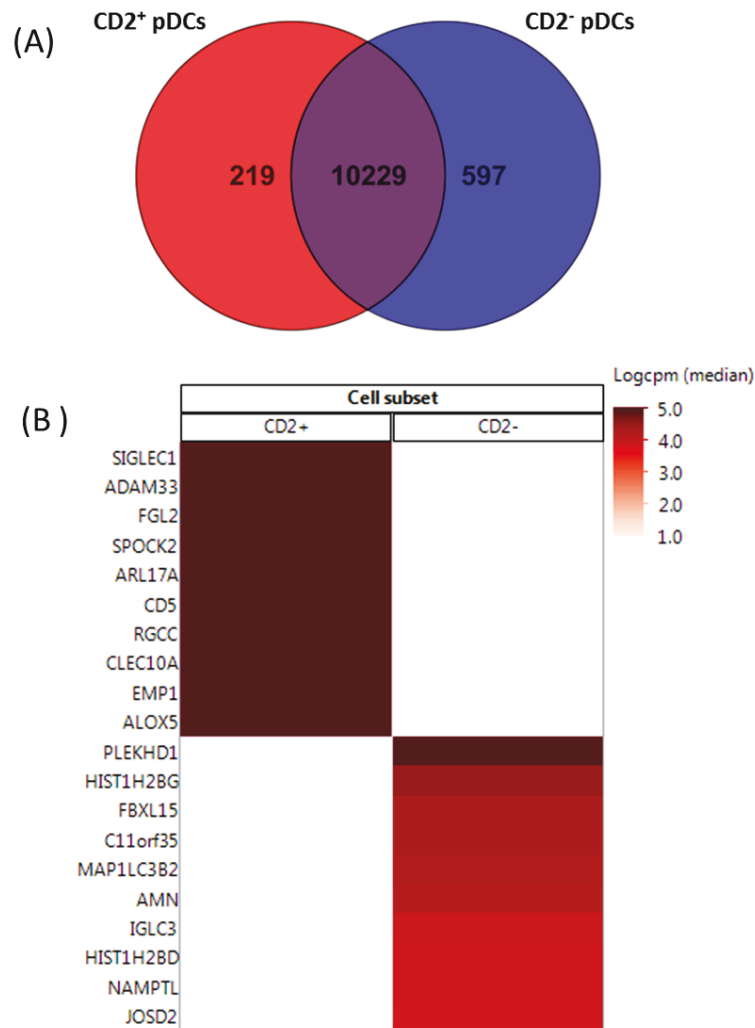


Figure 20. Common and unique gene signatures characterized in two pDC subsets. A) Venn diagram shows genes commonly and uniquely expressed by each pDC subset. (B) Top expressed unique genes with highest abundance in each pDC subset. Top 10 unique transcripts were selected based on expression levels. Raw counts were normalized to log₂ transformed counts per million (logcpm) and presented into a heatmap.

Top unique transcripts in CD2⁺ pDCs mainly included SIGLEC1 (endocytosis), ADAM33 (disintegrin family), CD5 (scavenger receptor activity), ALOX5 (inflammation) and previously introduced CLEC10A. Finally, top unique transcripts in CD2⁻ pDCs were identified including HIST1H2BG (broad antiviral activity), FBXL15 (ubiquitination mediator), MAP1LC3B2 (ubiquitin-like modifier), and JOSD2 (deubiquitinating enzyme).

To summarize, we analyzed transcriptional signatures of monocyte and DC subsets using RNA-Seq. Core gene signatures of myeloid APCs, monocytes, cDCs and pDCs were assessed. We also identified top unique genes which represented most significant transcriptional features in individual cell subsets.

Transcriptional Responses of Monocyte and DC Subsets to Influenza Vaccination Monocyte from the 2010 Apheresis Study

After identifying neutrophils and monocytes as major cellular sources of the innate IFN signature in response to influenza vaccination, we wished to understand whether distinct monocyte and DC subsets respond differently to influenza vaccination. We investigated transcription changes of monocyte and DC subsets at early time points, day1 and day 3, after flu vaccination. To this end, six healthy adult volunteers were recruited in the study and were randomly and evenly divided into two groups. They were vaccinated with TIV from 2010-2011 season (Fluzone®) (Table 3) with different H1N1 and H3N2 strains compared to previous season at day 0 and received a single body volume leukapheresis either at day 1 or day 3 and an additional apheresis at the steady state (day 60) (Figure 21).

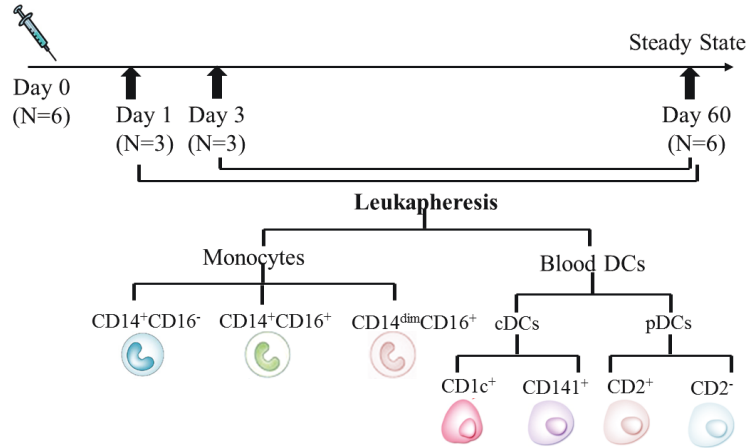


Figure 21. Human monocyte and DC subpopulations in healthy donors with TIV vaccination. Six healthy volunteers received 2010-2011 seasonal influenza vaccine (Fluzone®) at day 0. Leukapheresis samples were collected at day 1 and day 60 from three healthy donors and day 3 and day 60 from another three healthy donors. Leukapheresis sample were further sorted into seven cell subsets.

To identify transcriptional signatures expressed by each monocyte and DC cell subset in response to influenza vaccination, we analyzed the transcriptome in individual cell subset of the vaccinated subjects at days 1, 3 and 60 using RNA-Seq. Day 60 was used as the steady state. We first investigated the IFN signatures at early time points for each cell subset. Paired t-test with p-value cut-off 0.05 plus a fold change of 1.2 was used to identify differentially expressed interferon-stimulated genes (ISGs) (Schoggins et al., 2011) on day 1 or day 3 after the vaccination comparing with the steady state (day 60). Numbers of ISGs with up-regulation caused by the vaccination in each cell subset were summarized for each time point. In all three monocytes, there were similar numbers of IFN-inducible genes that were up-regulated on day 1 (Figure 22). In DC subsets, IFN signature was enriched in $CD1c^+$ cDCs but not $CD141^+$ cDCs. $CD2^+$ pDCs have more up-regulated ISGs than $CD141^+$ cDCs and $CD2^-$ pDCs on day 1 (Figure 22). On day 3, IFN-signature was diminished in all monocyte and DC subsets (Figure 22).

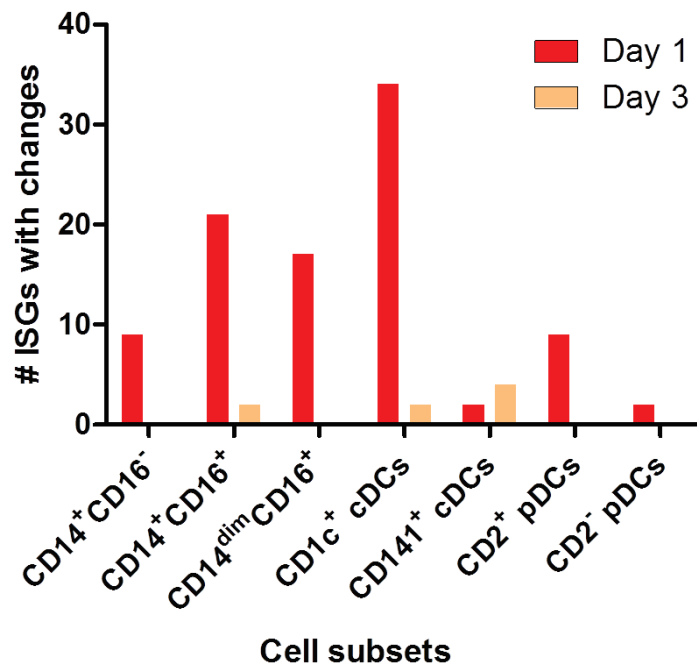


Figure 22. Numbers of interferon-stimulated genes (ISGs) with changes at day 1 and day 3 after influenza vaccination in monocyte and DC subsets.

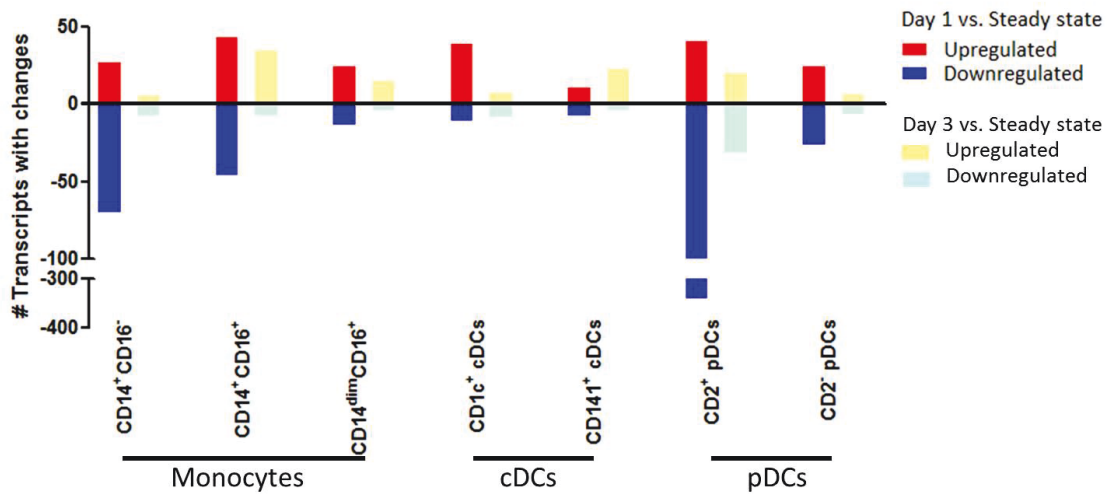


Figure 23. Most transcriptional changes upon vaccination occurred in monocytes and CD2⁺ pDCs. Transcripts were counted based on paired t-test ($p < 0.05$) plus a 1.5-fold change comparing day 1 or day 3 with day 60 using LogCPM for each cell subsets (unpaired t-test was used for the comparisons of day 3 and day 60 in CD2⁺ pDCs).

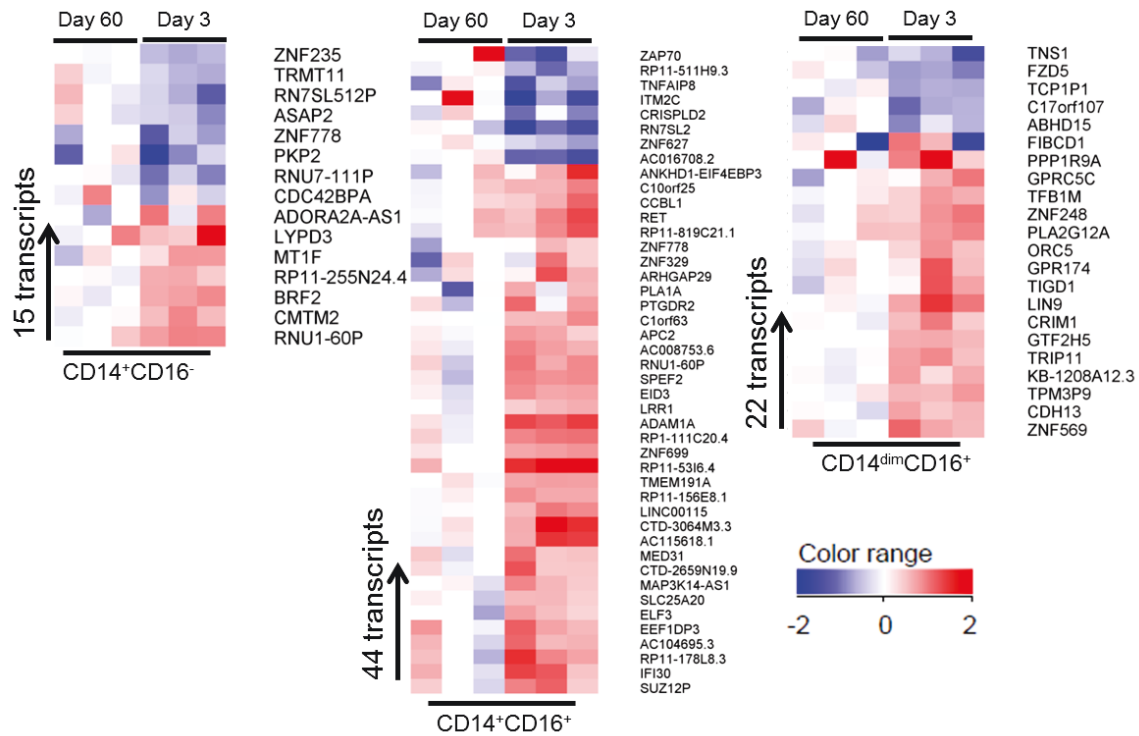


Figure 25. Genes with changes in each monocyte subsets after influenza vaccination. (A) Genes were selected based on paired t-test ($p < 0.05$) plus a 1.5-fold change comparing day 1 with day 60. Common and unique transcripts with changes elicited by vaccination were summarized in a venn diagram. (B) Genes were selected based on paired t-test ($p < 0.05$) plus a 1.5-fold change comparing day 3 with day 60.

We also identified other DEGs by comparing day 1 or day 3 with day 60 for each monocyte and DC subset. Genes were selected based on paired t-test ($p < 0.05$) plus a 1.5-fold change comparing day 1 or day 3 with the steady state (day 60) for each cell subset (Figure 23). Most transcriptional changes elicited by vaccination occurred in monocytes and CD2⁺ pDCs (Figure 23). In monocyte subsets, most DEGs were discovered in CD14⁺CD16⁻ and CD14⁺CD16⁺ monocytes on day 1. Chemokine CXCL3 and CCL20, and CLEC10A were down-regulated in CD14⁺CD16⁻ monocytes at day 1. IL31RA, CD38, and MHC- class II HLA-DOA, FCGR1A and FCGR1B were found to be up-regulated in CD14⁺CD16⁺ monocytes at day 1 (Figure 24). In addition, we

summarized the transcripts with changes elicited by vaccination for each monocyte subsets in a venn diagram. Most of those transcripts were unique but they were also transcripts with changes in common from different monocyte subsets. For instance, ANKRDD22 was upregulated in all three monocyte subsets and STAT1 was upregulated in two CD16⁺ monocyte subsets (Figure 24). On day 3, fewer genes with changes were identified to be DEGs in the monocyte subsets and CD14⁺CD16⁺ monocytes had more transcriptional changes as compared to other monocyte subsets (Figure 25).

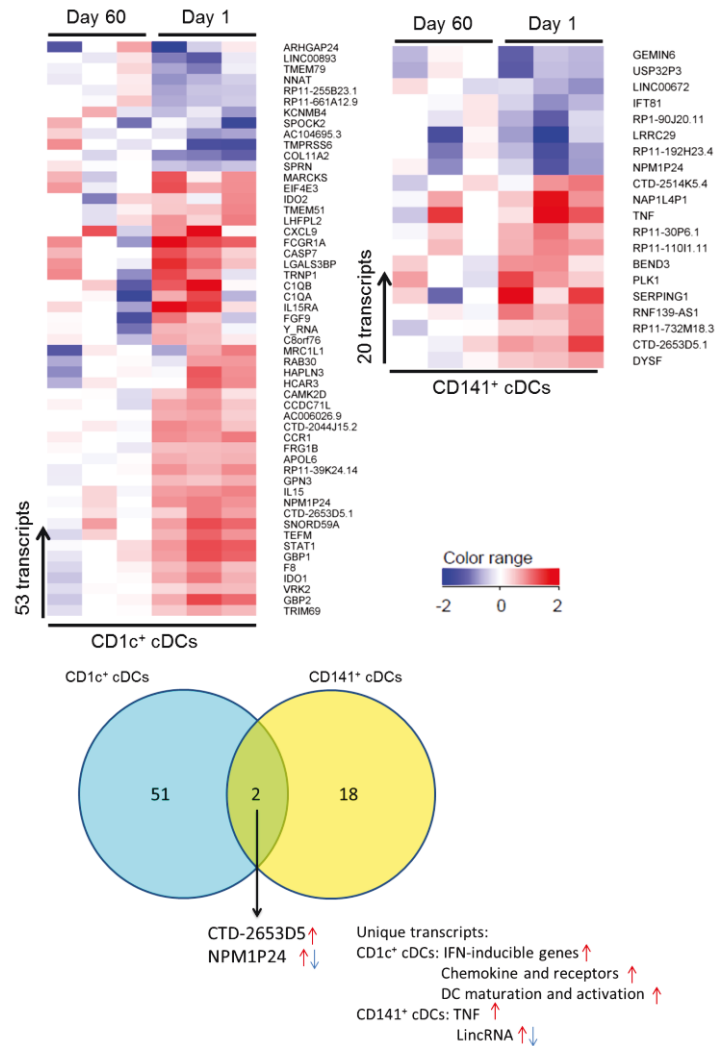


Figure 26. Genes with changes in each cDC subset after flu vaccination from 2010 cohort. Changes on transcriptional level in each cDC subset at day 1 post flu vaccination. Common and unique transcripts with changes elicited by vaccination were summarized in a venn diagram.

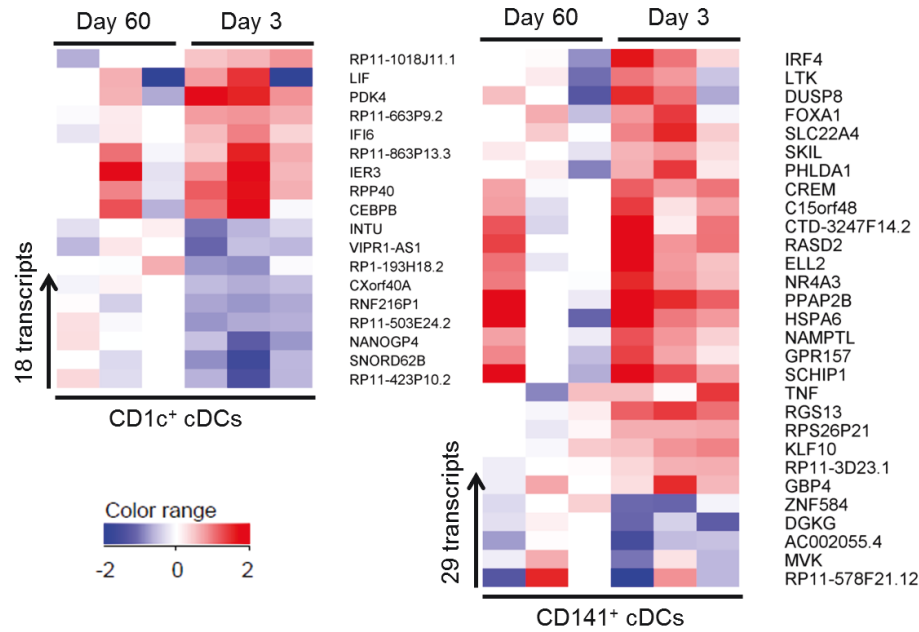


Figure 27. Genes with changes in each cDC subset after flu vaccination from 2010 cohort. Changes on transcriptional levels in each cDC subset at day 3 post flu vaccination

In cDC subsets, there were 53 DEGs in CD1c⁺ cDCs at day 1 when compared with day 60 steady state. Those DEGs including complement system molecules such as C1QA and C1QB, chemokine and chemokine receptors CXCL9 and CCR1, cytokine IL-15 and IL-15RA, IDO1 and IDO2 (Figure 26). There were fewer genes with changes at day 1 in CD141⁺ cDCs. TNF was found to be up-regulated at day 1 in CD141⁺ cDCs (Figure 26). Two commonly regulated genes were identified on day 1. CTD-2653D5 was upregulated while NPM1P24 was regulated in opposite directions. At day 3, more DEGs were present in response to vaccination in CD141⁺ cDCs. Those DEGs included some molecules with important immunological functions such as TNF (Figure 27).

Finally, we identified the DEGs in pDC subsets on day 1 and day 3 as compared with the steady state (day 60). There were 386 transcripts DEGs in CD2⁺ pDCs on day 1 compared with day 60. The majority of DEGs were down-regulated including MHC

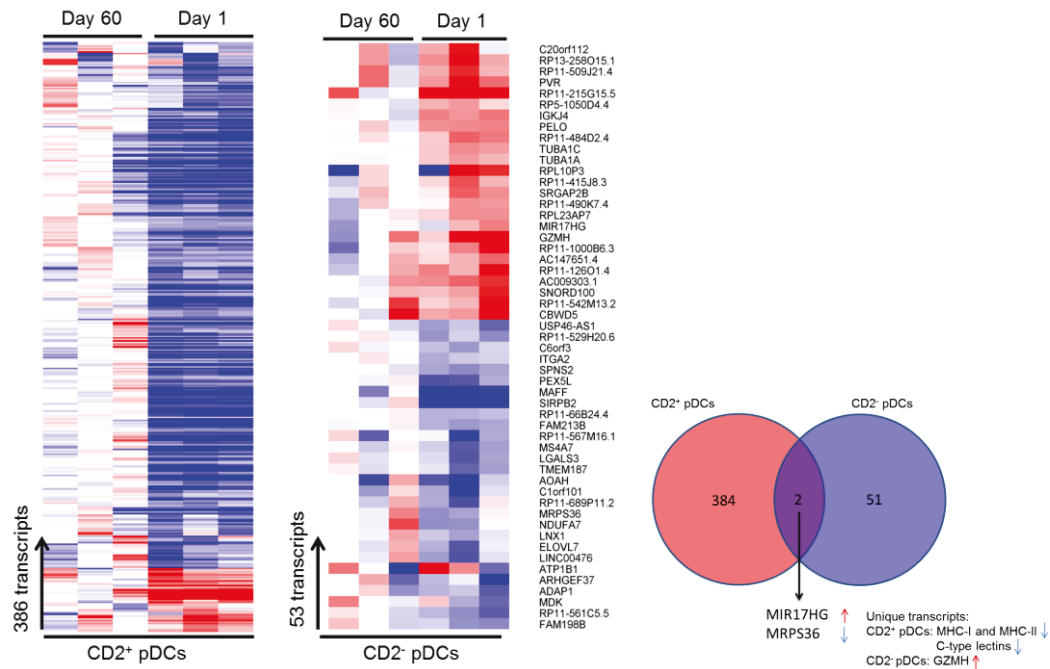


Figure 28. Genes with changes in each pDC subset after flu vaccination from 2010 cohort. Changes on transcriptional level in each cDC subset at day 1 post flu vaccination. Common and unique transcripts with changes elicited by vaccination were summarized in a venn diagram.

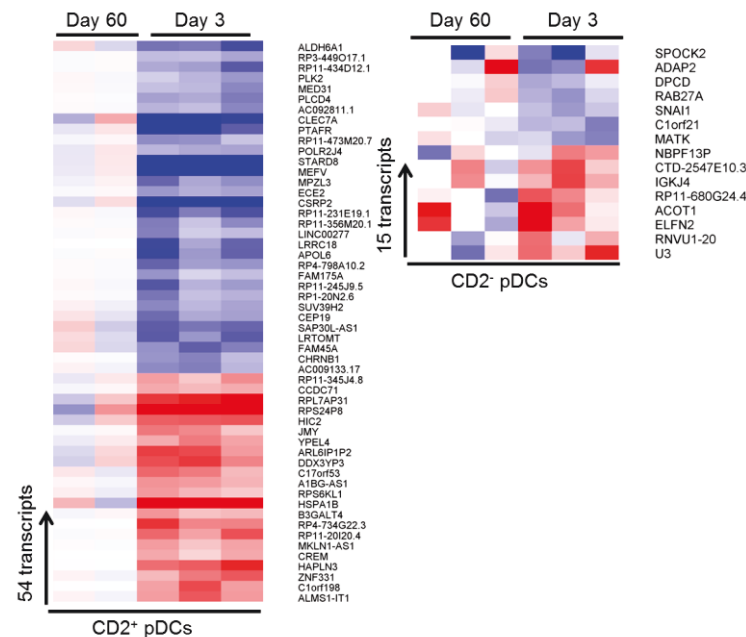


Figure 29. Genes with changes in each pDC subset after flu vaccination from 2010 cohort. Changes on transcriptional levels in each cDC subset at day 3 post flu vaccination.

molecules HLA-DRB5 (MHC-II) and HLA-H (MHC-I), C-type lectins CLEC12B and CLEC1B, and IL1RAP. The up-regulated molecules included CAMKK1, IL1B and IFN-related genes IRF2BPL and ISG15. Among 53 DEGs in CD2- pDCs on day 1 as compared to day 60, GZMH (granzyme H) was found to be up-regulated. Two common transcripts were identified including upregulation of MIR17H and downregulation of MRPS36 (Figure 28). On day 3, the numbers of transcripts with changes in pDC subsets were both significantly reduced. Most of these transcripts' biological functions still need to be annotated (Figure 29).

To summarize, an interferon signature after influenza vaccination was discovered at day 1 in monocytes, CD1c⁺ DCs and CD2⁺ pDCs but not in CD141⁺ DCs. Most transcriptional changes elicited by vaccination were shown in monocytes and CD2⁺ pDCs at day 1. The majority of transcripts with changes caused by vaccination are specific for each APC subset

Correlations between Baseline Transcriptional Signatures of APCs and Antibody Responses After Influenza Vaccination

Next, we wanted to study the biological significance of transcriptional profiles in blood APCs. We investigated the correlations between baseline transcriptional signatures of four blood APC populations and serological responses to influenza vaccination.

Study Design and Sample Selection Criteria

For the 2012 flu study, 26 healthy donors were recruited in the study. A 5 ml blood draw was collected from each individual at day 0 prior to influenza vaccination. Serum of healthy donors was also collected at day 0 and day 28 which is the peak of humoral

response after influenza vaccination (Figure 30). Starting from 5 million freshly ficolled PBMCs, four cell populations were sorted: CD14⁺ monocytes, CD1c⁺ and CD141⁺ cDCs, and BDCA2⁺ pDCs (Figure 31).

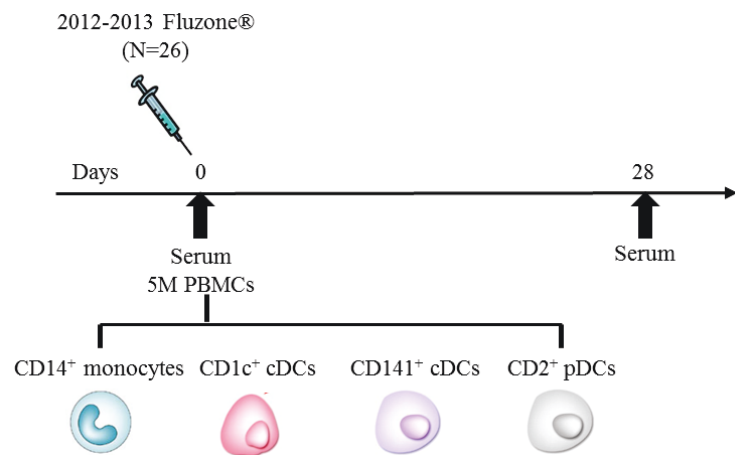


Figure 30. Study design of small blood draw study during 2012 flu season.

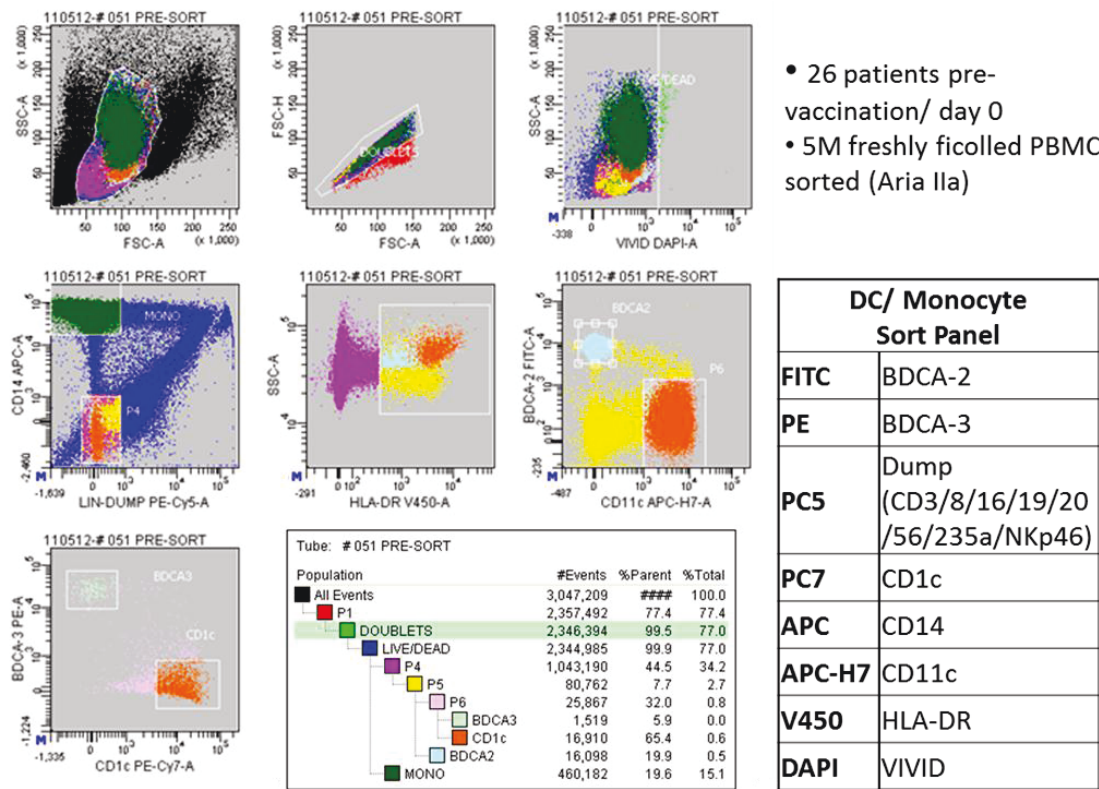


Figure 31. Gating strategy for monocyte and DC cell populations.

Table 7. Serologic responses of the 2012 small blood draw study. Virus-specific baseline and day 28 titers, fold change of each viral strain and best fold change among three strains are listed.

PatientID	Time Point	H1N1_HI_D0	H3N2_HI_D0	B_HI_D0	H1N1_HI_D28	H3N2_HI_D28	B_HI_D28	Fold_H1N1_HI	Fold_H3N2_HI	Fold_B_HI	HI_base	Best_HI_fold	H1N1_VN_D0	H3N2_VN_D0	B_VN_D0	H1N1_VN_D28	H3N2_VN_D28	B_VN_D28	Fold_H1N1_VN	Fold_H3N2_VN	Fold_B_VN	VN_base	Best_fold_VN
011_221_017	Day 0	6	403	40	96	806	80	16	2	2	6	16	7.9	403.2	50.4	403.2	806.3	100.8	50.8	2	2	7.9	50.8
011_221_029	Day 0	25	8	25	157.5	644.8	157.5	6.3	80.6	6.3	8	80.6	100.8	7.9	5	1280	640	160	12.7	80.6	32	7.9	80.6
011_221_030	Day 0	101	806	202	161.6	806	161.6	1.6	1	0.8	101	1.6	403.2	806.3	201.6	1016	806.3	160	2.5	1	0.8	403.2	2.5
011_221_018	Day 0	320	640	13	416	832	208	1.3	1.3	16	13	16	806.3	640	50.4	1280	806.3	127	1.6	1.3	2.5	50.4	2.5
011_221_019	Day 0	32	1280	5	102.4	1664	25	3.2	1.3	5	5	5	50.4	1280	5	403.2	1613	12.6	8	1.3	2.5	50.4	8
011_221_022	Day 0	320	101	5	640	404	101	2	4	20.2	5	20.2	1016	100.8	15.9	2032	403.2	127	2	4	8	15.9	8
011_221_025	Day 0	160	160	6	400	2032	1219	2.5	12.7	203.2	6	203.2	201.6	160	5	1016	2032	4064	5	12.7	812.7	5	812.7
011_221_031	Day 0	6	101	320	24	202	256	4	2	0.8	6	4	10	100.8	160	40	201.6	254	4	2	1.6	10	4
011_221_034	Day 0	20	13	13	320	330.2	131.3	16	25.4	10.1	13	25.4	20	12.6	15.9	806.3	320	254	40.3	25.4	16	20	40.3
011_221_036	Day 0	25	320	160	50	416	256	2	1.3	1.6	25	2	50.4	320	201.6	160	403.2	254	3.2	1.3	1.3	50.4	3.2
011_221_037	Day 0	202	160	80	323.2	640	160	1.6	4	2	160	4	254	160	80	640	640	254	2.5	4	3.2	160	4
011_221_040	Day 0	50	40	5	160	200	50.5	3.2	5	10.1	5	10.1	100.8	40	5	508	201.6	63.5	5	5	12.7	5	12.7
011_221_020	Day 0	202	320	63	404	416	50.4	2	1.3	0.8	202	2	160	320	50.4	1280	403.2	63.5	8	1.3	1.3	160	8
011_221_046	Day 0	160	202	25	512	262.6	100	3.2	1.3	4	25	4	403.2	508	127	1613	320	403.2	4	0.6	3.2	403.2	4
011_221_047	Day 0	13	25	5	52	62.5	5	4	2.5	1	13	4	50.4	10	5	100.8	25.2	10	2	2.5	2	10	2.5
011_221_048	Day 0	5	8	5	508	101.6	25	101.6	12.7	5	5	101.6	15.9	5	20	3225	50.4	127	203.2	10.1	6.3	15.9	203.2
011_221_049	Day 0	254	202	40	254	202	52	1	1	1.3	40	1.3	1280	127	127	1613	160	201.6	1.3	1.3	1.6	127	1.6
011_221_050	Day 0	8	8	32	512	406.4	51.2	64	50.8	1.6	8	64	40	10	100.8	3225	40	320	80.6	4	3.2	40	80.6
011_221_051	Day 0	32	5	5	64	160	5	2	32	1	5	32	63.5	6.3	10	254	160	63.5	4	25.4	6.3	6.3	25.4
011_221_052	Day 0	5	50	5	20	100	80	4	2	16	5	16	5	40	20	160	80	508	32	2	25.4	5	32
011_221_053	Day 0	5	5	5	5	5	5	1	1	1	5	1	6.3	7.9	6.3	25.2	15.9	7.9	4	2	1.3	6.3	4
011_221_055	Day 0	20	10	5	160	320	80	8	32	16	10	32	80	10	15.9	1280	403.2	160	16	40.3	10.1	10	40.3
011_221_056	Day 0	32	10	5	256	254	5	8	25.4	1	10	25.4	201.6	20	5	1280	50.4	80	6.3	2.5	16	5	16
011_221_057	Day 0	20	40	25	64	52	40	3.2	1.3	1.6	20	3.2	80	25.2	63.5	320	31.7	127	4	1.3	2	80	4
011_221_058	Day 0	20	5	5	2032	1280	5	101.6	256	1	5	256	50.4	5	5	5120	1016	7.9	101.6	203.2	1.6	5	203.2
011_221_024	Day 0	320	5	5	320	201.5	5	1	40.3	1	5	40.3	806.3	5	5	1280	201.6	5	1.6	40.3	1	5	40.3

Hemagglutination Inhibition (HI) assay and Viral Neutralization (VN) assay were conducted at both day 0 and day 28 to measure antibody mediated viral inhibition. 22 serological parameters were analyzed and summarized (Table 7) including baseline and day 28 titers for each viral strain, fold change of day 28 titer divided by day 0 titer for each viral strain, maximum fold change (best fold change) among three viral strains and the corresponding baseline titer (HI/VN base) from both HI and VN assays.

Transcriptional profiles of all sorted cell populations at baseline were analyzed using RNA-Seq. To assure sample and data quality, we checked for gene transcripts of lineage specific cell surface markers expressed on T, B, and NK cells to identify cellular contaminants. We identified CD141⁺ cDCs and BDCA2⁺ pDCs sorts with high expression of CD56 and CD3, indicating contamination with NK cells and T cells during

the sort (data not shown). Therefore, we took a strategy to pre-filter the transcripts for downstream analysis.

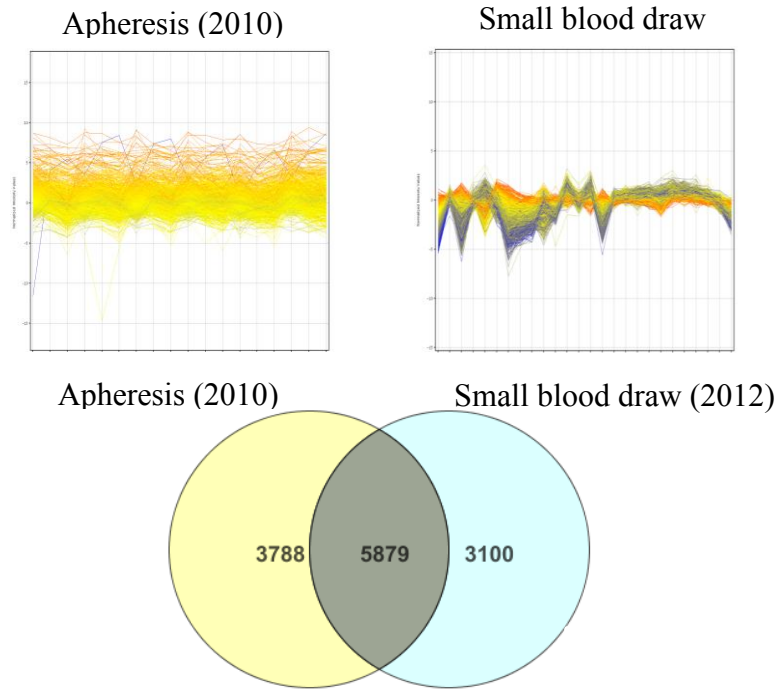


Figure 32. Commonly expressed genes of CD14⁺ monocytes sorted from 2010 apheresis and 2012 small blood draws. Line graphs showed genes present in CD14⁺ monocytes for each year of study. Common genes are at the intersection venn diagram.

Gene Selection Criteria

The RNA purity of samples with low cell counts might be impacted by cellular contaminants during the sorts and DNA contamination. To overcome this challenge, we focused on analyzing genes of CD14⁺ monocytes, CD1c⁺ and C141⁺ cDCs, and BDCA2⁺ pDCs that were expressed in 2010 apheresis sorted cell subsets (only day 60 steady state samples). If a transcript had a count ≥ 30 in $\geq 80\%$ of donors for an individual cell population, this gene was considered to be present.

For CD14⁺ monocytes, there were 9,667 genes identified as present genes from 2010 apheresis sorted cells and 8,979 genes were identified as present from 2012 small

blood draw sorted cells. We overlapped the gene sets from the two studies by a venn diagram and found 5,879 common genes for CD14⁺ monocytes (

Figure 32). The same strategy was applied to other APC subsets. 9,133 common transcripts were identified for CD1c⁺ cDCs; 715 common transcripts were identified for CD141⁺ cDCs; and 7,508 transcripts were identified for BDCA2⁺ pDCs. The downstream analysis only focused on those common transcripts for each cell subset.

Early Molecular Signatures Correlate with Antibody Responses

To identify early molecular signatures corresponding with antibody response, we performed correlation analysis between gene expressions at baseline and all 22 serological parameters for each APC subset. Spearman correlation was used to calculate coefficient factor between each transcript and serological parameter. P-value, correlation (R) and R² were calculated. Transcripts were filtered by requiring raw p-value ≤ 0.05 and R-square ≥ 0.3 with any serological parameter. The Number of transcripts passed the filter was summarized by each serological parameter for individual APC subset (Figure 33).

The largest numbers of transcripts that correlated with the serology was found in BDCA2⁺ pDCs. There were about 150 transcripts that correlated with fold change (day 28/ day 0) of B strain using VN assay (Fold_B_VN) in BDCA2⁺ pDCs. Fold change of titers in B stains (Fold_B_VN) was also found to be the top serological parameter in CD14⁺ monocytes and CD1c⁺ cDCs as compared to the fold changes in other strains. Therefore, we focused on investigating these transcripts that correlated with “Fold_B_VN” in each APC subset.

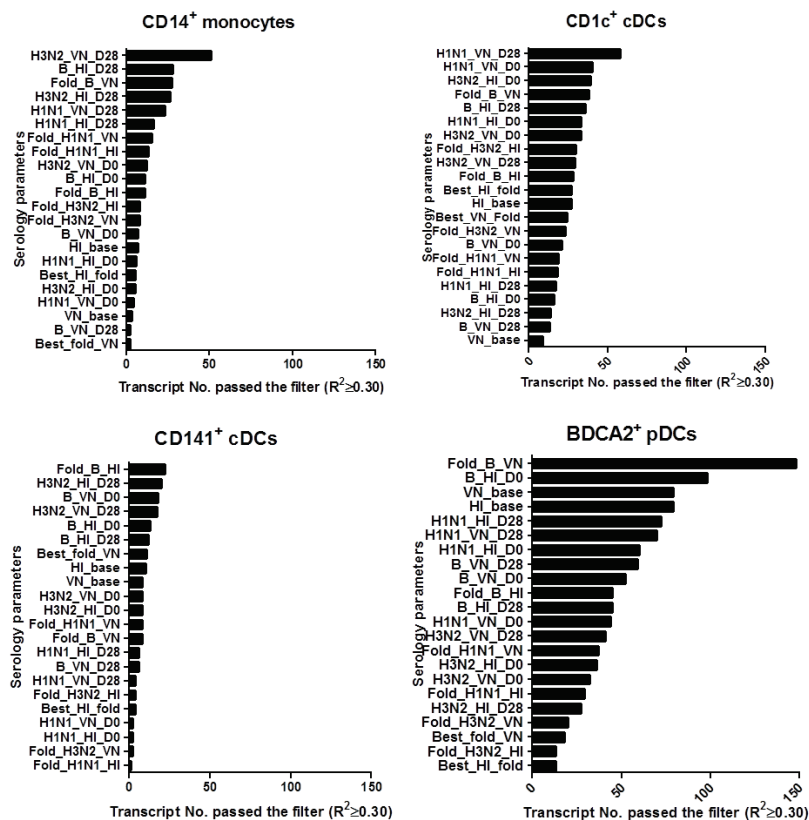


Figure 33. Numbers of transcripts correlating with each serology parameter. Transcripts were filtered by requiring the R-square ≥ 0.3

Table 8. Top genes ranked by correlation (R) with antibody response in CD14⁺ monocytes.

SYMBOL	TYPE	pValue	Spearman	Correlation	R-square
HP1BP3	protein_coding	0.000189301		0.67	0.45
EEF2	protein_coding	0.000232413		0.66	0.44
CLTA	protein_coding	0.00059236		0.65	0.39
RPL13	protein_coding	0.001093831		0.6	0.36
ARPC1B	protein_coding	0.001247564		0.6	0.36
ZNF664	protein_coding	0.001637198		0.59	0.34
HLA-B	protein_coding	0.001797699		0.58	0.34
ALYREF	protein_coding	0.002048111		0.58	0.33
EIF4H	protein_coding	0.002079449		0.58	0.33
PDCD6	protein_coding	0.002488768		0.57	0.32
TM2D3	protein_coding	0.00250722		0.57	0.32
PANK2	protein_coding	0.002839281		0.56	0.32
RPS6	protein_coding	0.002859931		0.56	0.31
COX5A	protein_coding	0.002901614		0.56	0.31
PSMA1	protein_coding	0.00296511		0.56	0.31
RPS16	protein_coding	0.003371519		0.55	0.31
HNRNPA1	protein_coding	0.003541894		0.55	0.3
NUPL2	protein_coding	0.003851011		0.55	0.3
RPL27A	protein_coding	0.003959012		0.55	0.3
LMO2	protein_coding	0.00404169		0.54	0.3
SIPA1L2	protein_coding	0.00404169	-0.54		0.3
CTD-2006C1.2	processed_transcript	0.00281876	-0.56		0.32
FAF1	protein_coding	0.002276241	-0.57		0.33
RP11-597D13.9	antisense	0.001352829	-0.59		0.35
KIAA1407	protein_coding	0.001363765	-0.59		0.35
NEK3	protein_coding	0.001331185	-0.6		0.35
WDR55	protein_coding	0.000948701	-0.61		0.37

Table 9. Top genes ranked by correlation (R) with antibody response in CD1c⁺ cDCs.

SYMBOL	TYPE	pValue	Spearman	
			Correlation	Rsquare
COPG1	protein_coding	9.465E-05	0.69	0.48
INPP5D	protein_coding	0.000117	0.68	0.47
ADD1	protein_coding	0.0002811	0.66	0.43
CTSB	protein_coding	0.0003132	0.65	0.42
SPPL3	protein_coding	0.0003552	0.65	0.42
GABARAP	protein_coding	0.00045	0.64	0.41
CD300A	protein_coding	0.0005122	0.63	0.4
IMP4	protein_coding	0.0007139	0.62	0.39
ITGAL	protein_coding	0.0008789	0.61	0.38
FAM120AOS	protein_coding	0.0015251	0.59	0.35
TLN1	protein_coding	0.0017293	0.58	0.34
FBXW2	protein_coding	0.0017977	0.58	0.34
RABGAP1	protein_coding	0.0018257	0.58	0.34
TBC1D5	protein_coding	0.0018685	0.58	0.34
ARFGAP2	protein_coding	0.0018685	0.58	0.34
PIK3CD	protein_coding	0.0020953	0.58	0.33
GPI	protein_coding	0.0022256	0.57	0.33
POLR2L	protein_coding	0.0023628	0.57	0.32
UBXN1	protein_coding	0.0025633	0.57	0.32
RXRB	protein_coding	0.0026591	0.56	0.32
ACTR1A	protein_coding	0.0027781	0.56	0.32
MLF2	protein_coding	0.0029865	0.56	0.31
SAE1	protein_coding	0.0030081	0.56	0.31
SERINC3	protein_coding	0.0031179	0.56	0.31
PHC2	protein_coding	0.0031179	0.56	0.31
KIAA0232	protein_coding	0.0031628	0.56	0.31
HIP1	protein_coding	0.0034437	0.55	0.3
WDR73	protein_coding	0.003468	0.55	0.3
NRBP1	protein_coding	0.0035419	0.55	0.3
TBL1X	protein_coding	0.0035919	0.55	0.3
RIN3	protein_coding	0.0035919	0.55	0.3
TRIM36	protein_coding	0.0036937	-0.55	0.3
HACE1	protein_coding	0.003798	-0.55	0.3
GLTSCR1L	protein_coding	0.0028393	-0.56	0.32
RAB40B	protein_coding	0.0030298	-0.56	0.31
PAQR3	protein_coding	0.0021596	-0.57	0.33
PAFAH2	protein_coding	0.0020953	-0.58	0.33
MRPL47	protein_coding	0.0008789	-0.61	0.38

Table 10. Top genes ranked by correlation (R) with antibody response in CD141⁺ cDCs.

SYMBOL	TYPE	With	pValue	Spearman	
				Correlation	Rsquare
PSMA2.2	protein_coding	Fold_B_VN	0.0020314	0.66	0.44
EEF2	protein_coding	Fold_B_VN	0.0044641	0.62	0.39
SRRM2	protein_coding	Fold_B_VN	0.0070343	0.6	0.36
PCNP	protein_coding	Fold_B_VN	0.0104045	0.57	0.33
MACF1	protein_coding	Fold_B_VN	0.0122706	0.56	0.32
GNB1	protein_coding	Fold_B_VN	0.0143966	-0.55	0.3
SECISBP2	protein_coding	Fold_B_VN	0.0033	-0.64	0.41
DOCK5	protein_coding	Fold_B_VN	0.0012223	-0.68	0.47

Table 11. Top genes ranked by correlation (R) with antibody response in BDCA2⁺ pDCs.

SYMBOL	TYPE	pValue	Spearman	
			Correlation	Rsquare
POLDIP3	protein_coding	8.53E-06	0.8	0.64
SULF2	protein_coding	0.000104	0.73	0.54
RAD18	protein_coding	0.000393	0.69	0.47
RAD51AP1	protein_coding	0.000566	0.68	0.46
FCGRT	protein_coding	0.000574	0.67	0.46
PSMD2	protein_coding	0.000582	0.67	0.45
NFX1	protein_coding	0.0006	0.67	0.45
SMPD3	protein_coding	0.000655	0.67	0.45
ACTG1	protein_coding	0.000931	0.66	0.43
C6orf48	protein_coding	0.000957	0.65	0.43
PEBP1	protein_coding	0.000997	0.65	0.43
PPIA	protein_coding	0.001053	0.65	0.42
HP51	protein_coding	0.001081	0.65	0.42
NR3C1	protein_coding	0.001302	0.64	0.41
ARFGAP2	protein_coding	0.001407	0.64	0.41
SCAF11	protein_coding	0.001463	0.64	0.4
C9orf91	protein_coding	0.001747	0.63	0.39
PIK3CD	protein_coding	0.002342	0.61	0.38
WAS	protein_coding	0.002342	0.61	0.38
RNF213	protein_coding	0.002371	0.61	0.38
BID	protein_coding	0.002399	0.61	0.38
GNA13	protein_coding	0.002457	0.61	0.37
SIRPB1	protein_coding	0.003172	0.6	0.36
NAA38	protein_coding	0.003209	0.6	0.36
MDH2	protein_coding	0.003434	0.6	0.35
SPN	protein_coding	0.003551	0.59	0.35
GMFR2	protein_coding	0.003631	0.59	0.35
EDEM1	protein_coding	0.003672	0.59	0.35
NDUFS6	protein_coding	0.003796	0.59	0.35
VAPA	protein_coding	0.003967	0.59	0.35
LGMN	protein_coding	0.004011	0.59	0.35
MAPK1IP1L	protein_coding	0.004236	0.59	0.34
LCP1	protein_coding	0.004282	0.58	0.34
FCER1A	protein_coding	0.004329	0.58	0.34
MBP	protein_coding	0.004376	0.58	0.34
SAMHD1	protein_coding	0.004618	0.58	0.34
NCOA4	protein_coding	0.004718	0.58	0.34
UQCRRH	protein_coding	0.004718	0.58	0.34
BCLAF1	protein_coding	0.004768	0.58	0.34
OIA1	protein_coding	0.004975	0.58	0.33
HNRNPC	protein_coding	0.005189	0.57	0.33
TTC7A	protein_coding	0.005244	0.57	0.33
SLC20A1	protein_coding	0.005411	0.57	0.33
GNB2L1	protein_coding	0.005641	0.57	0.32
CERS6	protein_coding	0.005641	0.57	0.32
SOD1	protein_coding	0.005819	0.57	0.32
ATP2A2	protein_coding	0.00594	0.57	0.32
PIIH	protein_coding	0.006125	0.57	0.32
CNPY3	protein_coding	0.006188	0.56	0.32
IDNK	protein_coding	0.006188	0.56	0.32
LSM14A	protein_coding	0.006643	0.56	0.31
PBX3	protein_coding	0.00671	0.56	0.31
TNFRSF1B	protein_coding	0.006846	0.56	0.31
MLF2	protein_coding	0.006846	0.56	0.31
RAD50	protein_coding	0.006915	0.56	0.31
DANCR	processed_transcript	0.006915	0.56	0.31
IDH3G	protein_coding	0.007054	0.56	0.31
RSL24D1	protein_coding	0.007196	0.56	0.31
PGGT1B	protein_coding	0.007196	0.56	0.31
PSMB8	protein_coding	0.007196	0.56	0.31
TGFB1	protein_coding	0.007636	0.55	0.31
PRKCB	protein_coding	0.007711	0.55	0.3
RAB7A	protein_coding	0.007711	0.55	0.3
HLA-DMB	protein_coding	0.008337	0.55	0.3
FNBP1	protein_coding	0.008499	0.55	0.3
HADHA	protein_coding	0.008665	0.55	0.3
ATP6V0B	protein_coding	0.008833	0.54	0.3
CECR1	protein_coding	0.008918	0.54	0.3
PSMD7	protein_coding	0.008918	0.54	0.3
SLC9A7	protein_coding	0.008918	0.54	0.3
DIRC2	protein_coding	0.008748396	-0.54	0.3
KIAA0922	protein_coding	0.008832727	-0.54	0.3
MCM9	protein_coding	0.008832727	-0.54	0.3
KLHL3	protein_coding	0.008832727	-0.54	0.3
ORC2	protein_coding	0.007340195	-0.55	0.31
ANO10	protein_coding	0.007711088	-0.55	0.3
ZDHHC13	protein_coding	0.007940956	-0.55	0.3
RDX	protein_coding	0.00809732	-0.55	0.3
TMCC3	protein_coding	0.008336621	-0.55	0.3
CENPL	protein_coding	0.00849937	-0.55	0.3
EXOC6B	protein_coding	0.006187655	-0.56	0.32
AASS	protein_coding	0.006187655	-0.56	0.32
SRCAP	protein_coding	0.006444322	-0.56	0.32
PKD1	protein_coding	0.006575928	-0.56	0.31
SUZ12	protein_coding	0.006642561	-0.56	0.31
RAPGEF2	protein_coding	0.006709752	-0.56	0.31
PLK1S1	processed_transcript	0.006845825	-0.56	0.31
TTC5	protein_coding	0.007124827	-0.56	0.31
PLCB4	protein_coding	0.007196028	-0.56	0.31
PCMTD2	protein_coding	0.007267816	-0.56	0.31
PDE3B	protein_coding	0.005525183	-0.57	0.33
NEDD4L	protein_coding	0.005582859	-0.57	0.33
METTL6	protein_coding	0.005582859	-0.57	0.33
PGM2L1	protein_coding	0.005582859	-0.57	0.33
SFXN5	protein_coding	0.005818593	-0.57	0.32
GPLD1	protein_coding	0.005818593	-0.57	0.32
FNBP1L	protein_coding	0.005878801	-0.57	0.32
C1orf112	protein_coding	0.005878801	-0.57	0.32
CITED2	protein_coding	0.006000769	-0.57	0.32
EOGT	protein_coding	0.004423618	-0.58	0.34
PTPN4	protein_coding	0.00447155	-0.58	0.34
BMP2K	protein_coding	0.00447155	-0.58	0.34
B8IP1	protein_coding	0.004568714	-0.58	0.34
TMEM135	protein_coding	0.004617953	-0.58	0.34
FCHO1	protein_coding	0.004667634	-0.58	0.34
RSRPY1	protein_coding	0.004717759	-0.58	0.34
LRRC37B	protein_coding	0.004819358	-0.58	0.33
RP11-434C1.1	lincRNA	0.004870837	-0.58	0.33
ATXN2	protein_coding	0.004922774	-0.58	0.33
ZNF546	protein_coding	0.004922774	-0.58	0.33
PLAG1	protein_coding	0.004975172	-0.58	0.33
ABCC4	protein_coding	0.003551294	-0.59	0.35
SLC30A7	protein_coding	0.003631458	-0.59	0.35
NFATC3	protein_coding	0.003754543	-0.59	0.35
AK9	protein_coding	0.003967442	-0.59	0.35
RALGAP1	protein_coding	0.004144947	-0.59	0.34
CACNB4	protein_coding	0.002996012	-0.6	0.36
GATAD1	protein_coding	0.003030607	-0.6	0.36
EHMT2	protein_coding	0.003100805	-0.6	0.36
LMO7	protein_coding	0.003136412	-0.6	0.36
CCNYL1	protein_coding	0.003319644	-0.6	0.36
PRIM2	protein_coding	0.003395409	-0.6	0.36
ADARB1	protein_coding	0.003395409	-0.6	0.36
WDR19	protein_coding	0.002456728	-0.61	0.37
TPK1	protein_coding	0.001882261	-0.62	0.38
E2F2	protein_coding	0.001929283	-0.62	0.38
DYNC2H1	protein_coding	0.002101761	-0.62	0.38
LCLAT1	protein_coding	0.002232781	-0.62	0.38
DNAJB4	protein_coding	0.001579458	-0.63	0.4
TOB2	protein_coding	0.001620003	-0.63	0.4
GRIP1	protein_coding	0.001640604	-0.63	0.4
RRAGD	protein_coding	0.001640604	-0.63	0.4
ARL15	protein_coding	0.001682472	-0.63	0.4
C1orf131	protein_coding	0.001746969	-0.63	0.39
GSAP	protein_coding	0.001813548	-0.63	0.39
ITGAX	protein_coding	0.0012353	-0.64	0.41
JDP2	protein_coding	0.001268223	-0.64	0.41
SPATA33	protein_coding	0.001389394	-0.64	0.41
SMYD4	protein_coding	0.000957101	-0.65	0.43
MCM2	protein_coding	0.000983608	-0.65	0.43
SLC9C2	protein_coding	0.001066914	-0.65	0.42
BRD3	protein_coding	0.000582497	-0.67	0.45
DCUN1D4	protein_coding	0.000608693	-0.67	0.45
GPATCH2	protein_coding	0.000723818	-0.67	0.44
MB21D1	protein_coding	0.000532992	-0.68	0.46
KIAA1715	protein_coding	0.000205115	-0.71	0.51
ARHGEF10	protein_coding	0.000161015	-0.72	0.52
CIRH1A	protein_coding	7.40335E-05	-0.74	0.55

Among the transcripts correlated with “Fold_B_VN” in CD14⁺ monocytes, there were MHC class I molecule HLA-B and proteasome PSMA1 that were involved in MHC class I antigen process pathway. Clathrin, CLTA, also had a positive correlation with the fold change of B strain which mediated endocytosis by forming clathrin-coated vesicles. Fas (TNFRSF6) associated factor 1, FAF1, negatively correlated and it was identified as a negative regulator of an NFkB signaling pathway (Table 8). The same analytical approach was applied to study CD1c⁺ cDCs. Positive correlation included immune-related genes involved in inflammation, activation of leukocytes, adhesion of DCs and movement of neutrophils such as CD300A, INPP5D, ITGAL, PIK3CD and TLN1 (Table 9). For CD141⁺ cDCs, many genes function still needed to be annotated (Table 10).

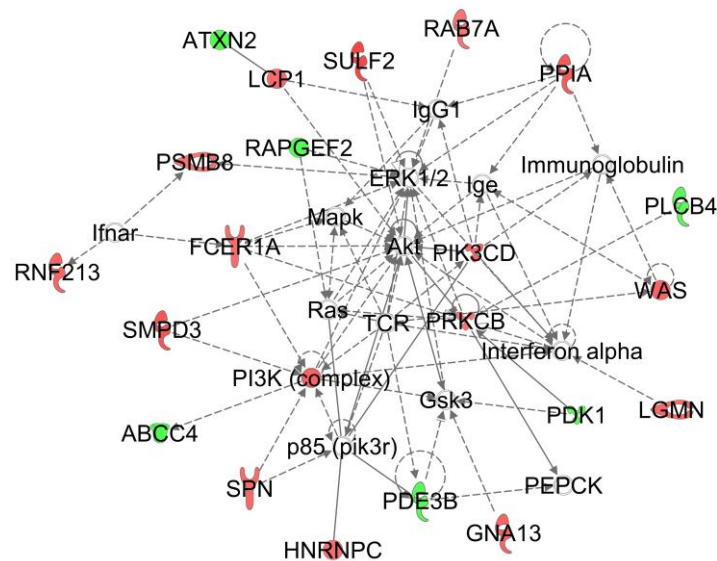


Figure 34. IPA network analysis of transcripts correlated with “Fold_B_VN” in BDCA2⁺ pDCs. Top network function involves immune-cell trafficking.

Finally, we investigated the transcripts that correlated with “Fold_B_VN” in BDCA2⁺ pDCs (Table 11). IPA network analysis was applied and the top functions of the correlated transcripts were identified as cell movement and immune- cell trafficking (Figure 34). Although type I IFN did not show direct correlation relationship with

investigated serological parameter, IFNAR and IFNA has been shown as the central nodes for FCER1A, PSMB8, RNF213 and LGMN (Figure 34).

To interpret our gene expression data on a global view, we employed Gene Set Enrichment Analysis (GSEA) which is a powerful analytical method to evaluate cumulative changes in the expression of gene sets defined based on prior biological knowledge. We pre-ranked our gene list based on the Spearman correlation R with “Fold_B_VN” for each APC subset and calculated a normalized enrichment score (NES) for each gene set adopted from individual blood modules. The NES reflected how often members of that gene set occur at the top (positive correlation) or bottom (negative correlation) of the pre-ranked gene list. Then we created a module map based on the NES for all APC subsets. We observed that many inflammation-related modules including M3.2, M4.6, M5.1 and M5.7 were enriched in pre-ranked gene list in CD14⁺ monocytes. It implies that transcripts with high ranking of correlation R overlapped with genes from inflammation modules. Monocyte module M4.14 was enriched in CD14⁺ monocytes which confirmed our analysis strategy. Additionally, there were also modules related to mitochondrial respiration/stress and protein synthesis were enriched in CD14⁺ monocytes. In CD1c⁺ cDCs, inflammation module M7.1 and interferon module M5.12 were enriched from our pre-ranked data set. In BDCA2⁺ pDCs, inflammation module M5.7 and a few modules related to mitochondrial respiration/stress and protein synthesis were also enriched (Figure 35).

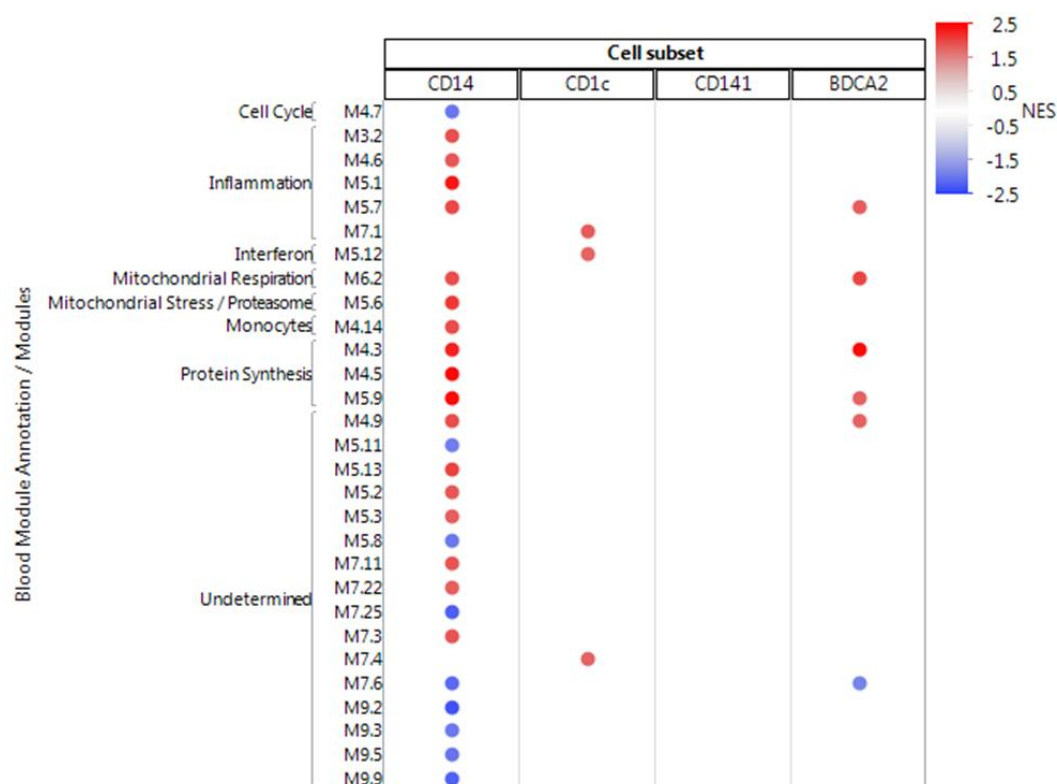


Figure 35. GSEA of transcripts correlated with Fold_B_VN using blood module gene sets. Transcripts were pre-ranked based on correlation R with Fold_B_VN for each APC subsets. Each gene set comprised genes from one blood module. GSEA was performed and the module map was generated using NES. Red dots represented positive NES and blue dots represented negative NES.

To summarize, we analyzed the correlation between gene expression of APC subsets at baseline and all available serological information. We identified large number of transcripts correlated with fold change of titers against B strain using VN assay across three investigated APC subsets. GSEA analysis showed inflammation-related modules were enriched in CD14⁺ monocytes. An IFN-related module M5.12 was enriched in CD1c⁺ cDCs and one inflammation module was enriched in CD1c⁺ cDCs and BDCA2⁺ pDCs, respectively.

CHAPTER FIVE

Discussion

Vaccination, the most successful preventive measure against infectious diseases, relies on the presentation of vaccine antigens to T and B cells by antigen-presenting cells (APCs). This process leads to the generation of protective immune responses mediated by antibodies produced by B cells and by cytotoxic molecules (granzyme and perforin) produced by CD8⁺ T cells. Many vaccines induce protective immunity via antibodies. However, not everybody can mount protective immune response to vaccines, as for example to influenza vaccine. The reasons underlying human variation in response to vaccination remain unclear. Systems biology approaches have been used to determine signatures that can be used to predict vaccine-induced immunity in humans, but whether there is a 'universal signature' that can be used to predict antibody responses to any vaccine is unknown.

Herein, we have applied microarray and RNAseq technologies to profile the transcripts of whole blood and blood cells subsets in order to understand their potential links with vaccine response. We have first established the global signatures of antibody responses to influenza vaccine and differentiated those from response to pneumococcal vaccine. We have then analyzed in-depth the transcriptional landscape of APCs in the context of influenza vaccination and finally, attempted to assess potential correlations between the status of APCs at baseline and vaccine responses. In the course of these studies, we have employed two technologies to assess the transcriptome, which we will discuss later.

Transcriptional Responses to Vaccination in Blood and Major Leukocytes

Our studies comparing transcriptional profiles in the blood in response to vaccination revealed that both seasonal influenza and pneumococcal vaccines induce rapid transcriptional changes already at day 1, consistent with the activation of innate immunity. Indeed, kinetic studies showed early innate immune responses already within hours after influenza vaccination (Obermoser et al., 2013). The two vaccines elicited quantitatively and qualitatively different transcriptional responses. Thus, in the influenza vaccine group the profiles were dominated by IFN-inducible transcripts whereas in the pneumococcal vaccine group they were mainly inflammation-related. IFN signature in vaccination is important since it has been suggested to be linked with vaccination outcomes. Indeed, Bucasas et al., observed up-regulation of interferon signaling genes like STAT1 and IRF9 in whole blood on day 1 after influenza vaccination which also correlated to the magnitude of serological response (Bucasas et al., 2011). In another study, a signature of IFN-related genes in PBMC on day 3 after flu vaccination was reported to correlate with serological response (Nakaya et al., 2011). In another project in human immunology project consortium (HIPC) program, Dr. Ramillo's group published that IFN signature was detected 7 days in the blood after the administration of live attenuated influenza vaccine (LAIV) in children (<5 years old) during 2011-2012 flu season. In their study, they also identified an IFN signature at day 1 in children who received TIV (inactivated vaccine) injection which was in line with our observation (Cao et al., 2014). 2011-2012 seasonal influenza vaccine consists of the same virus strains as in the 2010-2011 season, where we conducted our 2010 apheresis sorted APC studies. There are significant kinetic differences in IFN response in live vaccine and inactivated vaccine groups. In the live vaccine group, the virus needs time to establish replication in

the nasal mucosa which causes, probably with other factors, the delayed IFN signature observed in the blood. Thus, our results corroborate earlier studies. Furthermore, we have identified neutrophils and monocytes as the main cellular source of the day 1 influenza vaccine interferon signature in the blood.

Transcriptional Responses to Vaccination in Apheresis Sorted DC and Monocyte Subsets

After analyzing immune responses to vaccination from the blood and major leukocytes, we wished to expand our study to the subsets of monocytes and DCs. DCs are at a central position of initiating and regulating immune responses (Banchereau and Steinman, 1998). Although several subsets of human DCs have been identified, their roles in response to influenza vaccination have not been fully elucidated. Similarly, monocytes, the circulating precursors of DCs, have been classified into 3 major subsets but whether distinct monocyte subsets possess different functional specializations still remains a question. Due to the low frequency of CD141⁺ cDCs in the circulation, previous studies have characterized transcriptional profiles of blood cDCs by either focusing on CD1c⁺ cDCs only or only using microarrays (Segura et al., 2013; Watchmaker et al., 2014). Leukapheresis provided us with the opportunity to collect large amounts of white blood cells and to sort multiple cell populations from an individual. Monocytes are considered as a systemic reservoir of myeloid precursors for the regeneration of tissue macrophages and DCs (Geissmann et al., 2003; Randolph et al., 1999; Serbina and Pamer, 2006). Whole-genome array analysis represents an approach to better understand the functions of monocytes based on sorted subsets, using mice or other model systems (Auffray et al., 2007). Here, with the benefits of advancing

technology, we used RNA-Seq (Wold and Myers, 2008) to characterize monocytes and DCs in the steady state and early time points after influenza vaccination.

We systematically compared transcriptional profiles of the three sorted monocyte subsets and two DC subsets, CD1c⁺ and CD141⁺ DCs. We identified common and unique transcripts of all five myeloid APC subsets, or among monocyte or DC subsets. For example, in the analysis of the three monocyte subsets, we found CLEC4D and CCR2 were uniquely expressed in CD14⁺CD16⁻ monocytes which is consistent with the results in previous studies (Wong et al., 2011). CCR2, the receptor for monocyte chemoattractant protein-1 (MCP-1), mediates monocyte recruitment into inflamed tissues and its expression is upregulated by proinflammatory cytokines such as TNF (Sierra-Filardi et al., 2014). In addition, we also observed other unique genes enriched in CD14⁺CD16⁻ monocytes including a unique expression of long non-coding (LINC) RNA LINC00937 in CD14⁺CD16⁻ monocytes that was not detected by microarray (Wong et al., 2011). In CD14⁺CD16⁺ monocytes, uniquely expressed genes included LYPD3 (also known as C4.4A), which belongs to the Ly6 family. LYPD3 supports cell migration by binding laminins 1 and 5 (Paret et al., 2005). Another unique transcript found in CD14⁺CD16⁺ monocytes was GNLY, which is known as granulysin. Granulysin primarily was found to be expressed in cytotoxic T lymphocytes and NK cells, coexpressed in cytolytic granules with perforin and granzymes, and released via receptor-mediated granule exocytosis involved in killing tumors and microbes (Hanson et al., 1999; Kaspar et al., 2001; Stenger et al., 1998). Additionally, using recombinant granulysin, a more recent study demonstrated that this cytolytic feature is driven by its 9 kDa isoform whereas its 15 kDa isoform activates immature monocyte-derived DCs to differentiate into mature phenotype (Clayberger et al., 2012). Our result indicated that

CD14⁺CD16⁺ monocytes might be another cellular source of granulysin in vivo and/or they might be directly involved in DC differentiation. Recent work revealed that CD14^{dim}CD16⁺ monocytes are bona fide monocytes responding to a broad range of microbes by secreting proinflammatory cytokines TNF α , IL-1 β , and CCL3 (Cros et al., 2010; Wong et al., 2011). Our transcriptome analysis revealed that CD14⁺CD16⁻ overexpressed RNASE2, CD36, and TFEC, which are also over-expressed in CD1c⁺ cDC compared to CD141⁺ cDCs. These results suggest a relationship of CD1c⁺ cDCs and CD14⁺CD16⁻ monocytes. In our analysis of family molecules, CD14⁺CD16⁺ monocytes presented an intermediate phenotype between the classical and non-classical monocytes, which is in line with other molecular studies (Wong et al., 2011; Zawada et al., 2011).

Transcriptional programs of dendritic cell subsets have been investigated in the mouse system, human monocyte-derived DCs in vitro, and in human using microarray analysis (Banchereau et al., 2014; Miller et al., 2012; Segura et al., 2013). Our study used RNA-Seq to further analyze transcriptional profiles of all subsets of DCs found in human blood gathering more information from the transcriptome. Unique transcripts of CD1c⁺ DCs included FCER1A which was also identified to be expressed in CD1c⁺ DCs and facilitated IgE clearance as reported by another study (Greer et al., 2014). In addition, unique transcripts of CD1c⁺ DCs included FCGR2C (Fc γ receptor IIC), scavenger receptor cysteine-rich superfamily member CD163, and CD300e which appoints CD1c⁺ DCs with a phagocytic feature (Fabriek et al., 2005; Gasiorowski et al., 2013; Guilleams et al., 2014). Transcription factor ZEB2, identified as a unique transcript in CD1c⁺ DCs in our study has been previously reported to facilitate Langerhans cell (LC) mobilization associating with N-cadherin (Konradi et al., 2014). In CD141⁺ DCs, unique transcripts in our results are consistent with previously identified makers, XCR1,

CLEC9A and CADM1, accepted as common CD141⁺ DC markers across species (Bachem et al., 2010; Dutertre et al., 2014; Jongbloed et al., 2010). We also identified additional unique transcripts including ECE1 and TACSTD2. ECE1 was previously reported to be associated with transforming growth factor-beta (TGF- β 1) signaling in hepatic stellate cells after liver injury (Khimji et al., 2008). TACSTD, an EpCAM-Like Molecule, is a marker for human TGF- β 1-dependent epidermal LCs during development (Eisenwort et al., 2011). In the analysis of pre-selected family molecules, we found that the two cDC subsets showed very different expression patterns of transcription factors in the steady state. In addition to BATF3 and IRF8, which were previously implicated in CD141⁺ cDCs development (Helft et al., 2010), our analysis revealed conserved expression of IRF4, PRDM1, RNASE2 in CD1c⁺ cDCs. In mouse CD11b⁺ DCs, the counterpart of human CD1c⁺ cDC, IRF4 but not IRF8, plays a key role in promoting the expression of genes encoding for MHC class II pathway components and antigen processing and presentation molecules (Vander Lugt et al., 2014). PRDM1 (encoding Blimp-1) has been identified to have a selective role in the specification of human and mouse intestinal DC subsets. CD103 (integrin α E) and Sirp α (CD172a; a receptor for the signal-regulatory protein CD47) have been identified as conserved markers that defined three major subpopulations of conventional CD11c⁺ DCs in the human gut mucosa (Watchmaker et al., 2014). PRDM1 was found to be highly expressed in both human CD103⁺Sirp α ⁺ DCs and mouse CD103⁺CD11b⁺ DCs (Watchmaker et al., 2014); however, its functional role in dendritic cells still needs further investigation. RNASE2 (RNase A Family, 2) encodes eosinophil-derived neurotoxin (EDN), which is predicted to act as a transcription factor due to the presence of promiscuous InterPro DNA-binding domains (Hunter et al., 2009). RNASE2 was also described to possess antiviral

functions. Furthermore, RNASE2 was reported to be selectively chemotactic for dendritic cells but not for other type of leukocytes (Yang et al., 2003). Our result suggested that RNASE2 can be used as a marker to differentiate CD1c⁺ from CD141⁺ blood cDCs. High expression of RNASE2 in CD1c⁺ cDCs suggests a possible role in antiviral immunity. By comparing expression levels of antigen presentation genes and PRRs, our results also indicate that CD1c⁺ cDCs are more proficient at antigen processing and presentation, and recognizing a wide range of pathogens. We also investigated the difference of transcriptional profiles between CD2⁺ and CD2⁻ pDC subsets in the steady state. CD5 was found to be over-expressed in CD2⁺ pDCs. CD5 is thus a potential marker to divide CD2⁺ pDCs into CD2⁺CD5⁺ and CD2⁺CD5⁻ pDC subsets. CD2⁺CD5⁺ pDCs show a more mature phenotype with increased expression of CD80 and CD86 and therefore are more prone to participate in antigen presenting cell functions (Zhang et al., 2013). We also observed the unique expression of CLEC10A in CD2⁺ pDCs. Three unique transcripts in CD2⁻ pDCs, FBXL15, MAP1LC3B2 and JOSD2, are involved in ubiquitination (Cui et al., 2011; Seki et al., 2013).

To summarize, our in-depth studies of DC and monocyte subset transcriptional profiles using RNAseq provide a resource by cataloging differentially expressed genes. These differences are key to the functional specialization of these cell subsets.

Next, we investigated the early immune responses triggered by influenza vaccination in various APC subsets. In the 2010-2011 flu season, we expanded our study and investigated transcriptional changes of all subsets at day 1 and day 3 after vaccination in six healthy donors. An interferon signature after influenza vaccination was found at day 1 in monocytes subsets, CD1c⁺ DCs and CD2⁺ pDCs but not in CD141⁺ DCs. This result confirmed our previous observation in monocytes isolated from healthy donors one

day after vaccination (Obermoser et al., 2013). Furthermore, it also aligned with a recent work published by our group that CD14⁺ monocytes, blood CD1c⁺ but not CD141⁺ DCs responded to in vitro stimulation of TIV with an IFN signature (Banchereau et al., 2014). Moreover, we compared transcriptional changes at day 1 and day 3 for each monocyte subset in response to influenza vaccination. Most transcriptional changes were found in CD14⁺CD16⁻ and CD14⁺CD16⁺ monocytes on day 1. Chemokines are involved in various processes of monocyte recruitment including monocyte arrest and migration. CXCL3 (also called macrophage inflammatory protein-2-beta (MIP2b) acts as an arrest chemokine for monocyte adhesion on vascular cell adhesion molecule (VCAM)-1 under flow in the presence of P-selectin (Smith et al., 2005). The observed down-regulation of CXCL3 and CCL20 in our study may reflect that CD14⁺CD16⁻ monocytes are released from blood, migrating to the tissue. As discussed earlier, transcription factor analysis showed a closer relationship between CD14⁺CD16⁻ monocytes and CD1c⁺ cDCs. Down-regulation of CLEC10A in CD14⁺CD16⁻ monocytes at day 1 may indicate that this monocyte subset is involved in DC differentiation after vaccination. For CD14⁺CD16⁺ monocytes, we observed the up-regulation of ITGB7 (Integrin, Beta 7), IL31-RA, HLA-DOA and Fcγ receptor I at day 1. ITGB7 was identified as a marker for moDC maturation in a previous study (Aguilera-Montilla et al., 2013). IL31-RA is expressed in monocytes and macrophages and can bind IL-31 to induce pro-inflammatory effects (Kasraie et al., 2010). In human monocytes, FcγRI targets antigens to the MHC class II-rich late endosomes and leads to enhanced antigen processing and presentation to CD4⁺ T cells (Guilliams et al., 2014). CD14⁺CD16⁺ monocytes expressed high levels of MHC-II molecules in the steady state (Wong et al., 2011). Along with up-regulation of HLA-DOA, CD14⁺CD16⁺ monocytes probably present flu antigen via the MHC-class II

pathway. Besides up-regulated ISGs, biological functions of many transcripts that are changing in response to flu vaccination in CD14^{dim}CD16⁺ monocytes are not yet annotated. We also identified the common and unique transcripts with changes elicited by vaccination in monocyte subsets on day 1. The majority of transcripts with changes were unique to different monocyte subsets. Only one transcript, ANKRD22, was found to be upregulated in all three monocyte subsets. ANKRD22 was identified as an IFN γ -inducible gene in macrophages (Venner et al., 2014). It might be a key molecule involved in IFN response to vaccination in monocytes. STAT 1 was found to be upregulated in both CD16⁺ monocyte subsets. STAT1 and STAT2 proteins were identified as critical mediators of type I and type III IFN signaling that are essential components of the cellular antiviral response and adaptive immunity (Au-Yeung et al., 2013).

In cDCs, we discovered there were more genes with transcriptional changes elicited by influenza vaccination at day 1 in CD1c⁺ while CD141⁺ DC showed more differentially expressed genes on day 3 compared to the steady state. In CD1c⁺ cDCs at day 1, components of the complement system (C1QA and C1QB), E3 Ubiquitin-Protein Ligase (TRIM69), chemokine and chemokine receptors (CXCL9 and CCR1) and cytokines (IL-15 and IL-15RA) were all up-regulated. Our result showed the increased migration potentials of CD1c⁺ cDCs after the vaccination. A previous study showed that IL-15R α expression on mouse DCs is critical for NK cell activation via IL-15 trans-presentation to IL-2R β / γ_c receptors on NK cells (Koka et al., 2004). Our results may implicate CD1c⁺ cDCs involvement in NK cell activation upon influenza vaccination. We also observed the up-regulation of IDO1 and IDO2 (Indoleamine 2,3-Dioxygenase) at day 1. IDO1 is a DC maturation marker and is also related to T cell stimulatory activity

(Aguilera-Montilla et al., 2013). In CD141⁺ cDCs at day 1, the inflammatory marker tumor necrosis factor (TNF) was up-regulated, which may reflect that CD141⁺ cDCs initiated inflammatory responses to influenza vaccination. In addition, there are many other genes with transcriptional changes without annotation such as “RP11” family genes. There were only two transcripts, CTD-2653D5 and NPM1P24, upregulated in both cDC subsets after vaccination at day 1. However, their functions have not been described. On day 3, transcription factor CEBPB was up-regulated in CD1c⁺ cDCs. Previous studies showed that CEBPB regulates (trans-) differentiation and determines myeloid cell fate in the mouse (Stoilova et al., 2013). For CD141⁺ cDCs, TNF, IRF4 and GBP4 were found to be up-regulated. IRF4 has been identified to have a regulatory role in DCs by which it modulates IL-10 and IL-33 cytokine production to specifically promote Th2 differentiation and inflammation (Williams et al., 2013). Our result may indicate that CD141⁺ cDCs are prone to induce Th2 responses at day 3 in response to vaccination. This is in line with our recent publication demonstrating that CD141⁺ DCs but not CD1c⁺ DCs induce Th2 response via OX40L expression after LAIV stimulation (Yu et al., 2014).

CD2⁺ pDCs show the biggest number of transcripts changing in response to influenza vaccination on day 1 within all investigated APC subsets. IFN-related genes (IRF2BPL and ISG15) and pro-inflammatory cytokine (IL-1 β) were over-abundant but most transcripts were down-regulated. Down-regulated genes included C-type lectins (CLEC12B and CLEC1B), as well as MHC-I (HLA-H) and MHC-II molecules (HLA-DRB5), which may indicate that CD2⁺ pDCs migrate to the tissue for antigen detection and presentation. CD2⁺ pDCs seem to have more potential in antigen presentation with higher expression of costimulatory molecule CD80 upon activation as compared to CD2⁻

pDCs (Matsui et al., 2009). On the other hand, we observed the upregulation of granzyme H (GZMH) in CD2⁻ pDCs. Although no literature has focused on roles of GZMH in pDCs, our observation may provide another candidate to further study the killing mechanism of pDCs (Matsui et al., 2009). Two common transcripts with changes on day 1 were found in pDC subsets: upregulation of MIR17HG and downregulation of MRPS36. MIR17HG, affiliated with the class of lincRNAs, is a host gene for the MIR17-92 cluster comprising at least six microRNAs which may be involved in cell proliferation and differentiation (Park et al., 2014). On day 3, the numbers of transcripts changing in response to influenza vaccination were significantly reduced.

To summarize, our study provided new insights by defining the response of blood monocyte and DC subsets during the early immune responses to influenza vaccination in vivo. We were able to sort many rare APC cell populations from multiple time points post vaccination from healthy human subjects. However, we were limited in the numbers of healthy subjects that we were able to recruit in terms of the cost, timeline and logistics. Further validation of our results is needed, for example by investigating a larger cohort of healthy donors or using humanized mouse models (Yu et al., 2013).

Correlation between Baseline Signatures of APCs and Serologic Response

Finally, we wanted to address the question if serological response to influenza vaccination correlates with baseline transcriptional profiles in blood APCs. In order to scale up the numbers of donors needed for such a study, we used small blood draws (~ 5 mL of whole blood/ 5 M PBMC), instead of bead enriched apheresis sample like in the aforementioned studies. Because of technical challenges in sorting small cell numbers as

discussed in the results section, we focused our analysis only on genes present both in the small blood draw and the apheresis study.

Next, we investigated baseline molecular signatures that correlated with later antibody responses. The classical way of analyzing serology data is to define the high and low responders using the maximum fold change of titers among three viral strains as proposed by the FDA standard. The FDA defined seroconversion as an HAI titer of 1:40 or more and a minimum 4-fold increase of antibody titer after vaccination (Food and Drug Administration, 2007). Alternatively, the highest titer fold change, irrespective of strain, can be investigated (Nakaya et al., 2011). We took another approach by correlating all transcripts that were common with apheresis sorted APCs with all available serology information. In this way, we were able to determine if baseline transcriptional signatures correlated well with response to an individual viral strain in the vaccine.

Our analysis strategy helped us to identify fold change of antibody titers against the B influenza virus vaccine strain (as detected by viral neutralization assay) as the top serological parameter correlating with the highest numbers of transcripts at baseline. One possible explanation for this is that the 2012 influenza vaccine consists of B/Texas/6/2011 (a /Wisconsin/1/2010-like virus) which is a relatively novel vaccine strain regarding the formulation of influenza vaccines over the past ten years. The H1N1 and H3N2 viral strains have been included in the previous years. Indeed, most donors in our study did not have protective antibody titers (1:40) at baseline for the B strain, but many had titers of 1:40 or higher for the H1N1 and H3N2 strain. It is a well-known phenomenon that donors with pre-existing antibody titers yield a smaller fold-change in antibody titers in response to vaccination compared to subjects without pre-existing

antibody titers (“ceiling effect”). Thus in our study donors showed a higher magnitude of antibody response to vaccination in response to B strain compared to H1N1 and H3N2 vaccine strain. Consequently, the dynamic range of serological response was highest in response to B strain, and provided us the opportunity for detailed correlation analysis between baseline transcriptional signatures of APCs and fold change of titers against B strain detected by VN assay.

We determined that BDCA2⁺ pDCs showed the largest number of correlates. FAF1 is a Fas (TNFRSF6) associated factor is a negative regulator of an NFκB signaling pathway (Kinoshita et al., 2006). FAF1 showed negative correlation with “Fold_B_VN” in CD14⁺ monocytes and this implied that donors with an inflammation signature at baseline can mount a bigger antibody response to vaccination with the B strain. In CD1c⁺ cDCs, we identified genes correlating with the B strain antibody response were involved in several biological functions including inflammation and neutrophil movement. TLN1 along with FERMT3 were identified to be required for integrin activation. TLN1 is necessary for inducing LFA-1 extension which corresponds to intermediate affinity and induces neutrophils rolling (Lefort et al., 2012). However, its functional role in dendritic cells still needs to be investigated. CD141⁺ cDCs had very few common genes with apheresis sorted DCs and also few genes correlated with serological parameters. The correlated transcripts from BDCA2⁺ pDCs were involved in immune-cell trafficking. pDCs are well known type I IFN secreting cells which plays an important role in protecting against viral infection (Gilliet et al., 2008; Mathan et al., 2013). Our result did not show a direct correlation of IFN genes with serology, but some interferon-inducible genes were positively correlated. Finally, we combined GSEA and modular analysis to interpret our data. Many inflammation and mitochondria annotated

modules in CD14⁺ monocytes correlated with fold change of titers against B strain. Besides the inflammation module, CD1c⁺ cDCs also showed an IFN module correlating with antibody response to B strain. Interestingly, CD1c⁺ cDCs were also the main DC subset contributing to IFN signature on day 1 after vaccination. BDCA2⁺ pDCs showed positive correlation of both inflammation and mitochondria modules. Thus, our exploratory proof-of-concept analysis suggests that transcriptional profiling of blood APCs might offer prediction of immune response to vaccination. These findings will need to be validated in large-scale studies.

Our results also provide a strategy to tailor influenza vaccine adjuvants to impact specific APC subsets for better vaccination outcomes. Monocytes might be a key cell population to be considered for targeting since we observed an inflammation signature of monocytes at baseline correlating with later serologic response. We also observed the IFN signature in all monocyte subsets at day 1 in response to flu vaccination. IFN signature has been shown previously to be associated with antibody responses (Bucasas et al., 2011; Cao et al., 2014; Nakaya et al., 2011). A previous study has shown that CD14^{dim} monocytes patrol and sense virus and nucleic acids via TLR7/8 receptors (Cros et al., 2010). In a non-human primate study, TLR 7/8 and TLR9 ligand induce rapid expansion of monocytes, specifically elicit the activation of peripheral DCs, and promote the cytokine production correlating with chemokine and type-I IFN-inducible gene expression in the blood. Also injection of CpG-ODN (TLR9) mediated a sustainable inflammatory response in the blood (Kwissa et al., 2012). Targeting TLR7/8 and TLR9 receptors in monocytes might be an excellent way to induce both inflammation and interferon response, both of which are associated with inducing stronger serological response to seasonal influenza vaccination.

The live attenuated yellow fever vaccine 17D (YF-17D) is one of the most effective vaccines available which has been attributed to its capacity to activate multiple DC subsets via TLRs 2, 7, 8, and 9, induce a pro-inflammatory cytokine profile, and thereby stimulate polyvalent immune responses (Querec et al., 2006). Dr. Pulendran's group also showed that immunization of mice with synthetic nanoparticles containing antigens plus ligands that signal through TLR4 and TLR7 induces synergistic increases in antigen-specific, neutralizing antibodies compared to immunization with nanoparticles containing antigens plus a single TLR ligand. Antibody responses were dependent on direct triggering of both TLRs on B cells and dendritic cells, as well as on T-cell help. Immunization protected completely against lethal avian and swine influenza virus strains in mice, and induced robust immunity against pandemic H1N1 influenza in rhesus macaques (Kasturi et al., 2011).

Overall, our results provide a comprehensive comparative analysis of the transcriptional landscape of monocyte and blood subsets from human peripheral blood at the steady state and early time points after influenza vaccination. Furthermore, we provided a framework and tools for future studies to investigate the immune response to vaccines which may open up new avenues of improved vaccine design.

CHAPTER SIX

Conclusions

From this study, we had the following conclusions:

- Early innate immune response to the influenza vaccination peaks at day 1 with a prominent IFN signature followed by a smaller peak at day 7 caused by adaptive immune responses from whole blood samples.
- The major cellular sources contributing to this IFN signature at day 1 are neutrophils, monocytes, CD1c⁺ cDCs and CD2⁺ pDCs.
- Monocytes and CD2⁺ pDCs are the main contributors to global transcriptional changes occurring at day 1 after vaccination.
- Inflammation signature of APCs and an interferon signature in CD1c⁺ cDCs at baseline are correlated with specific serology response.

APPENDIX

APPENDIX

List of Current and Future Publications

Publications Related to the Topic of Dissertation

Wang Y, et al. Transcriptional Landscape of Circulating Dendritic Cells and Monocytes at Steady State and in Response to Influenza Vaccination (in preparation).

Wang Y, et al. Antibody responses to influenza vaccination correlate with the transcriptome of blood monocytes and dendritic cell subsets (in preparation).

Obermoser G, Presnell S, Domico K, Xu H, **Wang Y**, Anguiano E, Thompson-Snipes L, Ranganathan R, Zeitner B, Bjork A, Anderson D, Speake C, Ruchaud E, Skinner J, Alsina L, Sharma M, Dutartre H, Cepika A, Israelsson E, Nguyen P, Nguyen QA, Harrod AC, Zurawski SM, Pascual V, Ueno H, Nepom GT, Quinn C, Blankenship D, Palucka K, Banchereau J, Chaussabel D. Systems scale interactive exploration reveals quantitative and qualitative differences in response to influenza and pneumococcal vaccines. *Immunity*. 2013 Apr 18;38(4):831-44. doi: 10.1016/j.immuni.2012.12.008.

Yu CI, Becker C, **Wang Y**, Marches F, Helft J, Leboeuf M, Anguiano E, Pourpe S, Goller K, Pascual V, Banchereau J, Merad M, Palucka K. Human CD1c⁺ dendritic cells drive the differentiation of CD103⁺ CD8⁺ mucosal T cells via TGF- β . *Immunity*. 2013 Apr 18;38(4):831-44. doi: 10.1016/j.immuni.2012.12.008.

Yu CI, Becker C, Metang P, Marches F, **Wang Y**, Toshiyuki H, Banchereau J, Merad M, Palucka K. Human CD141⁺ Dendritic Cells Induce CD4⁺ T Cells To Produce Type 2 Cytokines. *J Immunol*. 2014 Sep 22. pii: 1401159.

Banchereau R, Baldwin N, Cepika AM, Athale S, Xue Y, Yu CI, Metang P, Cheruku A, Berthier I, Gayet I, **Wang Y**, Ohouo M, Snipes L, Xu H, Obermoser G, Blankenship D, Oh S, Ramilo O, Chaussabel D, Banchereau J, Palucka K, Pascual V. Transcriptional specialization of human dendritic cell subsets in response to microbial vaccines. *Nat Commun*. 2014 Oct 22;5:5283. doi: 10.1038/ncomms6283.

Additional Publications

- Rabinowitz KM, **Wang Y**, Chen E, Hovhannisyan Z, Chiang D, Berin MC, Dahan S, Chaussabel D, Ma'ayan A, Mayer L. Transforming Growth Factor- β Signaling Controls Activities of Human Intestinal CD8⁺ T Suppressor Cells, *Gastroenterology* (2012), doi: 10.1053/j.gastro.2012.12.001
- Boyd A, Bennuru S, **Wang Y**, Sanprasert V, Law M, Chaussabel D, Nutman TB, Semnani RT. Quiescent innate response to infective filariae by human langerhans cells suggests a strategy of immune evasion. *Infect Immun*. 2013 May;81(5):1420-9. doi: 10.1128/IAI.01301-12. Epub 2013 Feb 19.
- Bloom CI, Graham CM, Berry MP, Rozakeas F, Redford PS, **Wang Y**, Xu Z, Wilkinson KA, Wilkinson RJ, Kendrick Y, Devouassoux G, Ferry T, Miyara M, Bouvry D, Valeyre D, Gorochoy G, Blankenship D, Saadatian M, Vanhems P, Beynon H, Vancheeswaran R, Wickremasinghe M, Chaussabel D, Banchereau J, Pascual V, Ho LP, Lipman M, O'Garra A. Transcriptional blood signatures distinguish pulmonary tuberculosis, pulmonary sarcoidosis, pneumonias and lung cancers. *PLoS One*. 2013 Aug 5;8(8):e70630. doi: 10.1371/journal.pone.0070630.

BIBLIOGRAPHY

- Aguilera-Montilla, N., Chamorro, S., Nieto, C., Sanchez-Cabo, F., Dopazo, A., Fernandez-Salguero, P.M., Rodriguez-Fernandez, J.L., Pello, O.M., Andres, V., Cuenda, A., *et al.* (2013). Aryl hydrocarbon receptor contributes to the MEK/ERK-dependent maintenance of the immature state of human dendritic cells. *Blood* *121*, e108-117.
- Akira, S., and Takeda, K. (2004). Toll-like receptor signalling. *Nature reviews. Immunology* *4*, 499-511.
- Ambrose, C.S., Levin, M.J., and Belshe, R.B. (2011). The relative efficacy of trivalent live attenuated and inactivated influenza vaccines in children and adults. *Influenza and other respiratory viruses* *5*, 67-75.
- Ancuta, P., Liu, K.Y., Misra, V., Wacleche, V.S., Gosselin, A., Zhou, X., and Gabuzda, D. (2009). Transcriptional profiling reveals developmental relationship and distinct biological functions of CD16+ and CD16- monocyte subsets. *BMC genomics* *10*, 403.
- Anders, S., Pyl, P.T., and Huber, W. (2014). HTSeq – A Python framework to work with high-throughput sequencing data. *bioRxiv*.
- Andrzej Dzionek, A.F., Petra Schmidt, Sabine Cremer, Monika Zysk, Stefan Miltenyi, David W. Buck, and Jurgen Schmitz. (2000). BDCA-2, BDCA-3, and BDCA-4: Three Markers for Distinct Subsets of Dendritic Cells in Human Peripheral Blood. *The Journal of Immunology*. *165*, 6037-6046.
- Au-Yeung, N., Mandhana, R., and Horvath, C.M. (2013). Transcriptional regulation by STAT1 and STAT2 in the interferon JAK-STAT pathway. *Jak-Stat* *2*, e23931.
- Auffray, C., Fogg, D., Garfa, M., Elain, G., Join-Lambert, O., Kayal, S., Sarnacki, S., Cumano, A., Lauvau, G., and Geissmann, F. (2007). Monitoring of blood vessels and tissues by a population of monocytes with patrolling behavior. *Science* *317*, 666-670.
- Auffray, C., Sieweke, M.H., and Geissmann, F. (2009). Blood monocytes: development, heterogeneity, and relationship with dendritic cells. *Annual review of immunology* *27*, 669-692.
- Bachem, A., Guttler, S., Hartung, E., Ebstein, F., Schaefer, M., Tannert, A., Salama, A., Movassaghi, K., Opitz, C., Mages, H.W., *et al.* (2010). Superior antigen cross-presentation and XCR1 expression define human CD11c+CD141+ cells as homologues of mouse CD8+ dendritic cells. *The Journal of experimental medicine* *207*, 1273-1281.

- Banchereau, J., and Steinman, R.M. (1998). Dendritic cells and the control of immunity. *Nature*, 245–252.
- Banchereau, R., Baldwin, N., Cepika, A.M., Athale, S., Xue, Y., Yu, C.I., Metang, P., Cheruku, A., Berthier, I., Gayet, I., *et al.* (2014). Transcriptional specialization of human dendritic cell subsets in response to microbial vaccines. *Nature communications* 5, 5283.
- Barrat, F.J., Meeker, T., Gregorio, J., Chan, J.H., Uematsu, S., Akira, S., Chang, B., Duramad, O., and Coffman, R.L. (2005). Nucleic acids of mammalian origin can act as endogenous ligands for Toll-like receptors and may promote systemic lupus erythematosus. *The Journal of experimental medicine* 202, 1131-1139.
- Benjamini, Y., and Hochberg, Y. (1995). Controlling the False Discovery Rate: A Practical and Powerful Approach to Multiple Testing. *J.R. Stat.* , 289-300.
- Boltjes, A., and van Wijk, F. (2014). Human dendritic cell functional specialization in steady-state and inflammation. *Frontiers in immunology* 5, 131.
- Boonstra, A., Asselin-Paturel, C., Gilliet, M., Crain, C., Trinchieri, G., Liu, Y.J., and O'Garra, A. (2002). Flexibility of Mouse Classical and Plasmacytoid-derived Dendritic Cells in Directing T Helper Type 1 and 2 Cell Development: Dependency on Antigen Dose and Differential Toll-like Receptor Ligation. *Journal of Experimental Medicine* 197, 101-109.
- Boule, M.W., Broughton, C., Mackay, F., Akira, S., Marshak-Rothstein, A., and Rifkin, I.R. (2004). Toll-like receptor 9-dependent and -independent dendritic cell activation by chromatin-immunoglobulin G complexes. *The Journal of experimental medicine* 199, 1631-1640.
- Bucasas, K.L., Franco, L.M., Shaw, C.A., Bray, M.S., Wells, J.M., Nino, D., Arden, N., Quarles, J.M., Couch, R.B., and Belmont, J.W. (2011). Early patterns of gene expression correlate with the humoral immune response to influenza vaccination in humans. *The Journal of infectious diseases* 203, 921-929.
- Cao, R.G., Suarez, N.M., Obermoser, G., Lopez, S.M., Flano, E., Mertz, S.E., Albrecht, R.A., Garcia-Sastre, A., Mejias, A., Xu, H., *et al.* (2014). Differences in antibody responses between trivalent inactivated influenza vaccine and live attenuated influenza vaccine correlate with the kinetics and magnitude of interferon signaling in children. *The Journal of infectious diseases* 210, 224-233.
- CDC (2010). The 2009 H1N1 Pandemic: Summary Highlights, April 2009-April 2010.
- Chaussabel, D., Pascual, V., and Banchereau, J. (2010). Assessing the human immune system through blood transcriptomics. *BMC biology* 8, 84.

- Chaussabel, D., Quinn, C., Shen, J., Patel, P., Glaser, C., Baldwin, N., Stichweh, D., Blankenship, D., Li, L., Munagala, I., *et al.* (2008). A modular analysis framework for blood genomics studies: application to systemic lupus erythematosus. *Immunity* 29, 150-164.
- Christensen, S.R., Shupe, J., Nickerson, K., Kashgarian, M., Flavell, R.A., and Shlomchik, M.J. (2006). Toll-like receptor 7 and TLR9 dictate autoantibody specificity and have opposing inflammatory and regulatory roles in a murine model of lupus. *Immunity* 25, 417-428.
- Clayberger, C., Finn, M.W., Wang, T., Saini, R., Wilson, C., Barr, V.A., Sabatino, M., Castiello, L., Stroncek, D., and Krensky, A.M. (2012). 15 kDa granulysin causes differentiation of monocytes to dendritic cells but lacks cytotoxic activity. *Journal of immunology* 188, 6119-6126.
- Clements, M.L., Betts, R.F., Tierney, E.L., and Murphy, B.R. (1986). Serum and nasal wash antibodies associated with resistance to experimental challenge with influenza A wild-type virus. *Journal of clinical microbiology* 24, 157-160.
- Cros, J., Cagnard, N., Woollard, K., Patey, N., Zhang, S.Y., Senechal, B., Puel, A., Biswas, S.K., Moshous, D., Picard, C., *et al.* (2010). Human CD14^{dim} monocytes patrol and sense nucleic acids and viruses via TLR7 and TLR8 receptors. *Immunity* 33, 375-386.
- Cui, Y., He, S., Xing, C., Lu, K., Wang, J., Xing, G., Meng, A., Jia, S., He, F., and Zhang, L. (2011). SCFFBXL(1)(5) regulates BMP signalling by directing the degradation of HECT-type ubiquitin ligase Smurf1. *The EMBO journal* 30, 2675-2689.
- de Almeida, M.C., Silva, A.C., Barral, A., and Barral Netto, M. (2000). A simple method for human peripheral blood monocyte isolation. *Memorias do Instituto Oswaldo Cruz* 95, 221-223.
- Dutertre, C.A., Wang, L.F., and Ginhoux, F. (2014). Aligning bona fide dendritic cell populations across species. *Cellular immunology* 291, 3-10.
- Eisenwort, G., Jurkin, J., Yasmin, N., Bauer, T., Gesslbauer, B., and Strobl, H. (2011). Identification of TROP2 (TACSTD2), an EpCAM-like molecule, as a specific marker for TGF-beta1-dependent human epidermal Langerhans cells. *The Journal of investigative dermatology* 131, 2049-2057.
- Fabrick, B.O., Dijkstra, C.D., and van den Berg, T.K. (2005). The macrophage scavenger receptor CD163. *Immunobiology* 210, 153-160.
- Fiore, A.E., Shay, D.K., Broder, K., Iskander, J.K., Uyeki, T.M., Mootrey, G., Bresee, J.S., Cox, N.J., and CDC (2009). Prevention and control of seasonal influenza with vaccines: recommendations of the Advisory Committee on Immunization Practices (ACIP), 2009. *MMWR Recomm Rep.* 58, 1-52.

- Food and Drug Administration (2007). Guidance for Industry: Clinical Data Needed to Support the Licensure of Pandemic Influenza Vaccines. (Office of Communication, Training and Manufacturers Assistance, Rockville, Maryland, 2007).
- Gasiorowski, R.E., Ju, X., Hart, D.N., and Clark, G.J. (2013). CD300 molecule regulation of human dendritic cell functions. *Immunology letters* 149, 93-100.
- Gaucher, D., Therrien, R., Kettaf, N., Angermann, B.R., Boucher, G., Filali-Mouhim, A., Moser, J.M., Mehta, R.S., Drake, D.R., 3rd, Castro, E., *et al.* (2008). Yellow fever vaccine induces integrated multilineage and polyfunctional immune responses. *The Journal of experimental medicine* 205, 3119-3131.
- Geijtenbeek, T.B., and Gringhuis, S.I. (2009). Signalling through C-type lectin receptors: shaping immune responses. *Nature reviews. Immunology* 9, 465-479.
- Geiss, G.K., Bumgarner, R.E., Birditt, B., Dahl, T., Dowidar, N., Dunaway, D.L., Fell, H.P., Ferree, S., George, R.D., Grogan, T., *et al.* (2008). Direct multiplexed measurement of gene expression with color-coded probe pairs. *Nature biotechnology* 26, 317-325.
- Geissmann, F., Jung, S., and Littman, D.R. (2003). Blood monocytes consist of two principal subsets with distinct migratory properties. *Immunity* 19, 71-82.
- Gilliet, M., Cao, W., and Liu, Y.J. (2008). Plasmacytoid dendritic cells: sensing nucleic acids in viral infection and autoimmune diseases. *Nature reviews. Immunology* 8, 594-606.
- Greer, A.M., Wu, N., Putnam, A.L., Woodruff, P.G., Wolters, P., Kinet, J.P., and Shin, J.S. (2014). Serum IgE clearance is facilitated by human FcεpsilonRI internalization. *The Journal of clinical investigation* 124, 1187-1198.
- Grohskopf, L.A., Olsen, S.J., Sokolow, L.Z., Bresee, J.S., Cox, N.J., Broder, K.R., Karron, R.A., Walter, E.B., Influenza Division, N.C.f.I., and Respiratory Diseases, C.D.C. (2014). Prevention and Control of Seasonal Influenza with Vaccines: Recommendations of the Advisory Committee on Immunization Practices (ACIP) - United States, 2014-15 Influenza Season. *MMWR. Morbidity and mortality weekly report* 63, 691-697.
- Guilliams, M., Bruhns, P., Saeys, Y., Hammad, H., and Lambrecht, B.N. (2014). The function of Fcγ receptors in dendritic cells and macrophages. *Nature reviews. Immunology* 14, 94-108.
- Haller Hasskamp, J., Zapas, J.L., and Elias, E.G. (2005). Dendritic cell counts in the peripheral blood of healthy adults. *American journal of hematology* 78, 314-315.

- Haniffa, M., Shin, A., Bigley, V., McGovern, N., Teo, P., See, P., Wasan, P.S., Wang, X.N., Malinarich, F., Malleret, B., *et al.* (2012). Human tissues contain CD141^{hi} cross-presenting dendritic cells with functional homology to mouse CD103⁺ nonlymphoid dendritic cells. *Immunity* 37, 60-73.
- Hanson, D.A., Kaspar, A.A., Poulain, F.R., and Krensky, A.M. (1999). Biosynthesis of granulysin, a novel cytolytic molecule. *Molecular immunology* 36, 413-422.
- Harrow, J., Frankish, A., Gonzalez, J.M., Tapanari, E., Diekhans, M., Kokocinski, F., Aken, B.L., Barrell, D., Zadissa, A., Searle, S., *et al.* (2012). GENCODE: the reference human genome annotation for The ENCODE Project. *Genome research* 22, 1760-1774.
- Heath, W.R., and Carbone, F.R. (2001). Cross-presentation in viral immunity and self-tolerance. *Nat Rev Immunol.* 1, 126-134.
- Helft, J., Ginhoux, F., Bogunovic, M., and Merad, M. (2010). Origin and functional heterogeneity of non-lymphoid tissue dendritic cells in mice. *Immunol Rev.* 234, 55-75.
- Hemont, C., Neel, A., Heslan, M., Braudeau, C., and Josien, R. (2013). Human blood mDC subsets exhibit distinct TLR repertoire and responsiveness. *Journal of leukocyte biology* 93, 599-609.
- Hunter, S., Apweiler, R., Attwood, T.K., Bairoch, A., Bateman, A., Binns, D., Bork, P., Das, U., Daugherty, L., Duquenne, L., *et al.* (2009). InterPro: the integrative protein signature database. *Nucleic acids research* 37, D211-215.
- Ito, T., Wang, Y.H., Duramad, O., Hori, T., Delespesse, G.J., Watanabe, N., Qin, F.X., Yao, Z., Cao, W., and Liu, Y.J. (2005). TSLP-activated dendritic cells induce an inflammatory T helper type 2 cell response through OX40 ligand. *The Journal of experimental medicine* 202, 1213-1223.
- Iwasaki, H., and Akashi, K. (2007). Myeloid lineage commitment from the hematopoietic stem cell. *Immunity* 26, 726-740.
- Joffre, O.P., Segura, E., Savina, A., and Amigorena, S. (2012). Cross-presentation by dendritic cells. *Nature reviews. Immunology* 12, 557-569.
- Jongbloed, S.L., Kassianos, A.J., McDonald, K.J., Clark, G.J., Ju, X., Angel, C.E., Chen, C.J., Dunbar, P.R., Wadley, R.B., Jeet, V., *et al.* (2010). Human CD141⁺ (BDCA-3)⁺ dendritic cells (DCs) represent a unique myeloid DC subset that cross-presents necrotic cell antigens. *The Journal of experimental medicine* 207, 1247-1260.
- Kadowaki, N., Antonenkov, S., Lau, J., and Liu, Y. (2000). Natural interferon alpha/beta-producing cells link innate and adaptive immunity. *J. Exp. Med.* 192, 219-226.

- Kaspar, A.A., Okada, S., Kumar, J., Poulain, F.R., Drouvalakis, K.A., Kelekar, A., Hanson, D.A., Kluck, R.M., Hitoshi, Y., Johnson, D.E., *et al.* (2001). A distinct pathway of cell-mediated apoptosis initiated by granulysin. *Journal of immunology* *167*, 350-356.
- Kasraie, S., Niebuhr, M., and Werfel, T. (2010). Interleukin (IL)-31 induces pro-inflammatory cytokines in human monocytes and macrophages following stimulation with staphylococcal exotoxins. *Allergy* *65*, 712-721.
- Kasturi, S.P., Skountzou, I., Albrecht, R.A., Koutsonanos, D., Hua, T., Nakaya, H.I., Ravindran, R., Stewart, S., Alam, M., Kwissa, M., *et al.* (2011). Programming the magnitude and persistence of antibody responses with innate immunity. *Nature* *470*, 543-547.
- Kelly, A., Fahey, R., Fletcher, J.M., Keogh, C., Carroll, A.G., Siddachari, R., Geoghegan, J., Hegarty, J.E., Ryan, E.J., and O'Farrelly, C. (2014). CD141⁺ myeloid dendritic cells are enriched in healthy human liver. *J Hepatol.* *60*, 135-142.
- Khimji, A.K., Shao, R., and Rockey, D.C. (2008). Divergent transforming growth factor-beta signaling in hepatic stellate cells after liver injury: functional effects on ECE-1 regulation. *The American journal of pathology* *173*, 716-727.
- Kim, D., Pertea, G., Trapnell, C., Pimentel, H., Kelley, R., and Salzberg, S.L. (2013). TopHat2: accurate alignment of transcriptomes in the presence of insertions, deletions and gene fusions. *Genome biology* *14*, R36.
- Kinoshita, T., Kondoh, C., Hasegawa, M., Imamura, R., and Suda, T. (2006). Fas-associated factor 1 is a negative regulator of PYRIN-containing Apaf-1-like protein 1. *International immunology* *18*, 1701-1706.
- Koka, R., Burkett, P., Chien, M., Chai, S., Boone, D.L., and Ma, A. (2004). Cutting Edge: Murine Dendritic Cells Require IL-15R to Prime NK Cells. *The Journal of Immunology* *173*, 3594-3598.
- Konradi, S., Yasmin, N., Haslwanter, D., Weber, M., Gesslbauer, B., Sixt, M., and Strobl, H. (2014). Langerhans cell maturation is accompanied by induction of N-cadherin and the transcriptional regulators of epithelial-mesenchymal transition ZEB1/2. *European journal of immunology* *44*, 553-560.
- Krishnaswamy, J.K., Chu, T., and Eisenbarth, S.C. (2013). Beyond pattern recognition: NOD-like receptors in dendritic cells. *Trends in immunology* *34*, 224-233.
- Kwissa, M., Nakaya, H.I., Oluoch, H., and Pulendran, B. (2012). Distinct TLR adjuvants differentially stimulate systemic and local innate immune responses in nonhuman primates. *Blood* *119*, 2044-2055.

- La Montagne, J.R., Noble, G.R., Quinnan, G.V., Curlin, G.T., Blackwelder, W.C., Smith, J.I., Ennis, F.A., and Bozeman, F.M. (1983). Summary of clinical trials of inactivated influenza vaccine - 1978. *Reviews of infectious diseases* 5, 723-736.
- Lande, R., Gregorio, J., Facchinetti, V., Chatterjee, B., Wang, Y.H., Homey, B., Cao, W., Wang, Y.H., Su, B., Nestle, F.O., *et al.* (2007). Plasmacytoid dendritic cells sense self-DNA coupled with antimicrobial peptide. *Nature* 449, 564-569.
- Lauvau, G., Chorro, L., Spaulding, E., and Soudja, S.M. (2014). Inflammatory monocyte effector mechanisms. *Cellular immunology*.
- Lefort, C.T., Rossaint, J., Moser, M., Petrich, B.G., Zarbock, A., Monkley, S.J., Critchley, D.R., Ginsberg, M.H., Fassler, R., and Ley, K. (2012). Distinct roles for talin-1 and kindlin-3 in LFA-1 extension and affinity regulation. *Blood* 119, 4275-4282.
- Li, H., Handsaker, B., Wysoker, A., Fennell, T., Ruan, J., Homer, N., Marth, G., Abecasis, G., Durbin, R., and Genome Project Data Processing, S. (2009). The Sequence Alignment/Map format and SAMtools. *Bioinformatics* 25, 2078-2079.
- Li, S., Rouphael, N., Duraisingham, S., Romero-Steiner, S., Presnell, S., Davis, C., Schmidt, D.S., Johnson, S.E., Milton, A., Rajam, G., *et al.* (2014). Molecular signatures of antibody responses derived from a systems biology study of five human vaccines. *Nature immunology* 15, 195-204.
- Lovering, R.C., Camon, E.B., Blake, J.A., and Diehl, A.D. (2008). Access to immunology through the Gene Ontology. *Immunology* 125, 154-160.
- Lundberg, K., Rydnert, F., Greiff, L., and Lindstedt, M. (2014). Human blood dendritic cell subsets exhibit discriminative pattern recognition receptor profiles. *Immunology* 142, 279-288.
- MacDonald, K.P., Munster, D.J., Clark, G.J., Dzionek, A., Schmitz, J., and Hart, D.N. (2002). Characterization of human blood dendritic cell subsets. *Blood* 100, 4512-4520.
- Manz, M.G., Traver, D., Miyamoto, T., Weissman, I.L., and Akashi, K. (2001). Dendritic cell potentials of early lymphoid and myeloid progenitors. *Blood* 97, 3333-3341.
- Mathan, T.S., Figdor, C.G., and Buschow, S.I. (2013). Human plasmacytoid dendritic cells: from molecules to intercellular communication network. *Frontiers in immunology* 4, 372.
- Matsui, T., Connolly, J.E., Michnevitz, M., Chaussabel, D., Yu, C.I., Glaser, C., Tindle, S., Pypaert, M., Freitas, H., Piqueras, B., *et al.* (2009). CD2 distinguishes two subsets of human plasmacytoid dendritic cells with distinct phenotype and functions. *Journal of immunology* 182, 6815-6823.

- Miller, J.C., Brown, B.D., Shay, T., Gautier, E.L., Jojic, V., Cohain, A., Pandey, G., Leboeuf, M., Elpek, K.G., Helft, J., *et al.* (2012). Deciphering the transcriptional network of the dendritic cell lineage. *Nature immunology* *13*, 888-899.
- Nagalakshmi, U., Wang, Z., Waern, K., Shou, C., Raha, D., Gerstein, M., and Snyder, M. (2008). The transcriptional landscape of the yeast genome defined by RNA sequencing. *Science* *320*, 1344-1349.
- Nair, H., Brooks, W.A., Katz, M., Roca, A., Berkley, J.A., Madhi, S.A., Simmerman, J.M., Gordon, A., Sato, M., Howie, S., *et al.* (2011). Global burden of respiratory infections due to seasonal influenza in young children: a systematic review and meta-analysis. *Lancet* *378*, 1917-1930.
- Nakaya, H.I., Wrammert, J., Lee, E.K., Racioppi, L., Marie-Kunze, S., Haining, W.N., Means, A.R., Kasturi, S.P., Khan, N., Li, G.M., *et al.* (2011). Systems biology of vaccination for seasonal influenza in humans. *Nature immunology* *12*, 786-795.
- Neuzil, K.M., Dupont, W.D., Wright, P.F., and Edwards, K.M. (2001). Efficacy of inactivated and cold-adapted vaccines against influenza A infection, 1985 to 1990: the pediatric experience. *The Pediatric infectious disease journal* *20*, 733-740.
- Nizzoli, G., Krietsch, J., Weick, A., Steinfelder, S., Facciotti, F., Gruarin, P., Bianco, A., Steckel, B., Moro, M., Crosti, M., *et al.* (2013). Human CD1c+ dendritic cells secrete high levels of IL-12 and potently prime cytotoxic T-cell responses. *Blood* *122*, 932-942.
- Obermoser, G., Presnell, S., Domico, K., Xu, H., Wang, Y., Anguiano, E., Thompson-Snipes, L., Ranganathan, R., Zeitner, B., Bjork, A., *et al.* (2013). Systems scale interactive exploration reveals quantitative and qualitative differences in response to influenza and pneumococcal vaccines. *Immunity* *38*, 831-844.
- Okoniewski, M.J., and Miller, C.J. (2006). Hybridization interactions between probesets in short oligo microarrays lead to spurious correlations. *BMC bioinformatics* *7*, 276.
- Ovcharenko, D., Jarvis, R., Hunicke-Smith, S., Kelnar, K., and Brown, D. (2005). High-throughput RNAi screening in vitro: from cell lines to primary cells. *Rna* *11*, 985-993.
- Palucka, A.K., Ueno, H., Fay, J.W., and Banchereau, J. (2007). Taming cancer by inducing immunity via dendritic cells. *Immunol Rev.* *220*, 129-150.
- Palucka, K., Banchereau, J., and Mellman, I. (2010). Designing vaccines based on biology of human dendritic cell subsets. *Immunity* *33*, 464-478.

- Paret, C., Bourouba, M., Beer, A., Miyazaki, K., Schnolzer, M., Fiedler, S., and Zoller, M. (2005). Ly6 family member C4.4A binds laminins 1 and 5, associates with galectin-3 and supports cell migration. *International journal of cancer. Journal international du cancer* 115, 724-733.
- Park, D., Lee, S.C., Park, J.W., Cho, S.Y., and Kim, H.K. (2014). Overexpression of miR-17 in gastric cancer is correlated with proliferation-associated oncogene amplification. *Pathology international* 64, 309-314.
- Passlick, B., Flieger, D., and Ziegler-Heitbrock, H.W. (1989). Identification and characterization of a novel monocyte subpopulation in human peripheral blood. *Blood* 74, 2527-2534.
- Pulendran, B., Oh, J.Z., Nakaya, H.I., Ravindran, R., and Kazmin, D.A. (2013). Immunity to viruses: learning from successful human vaccines. *Immunological reviews* 255, 243-255.
- Querec, T., Bennouna, S., Alkan, S., Laouar, Y., Gorden, K., Flavell, R., Akira, S., Ahmed, R., and Pulendran, B. (2006). Yellow fever vaccine YF-17D activates multiple dendritic cell subsets via TLR2, 7, 8, and 9 to stimulate polyvalent immunity. *The Journal of experimental medicine* 203, 413-424.
- Querec, T.D., Akondy, R.S., Lee, E.K., Cao, W., Nakaya, H.I., Teuwen, D., Pirani, A., Gernert, K., Deng, J., Marzolf, B., *et al.* (2009). Systems biology approach predicts immunogenicity of the yellow fever vaccine in humans. *Nature immunology* 10, 116-125.
- Randolph, G.J., Inaba, K., Robbiani, D.F., Steinman, R.M., and Muller, W.A. (1999). Differentiation of phagocytic monocytes into lymph node dendritic cells in vivo. *Immunity* 11, 753-761.
- Real, E., Kaiser, A., Raposo, G., Amara, A., Nardin, A., Trautmann, A., and Donnadieu, E. (2004). Immature Dendritic Cells (DCs) Use Chemokines and Intercellular Adhesion Molecule (ICAM)-1, But Not DC-Specific ICAM-3-Grabbing Nonintegrin, to Stimulate CD4⁺ T Cells in the Absence of Exogenous Antigen. *The Journal of Immunology* 173, 50-60.
- Reber, A.J., Chirkova, T., Kim, J.H., Cao, W., Biber, R., Shay, D.K., and Sambhara, S. (2012). Immunosenescence and Challenges of Vaccination against Influenza in the Aging Population. *Aging and disease* 3, 68-90.
- Ringner, M. (2008). What is principal component analysis? *Nature biotechnology* 26, 303-304.
- Robinson, M.D., McCarthy, D.J., and Smyth, G.K. (2010). edgeR: a Bioconductor package for differential expression analysis of digital gene expression data. *Bioinformatics* 26, 139-140.

- Royce, T.E., Rozowsky, J.S., and Gerstein, M.B. (2007). Toward a universal microarray: prediction of gene expression through nearest-neighbor probe sequence identification. *Nucleic acids research* 35, e99.
- Schenten, D., and Medzhitov, R. (2011). The control of adaptive immune responses by the innate immune system. *Advances in immunology* 109, 87-124.
- Schmitt, N., Morita, R., Bourdery, L., Bentebibel, S.E., Zurawski, S.M., Banchereau, J., and Ueno, H. (2009). Human dendritic cells induce the differentiation of interleukin-21-producing T follicular helper-like cells through interleukin-12. *Immunity* 31, 158-169.
- Schoggins, J.W., Wilson, S.J., Panis, M., Murphy, M.Y., Jones, C.T., Bieniasz, P., and Rice, C.M. (2011). A diverse range of gene products are effectors of the type I interferon antiviral response. *Nature* 472, 481-485.
- Schotsaert, M., and Garcia-Sastre, A. (2014). Influenza Vaccines: A Moving Interdisciplinary Field. *Viruses* 6, 3809-3826.
- Segura, E., Touzot, M., Bohineust, A., Cappuccio, A., Chiochia, G., Hosmalin, A., Dalod, M., Soumelis, V., and Amigorena, S. (2013). Human inflammatory dendritic cells induce Th17 cell differentiation. *Immunity* 38, 336-348.
- Segura, E., Valladeau-Guilemond, J., Donnadieu, M.H., Sastre-Garau, X., Soumelis, V., and Amigorena, S. (2012). Characterization of resident and migratory dendritic cells in human lymph nodes. *The Journal of experimental medicine* 209, 653-660.
- Seki, T., Gong, L., Williams, A.J., Sakai, N., Todi, S.V., and Paulson, H.L. (2013). JosD1, a membrane-targeted deubiquitinating enzyme, is activated by ubiquitination and regulates membrane dynamics, cell motility, and endocytosis. *The Journal of biological chemistry* 288, 17145-17155.
- Serbina, N.V., and Pamer, E.G. (2006). Monocyte emigration from bone marrow during bacterial infection requires signals mediated by chemokine receptor CCR2. *Nature immunology* 7, 311-317.
- Shi, C., and Pamer, E.G. (2011). Monocyte recruitment during infection and inflammation. *Nature reviews. Immunology* 11, 762-774.
- Sierra-Filardi, E., Nieto, C., Dominguez-Soto, A., Barroso, R., Sanchez-Mateos, P., Puig-Kroger, A., Lopez-Bravo, M., Joven, J., Ardavin, C., Rodriguez-Fernandez, J.L., et al. (2014). CCL2 shapes macrophage polarization by GM-CSF and M-CSF: identification of CCL2/CCR2-dependent gene expression profile. *Journal of immunology* 192, 3858-3867.
- Smith, D.F., Galkina, E., Ley, K., and Huo, Y. (2005). GRO family chemokines are specialized for monocyte arrest from flow. *American journal of physiology. Heart and circulatory physiology* 289, H1976-1984.

- Steel, J., Lowen, A.C., Pena, L., Angel, M., Solorzano, A., Albrecht, R., Perez, D.R., Garcia-Sastre, A., and Palese, P. (2009). Live attenuated influenza viruses containing NS1 truncations as vaccine candidates against H5N1 highly pathogenic avian influenza. *Journal of virology* 83, 1742-1753.
- Steinman, R.M. (2007). Lasker Basic Medical Research Award. Dendritic cells: versatile controllers of the immune system. *Nat. Med.* 13, 1155-1159.
- Steinman, R.M. (2008). Dendritic cells in vivo: a key target for a new vaccine science. *Immunity* 29, 319-324.
- Steinman, R.M., Hawiger, D., Liu, K., Bonifaz, L., Bonnyay, D., Mahnke, K., Iyoda, T., Ravetch, J., Dhodapkar, M., Inaba, K., and Nussenzweig, M. (2003). Dendritic Cell Function in Vivo during the Steady State: A Role in Peripheral Tolerance. *Ann N Y Acad Sci.* 987, 15-25.
- Stenger, S., Hanson, D.A., Teitelbaum, R., Dewan, P., Niazi, K.R., Froelich, C.J., Ganz, T., Thoma-Uszynski, S., Melian, A., Bogdan, C., *et al.* (1998). An antimicrobial activity of cytolytic T cells mediated by granulysin. *Science* 282, 121-125.
- Stoilova, B., Kowenz-Leutz, E., Scheller, M., and Leutz, A. (2013). Lymphoid to myeloid cell trans-differentiation is determined by C/EBPbeta structure and post-translational modifications. *PloS one* 8, e65169.
- Taubenberger, J.K., and Morens, D.M. (2008). The Pathology of Influenza Virus Infections. 499–522.
- Thompson, W.W., Moore, M.R., Weintraub, E., Cheng, P.Y., Jin, X., Bridges, C.B., Bresee, J.S., and Shay, D.K. (2009). Estimating influenza-associated deaths in the United States. *American journal of public health* 99 Suppl 2, S225-230.
- Thompson, W.W., Shay, D.K., Weintraub, E., Brammer, L., Bridges, C.B., Cox, N.J., and Fukuda, K. (2004). Influenza-associated hospitalizations in the United States. *JAMA : the journal of the American Medical Association* 292, 1333-1340.
- Traver, D., Akashi, K., Manz, M., Merad, M., Miyamoto, T., Engleman, E.G., and Weissman, I.L. (2000). Development of CD8alpha-positive dendritic cells from a common myeloid progenitor. *Science* 290, 2152-2154.
- Treanor, J.J., El Sahly, H., King, J., Graham, I., Izikson, R., Kohberger, R., Patriarca, P., and Cox, M. (2011). Protective efficacy of a trivalent recombinant hemagglutinin protein vaccine (FluBlok(R)) against influenza in healthy adults: a randomized, placebo-controlled trial. *Vaccine* 29, 7733-7739.
- Tsang, J.S., Schwartzberg, P.L., Kotliarov, Y., Biancotto, A., Xie, Z., Germain, R.N., Wang, E., Olnes, M.J., Narayanan, M., Golding, H., *et al.* (2014). Global analyses of human immune variation reveal baseline predictors of postvaccination responses. *Cell* 157, 499-513.

- Vander Lugt, B., Khan, A.A., Hackney, J.A., Agrawal, S., Lesch, J., Zhou, M., Lee, W.P., Park, S., Xu, M., DeVoss, J., *et al.* (2014). Transcriptional programming of dendritic cells for enhanced MHC class II antigen presentation. *Nature immunology* *15*, 161-167.
- Vaquerizas, J.M., Kummerfeld, S.K., Teichmann, S.A., and Luscombe, N.M. (2009). A census of human transcription factors: function, expression and evolution. *Nature reviews. Genetics* *10*, 252-263.
- Venner, J.M., Famulski, K.S., Badr, D., Hidalgo, L.G., Chang, J., and Halloran, P.F. (2014). Molecular landscape of T cell-mediated rejection in human kidney transplants: prominence of CTLA4 and PD ligands. *American journal of transplantation : official journal of the American Society of Transplantation and the American Society of Transplant Surgeons* *14*, 2565-2576.
- Villadangos, J.A., and Schnorrer, P. (2007). Intrinsic and cooperative antigen-presenting functions of dendritic-cell subsets in vivo. *Nature reviews. Immunology* *7*, 543-555.
- Wang, S., Taaffe, J., Parker, C., Solorzano, A., Cao, H., Garcia-Sastre, A., and Lu, S. (2006). Hemagglutinin (HA) proteins from H1 and H3 serotypes of influenza A viruses require different antigen designs for the induction of optimal protective antibody responses as studied by codon-optimized HA DNA vaccines. *Journal of virology* *80*, 11628-11637.
- Wang, Z., Gerstein, M., and Snyder, M. (2009). RNA-Seq: a revolutionary tool for transcriptomics. *Nature reviews. Genetics* *10*, 57-63.
- Watchmaker, P.B., Lahl, K., Lee, M., Baumjohann, D., Morton, J., Kim, S.J., Zeng, R., Dent, A., Ansel, K.M., Diamond, B., *et al.* (2014). Comparative transcriptional and functional profiling defines conserved programs of intestinal DC differentiation in humans and mice. *Nature immunology* *15*, 98-108.
- Whitley, P., Moturi, S., Santiago, J., Johnson, C., and Setterquist, R. (2005). Improved Microarray Sensitivity using Whole Blood RNA Samples. *Ambion TechNotes* *12*, 20-23
- Williams, J.W., Tjota, M.Y., Clay, B.S., Vander Lugt, B., Bandukwala, H.S., Hrusch, C.L., Decker, D.C., Blaine, K.M., Fixsen, B.R., Singh, H., *et al.* (2013). Transcription factor IRF4 drives dendritic cells to promote Th2 differentiation. *Nature communications* *4*, 2990.
- Wold, B., and Myers, R.M. (2008). Sequence census methods for functional genomics. *Nature methods* *5*, 19-21.

- Wong, K.L., Tai, L.L., Wong, W.C., Han, H., Sem, X., Yeap, W.H., Kourilsky, P., and Wong, S.C. (2011). Gene expression profiling reveals the defining features of the classical, intermediate, and nonclassical human monocyte subsets. *Blood* 118, 16-31.
- Wong, S.S., and Webby, R.J. (2013). Traditional and new influenza vaccines. *Clinical microbiology reviews* 26, 476-492.
- World Health Organization (2014). Fact sheet on influenza.
- Yang, D., Rosenberg, H.F., Chen, Q., Dyer, K.D., Kurosaka, K., and Oppenheim, J.J. (2003). Eosinophil-derived neurotoxin (EDN), an antimicrobial protein with chemotactic activities for dendritic cells. *Blood* 102, 3396-3403.
- Yu, C.I., Becker, C., Metang, P., Marches, F., Wang, Y., Toshiyuki, H., Banchereau, J., Merad, M., and Palucka, A.K. (2014). Human CD141⁺ Dendritic Cells Induce CD4⁺ T Cells To Produce Type 2 Cytokines. *Journal of immunology* 193, 4335-4343.
- Yu, C.I., Becker, C., Wang, Y., Marches, F., Helft, J., Leboeuf, M., Anguiano, E., Pourpe, S., Goller, K., Pascual, V., *et al.* (2013). Human CD1c⁺ dendritic cells drive the differentiation of CD103⁺ CD8⁺ mucosal effector T cells via the cytokine TGF-beta. *Immunity* 38, 818-830.
- Zawada, A.M., Rogacev, K.S., Rotter, B., Winter, P., Marell, R.R., Fliser, D., and Heine, G.H. (2011). SuperSAGE evidence for CD14⁺⁺CD16⁺ monocytes as a third monocyte subset. *Blood* 118, e50-61.
- Zhang, X., Lepelley, A., Azria, E., P., L., Roguet, G., Schwartz, O., Launay, O., Leclerc, C., and Lo-Man, R. (2013). Neonatal Plasmacytoid Dendritic Cells (pDCs) Display Subset Variation but Can Elicit Potent Anti-Viral Innate Responses. *PloS one* 8.
- Ziegler-Heitbrock, L. (2007). The CD14⁺ CD16⁺ blood monocytes: their role in infection and inflammation. *Journal of leukocyte biology* 81, 584-592.
- Ziegler-Heitbrock, L., Ancuta, P., Crowe, S., Dalod, M., Grau, V., Hart, D.N., Leenen, P.J., Liu, Y.J., MacPherson, G., Randolph, G.J., *et al.* (2010). Nomenclature of monocytes and dendritic cells in blood. *Blood* 116, e74-80.